POLITECNICO DI MILANO

Scuola di ingegneria Industriale e dell'informazione

Corso di Laurea Magistrale in

Ingegneria Meccanica

Modelling and control

of a device that converts wave motion

into electrical energy

Supervisor:

Prof. Francesco Castelli Dezza

Co-supervisor:

Prof. Sergio Martinez Gonzalez,
Prof. Vincenzo Dossena

Candidates:

Gianmarco Bertelli 796774

Massimo Brovedani 796930

Academic year 2013/2014

ACKNOWLEDGMENTS

The following work has been possible thanks to prof. Francesco Castellidezza, Politecnico di Milano, and prof. Sergio Martinez, Politécnica de Madrid, who followed periodically our project from the very beginning. Professor Castelidezza has always been available to give feedback and advises despite the distance and prof. Martinez who, through his attentiveness, helped us achieving a successful work. We then want to acknowledge Prof. Dossena and Prof. Collina and Dr. Hugo Mendoza Ph.D. that for all this time showed interest to our project and offered help. Moreover, we feel grateful to Prof. Belloli since he has always contributed with useful academic and life advises.

We must thank our common Italian and foreigner friends that accompanies us through these demanding years of university. In particular our best regards Carlotta, Dario, Dido, Est, Fano, Francesca, Giulia, Il Cubo, Leo, Lore, Luisa, Mirella, Peppe, Ugo, Veronica, from our great time in Milan; Carlitos, Gabriel, Giordy, Giulia, Isabela, Jeff, Luca, Maria, Mariana, Marilena, Michela, Mike, Nestor, Nieves, Pablo, Ricardo, Samantha, Stabbo, Thomas, from our astonishing international experience.

Despite we work as unique entity for this project, we have also additional personal acknowledgments and we would like to list them in the following columns

The first one I would like to thank is someone who, despite is not physically here, is always in my hearth and always indicates me the way to follow. She insisted a lot in order to make me apply for mechanical engineering, she instilled on me her passion for knowledge and she did the most to convince me to undertake international experiences since I was

I would like to thank my family, my dad Ruggero, my mum Anna and my grandmas Rosaria and Dina that with their counsels and behaviors showed, but not imposed, the path to follow.

I want to thank my “sister” Carlotta that since I was a boy of sixteen years old showed me another way of seeing the world, fostering my critical way of

child. This person is my sweet mum Maria. A huge thank must be said also to my great dad Ivo, who always followed me and sustained me during my studies. My success at the university has been possible also to my second family, that has always been attentive on me and has always helped me a lot when I went back home. I want hence to acknowledge Nani, Bepi, Glauco and Vania. I then thank my sister Veronica, who always shows herself proud of me, and my aunt Magda, that is always available to help me. Keeping around my home town, I want to thank the wonderful group of friends that I developed there. In particular, I want to praise the quality as best friends of Giordy and Luca, who have always been in contact with me and have always visited me around the world with passion and happiness. The same merit goes to my best girlfriends Michela and Marilena, always in touch with me and caring about my path. I report again the important role that my international and Italian friends covered in these years, and I want to acknowledge them also personally. By the end, I thank my high school professors, without whom I wouldn't have developed my attitude and thinking and helping me out through some bad moments, creating the man that I am; and my "brother" Raffaele that since I was 4 years old has been by my side and even with more than 800 km of distance he taught me how a man can be happy and smile in every situation, how much is beautiful to compete and to make people laugh, making the friend that I am.

Thanks to Civic, Paolone, with whom I share memories, as teenagers and as young man, of jokes, happiness and tranquility, Dilly, Ele, that endured my jokes during my adolescence and that lightened up all my visits in Modena even in the darker moments, Alle, Laura that shared the best trips that I did both in Spain and in Greece and to Gandalf, Stabbo, Lippa, Cianciu that made my experience in China unique.

My thanks must also go to two of my high school professors, Lucia Gaiani and Giuseppe Sturiale, that believed in my potential and invested in me their time to make me not just a good student but a hungry one.

personality in this way. The last person I want to remember is my first teacher, who else unfortunately is not here with us anymore, maestra Paola, who is the first person who noticed my passion for studying and working hard, and who always gave me great advises.

And to my companions Massimo, Dario and Leonardo with whom I started and shared an indelible chapter of my life.

These people allow us to open our mind and pointed us the gateway for success

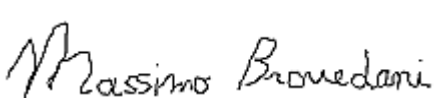

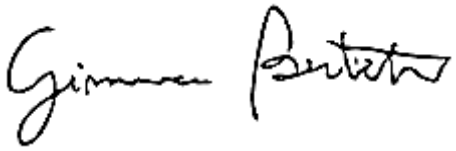

CONTENTS

LIST OF FIGURES

LIST OF TABLES

ABSTRACT

La carenza di aspettative dalla produzione di potenza attraverso fonti tradizionali e l'urgenza di trovare un buon compromesso fra economicità ed energia pulita portano il mondo delle rinnovabili ad essere un contesto aperto a nuovi studi e nuove ricerche. Accanto alle energie rinnovabili tradizionali si affiancano quindi energie rinnovabili alternative, come quella contenuta nel mare, che compone due terzi del nostro pianeta. Un impianto che converte l'energia delle onde in energia elettrica è oggetto di studio e di miglioramento in corso. Questo processo richiede ancora molto per portare a delle soluzioni economiche e considerabili rispetto a quelle messe tuttora a disposizione dalle risorse tradizionali. Il nostro studio non è un tentativo di ridurre costi progettuali e non riguarda una proposta impianstica, ma un passo verso una produzione più efficiente attraverso questa tecnologia innovativa, il che si tradurrebbe in una riduzione di costi di esercizio. Lo studio quindi parte con la modellizazione e la caratterizzazione delle varie componenti dell'impianto preso in considerazione, e prosegue con l'ottimizzazione della strategia di controllo del sistema al fine di ottenere una maggiore estrazione di energia, per cui una migliore efficienza. Lo studio è numerico ed utilizza software di calcolo ed elementi finiti per l'ottenimento dei risultati. Alla fine, questi vengono comparati con soluzioni non ottime ed una stima di una potenza media viene fornita.

The lack of expectations from power production through traditional sources along with the need of a compromise between cost saving and clean energy make the world of renewable energies an open and undiscovered reality. For this purposes, innovative renewable energies started to grow next to the traditional ones. An example is given by the energy contained in to the sea, which composes two third of our planet. A plant converting wave energy into electric energy is still an object of deep study and potential improvement. This process requires a lot in order to make this solution economically comparable with what the actual traditional energies offer. Our study is not an attempt to

propose a reduction of installation costs through a determinate plant structure. It is, instead, a step towards a more efficient production through this innovative technology, which would drive too to smaller exercise costs. The study hence starts with the modelization and the characterization of all the components belonging to a particular system of wave energy conversion, and it carries on with the optimization of the control strategy of the same plant, in order to extract more energy, hence, to achieve a better efficiency. The study is numerical and exploits calculus and even FEM software in order to get to the results. By the end, what we achieved is compared with not optimized solution and a global esteem of power generation is provided.

La falta de expectativas en la producción energética a través de las fuentes tradicionales y la urgencia de encontrar un compromiso entre el ahorro económico y la energía limpia, hace que el mundo de las energías renovables sea una realidad actual y a estudiar. Debido a estas innovativas estrategias, en la última década las energías renovables han ganado mucha importancia en los proyectos de investigación. Un claro ejemplo es la energía mareomotriz, una tecnología que convierte la energía de las olas en electricidad es, definitivamente, un campo potencial de estudio e investigación ya que dos terceras partes de la tierra es agua. Esta fuente de energía necesita todavía desarrollarse para poder llegar a competir en el mercado eléctrico con las clásicas fuentes energéticas. Uno de los principales problemas que tiene es el coste de instalación y sobre el cual están centradas la mayoría de las líneas de investigación. En nuestro estudio, en vez de centrarnos en este problema, hemos querido mejorar su eficiencia energética logrando reducir el coste de producción. El proyecto comienza con la modelización y la caracterización de todos los componentes de la planta que extrae la energía de las olas, y concluye con la optimización de la estrategia de control consiguiendo mayor energía eléctrica y mejorar así la eficiencia del modelo. Se realizará un estudio numérico utilizando MATLAB y su interfaz Simulink, además del programa FEM para verificar la interacción entre las olas y la instalación. Finalmente, para demostrar la validez de

nuestro estudio, se comparará con el control sin optimizar y se realizará una estimación de la producción media.

INTRODUCTION

The work is presented in four different chapters that cover all the necessary steps to model the Wave Energy Converter and to study a sub-optimal control that maximize the energy extraction.

The first chapter is an overview on how the electric energy is mainly produced and on the actual state of marine energy converters. Firstly, we underline the problems connected with fossil fuel energy generation explaining why we think that an exploitation of marine energy could lead to an improvement of the actual critical condition; secondly, we analyzed the state of the art of the wave energy converters choosing among them a plant to model and control. The choice was done considering the information availability, the project phase and the plant structure.

The second chapter regards the modelization of the plant and its validation. The plant we choose resembles a prototype plant in Denmark, the Wave Star WEC. The Wave Star WEC is composed by different parts that interact between themselves. The energy conversion process starts from the exploitation of the movement of a buoy generated by the waves; this buoy is connected through a mechanical arm to a cylinder that pumps a hydraulic fluid inside a hydraulic circuit. The hydraulic circuit is characterized by three pressures lines each of which is connected to a bunch of accumulators. Parts of the hydraulic circuit, the high and the low pressure lines, are then connected to a constant stroke hydraulic motor that is keyed with an asynchronous generator, which produces the energetic output of our system. Since we modeled just one buoy, we can't consider our model exactly equal to the Wave Star Prototype. However, this will not influence the control strategy and the optimization procedure. Each component of the plant has been studied and validated singularly before gathering all the parts together. To model the interaction between the buoy and the wave we used the well-known linear wave theory and we exploit the results given by the commercial code ANSYS AQWA. To characterize the behavior of all the components we used a highly analytical and meticulous description

through differential and algebraic equations, each of which is deeply justified through a physical and critical analysis of the process. For instance, we modeled the hydraulic cylinder considering the behavior of the pressure inside each chamber, through the mass conservation theory, and we modeled the friction in a detailed way. However, we neglected the mass of the cylinder that is very small compared to the mass of the mechanical arm. The modelization for each component has been carried out in parallel with the validation. Since we didn't have an available physical prototype we compared our results with the results given by the reliable Simscape library. By the end of the chapter, we gathered all the components together by creating a Simulink model that describes our whole plant. The final validation occurs through the comparison between two whole models, the Simscape one and ours.

The third chapter regards the study, the optimization procedure and the implementation of our control strategy. The aim is to optimize the energy extraction of the plant. The study starts from a regular wave phenomenon and then moves to the real irregular waves. The control structure for these two cases does not change; it is a four quadrant control and the fact of keeping the same structure between regular and irregular waves is justified and yields our control a sub-optimal one. The optimal control, in fact, is impossible to be perfectly achieved since it would require the knowledge of the future. The optimization procedure has been carried out by parts, since there are many parameters to be optimized. Through an iteration process, we obtained the final optimal values. This choice has been done considering a compromise between time consumption and result accuracy; a whole optimization would have lead to a too long procedure due to the high number of parameters and their dependence on the wave states. In fact, our control is based on a reference force to be tracked; this reference force is based on a spring based reactive control and depends, hence, on two parameters. In addition to these two values we need to optimize the control time and the working pressures. This optimization is driven by a compromise between tracking and losses in the hydraulic circuit. The implementation of the control sees three different constrains. First, we have to track the reference force by controlling the manifold; secondly, we have to avoid the depletion of

the accumulators through a slight modification of the manifold control strategy. Finally, we need to keep the desired drop between the pressure lines, by controlling the feeding frequency of the generator.

In the fourth and last chapter, we gather all the results achieved for different wave states and we compared our control with others not optimized. The comparison made by listing the states variables and outputs that are strictly connected to energy conversion We show the behavior of the system and its main variables for a real time of more than half an hour, with a chosen wave state. We then express an hypothetical mean power generation.

INTRODUZIONE

Il lavoro svolto si estende in Quattro capitoli che coprono un percorso che parte dalla modellizzazione di un impianto di conversione dell'energia contenuta nella onde marine in energia elettrica, allo studio di un controllo subottimo al fine di massimizzare l'estrazione della stessa.

Il primo capitolo discorre brevemente sulla situazione odierna per quanto riguarda la produzione energetica e descrive lo stato attuale dei convertitori di energia marina. Inizialmente vengono messi in evidenza i problemi correlati alla produzione energetica attraverso combustibili fossili, spiegando in parallelo il motivo per cui lo sfruttamento dell' energia contenuta nel mare possa aiutare a migliorare la situazione critica attuale. Successivamente viene analizzato lo stato dell'arte degli impianti per la conversione dell'energia marina classificandoli in base alla tecnologia, e viene scelto l'impianto oggetto del nostro studio. La scelta viene effettuata sulla base delle informazioni disponibli, della fase di avanzamento progettuale e della struttura dell'impianto.

Il secondo capitolo tratta della modellizzazione dell impianto e della sua validazione. La tecnologia scelta è quella del Wave Star, impianto presente in Danimarca ancora a livello di prototipo, e diviso in diverse componenti interagenti fra di loro. Il processo di conversione prende luogo dal movimento di una boa generato dalla forza delle onde su cui la stessa galleggia; la boa è connessa ad un braccio meccanico, che a sua volta muove uno stantuffo all'interno di un cilindro idraulico, che agisce da pompa per pressurizzare un fluido nel circuito idraulico. Il circuito idraulico è caratterizzato da tre linee di pressione, ognuna della quali è connessa ad una serie di accumulatori. Parte del circuito, vale a dire le linee di alta e bassa pressione, sono connesse ad un motore idraulico a cilindrata costante, calettato con un generatore asincrono, dal quale viene generato l'output energetico del nostro sistema. Avendo modellizzato solo una boa, non possiamo considerare il modello del nostro impianto esattamente uguale al prototipo Wave Star.

Tuttavia, questo non influenzerà minimamente la bontà dei risultati e la validità della procedura di ottimizzazione utilizzata. Ogni singola parte dell'impianto viene studiata singolarmente prima di assemblare il tutto nel modello finale. Per modellare l'interazione fra boa e onda sfruttiamo la linear wave theory ed i risultati di un software commerciale chiamato ANSYS AQWA. Al fine di ottenere una descrizione di ogni singolo componente, utilizziamo un approccio altamente analitico e meticoloso attraverso delle equazioni differenziali e algebriche, che vengono giustificate attraverso un'analisi profonda e critica sulla fisica del processo. Per riportare un esempio, caratterizziamo l'andamento delle pressioni nelle camere attraverso la legge della conservazione della massa di fluido, e allo stesso tempo teniamo conto in maniera dettagliata dell'attrito all'interno del cilindro. In aggiunta, abbiamo deciso di trascurare la massa dello stantuffo, visto il valore esiguo se comparato con il braccio meccanico connesso alla boa. La modellizzazione di ogni componente è stata effettuata in parallelo con la validazione. Data l'assenza di un laboratorio dove testare il nostro modello, la validazione è avvenuta attraverso un confronto con un modello equivalente, creato tramite l'affidabile, e più volte testata, libreria Simscape. Alla fine del capitolo, uniamo tutti i componenti al fine di creare l'impianto nella sua globalità. La validazione finale avviene tramite il confronto dei risultati fra i due modelli totali, quello Simscape ed il nostro.

Il terzo capitolo concerne lo studio, l'ottimizzazione e l'implementazione della nostra strategia di controllo sull'impianto. L'obbiettivo è la massimizzazione dell'energia estratta. Lo studio parte da un'onda regolare e segue con l'estensione a spettri complessi di onde. La struttura del controllo nei due casi non cambia, essendo sempre un controllo a quattro quadranti. Il fatto che la forma del controllo rimanga la stessa viene giustificato e rende il controllo, nel caso di onde irregulari, un controllo subottimo. Si vedrà, infatti, come il raggiungimento di un controllo ottimo sia impossibile, poichè prevederebbe una conoscenza precisa del futuro. La procedura di ottimizzazione è stata svolta suddividendo il problema totale in sottoproblemi, visto che i parametri aventi punto di ottimo sono numerosi. Tramite una procedura iterativa, spiegata nel dettaglio, arriviamo a dei risultati ottimi finali. L'adozione di tale strategia iterativa è stata una scelta guidata da un

compromesso fra tempo speso e precisione dei risultati; un'ottimizzazione globale, infatti, avrebbe implicato un tempo eccessivamente lungo per l'ottenimento dei risultati, a causa del numero dei parametri coinvolti in tale procedura e della loro dipendenza dallo stato del mare. Il nostro controllo si basa su una forza di riferimento da seguire ed è un controllo spring based; è quindi basato su due parametri. In aggiunta a quest'ultimi si mette in evidenza l'importanza di ottimizzare pure il tempo di controllo e le pressioni di lavoro per le linee connesse al motore. Tale ottimizzazione è frutto di un compromesso fra un buon inseguimento della forza di riferimento ed una limitazione delle perdite idrauliche nel circuito. L'implementazione del controllo deve tener conto, alla fine, di tre vincoli. Primo, è necessario inseguire la forza attraverso un'adeguata apertura e chiusura delle valvole che connettono cilindro e accumulatori. Successivamente, bisogna evitare lo svuotamento degli accumulatori, modificando leggermente la strategia di controllo delle valvole. Infine, è anche importante mantenere la desiderata ed ottimizzata differenza di pressione fra le linee, agendo sulla frequenza e voltaggio di alimentazione del generatore asincrono.

Nell'ultimo capitolo, raccogliamo tutti i risultati ottenuti, utilizzando come input diversi stati d'onda. Dato uno stato d'onda, compariamo una soluzione ottima con quelle non ottime. Il confronto fra i controlli viene effettuato attraverso variabili e output strettamente connessi al processo di conversione dell'energia. Sempre fissando l'input, mostriamo il comportamento del sistema e delle sue variabili principali attraverso una simulazione che corrisponde a mezzora di tempo reale. Esprimiamo infine un'ipotetica potenza media dell'impianto.

1 First Chapter: Overview and Classification of the Technologies

1.1 Problems connected with Fossil Fuel Energy Consumption:

Since human being has always been an economical subject, he applies an economical point of view on each decision, in order to achieve the best result with the least effort. One of the protagonist of the last century was the development of the industries, and so the technologies, that brought to a better energy exploitation. By means of energy and all the devices that use it, humanity was able to achieve results that one hundred years before were not even imaginable, and so it greatly fulfilled its needs and requirements.

In the recent past almost all the energy was produced by means of fossil fuels, which are the results of a natural process that lasted millions of years. Through them and their flexibility everything was achievable with an insignificant amount of money thanks to their high energetic density, simplicity of storage and the high reserves to production ratio.

The same industrial development made the consumption increase rapidly, above all after the seventies where we can observe [Figure 1-1] that the energy consumption is almost doubled from 1970 to 2004.

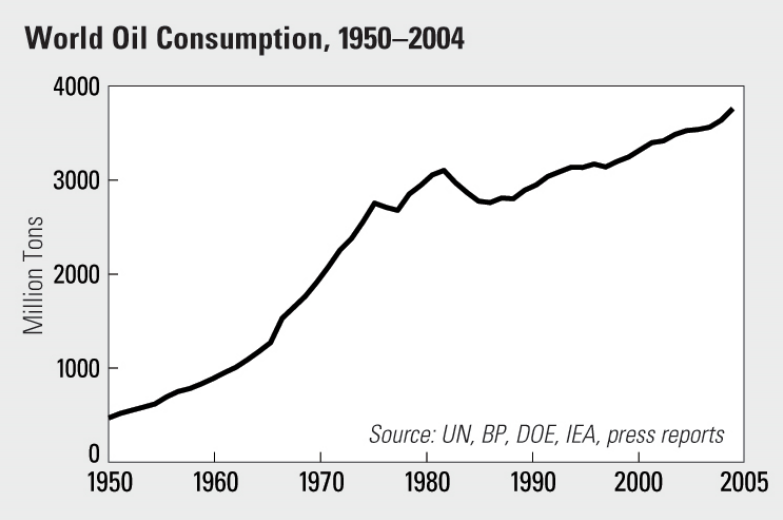

Figure 1-1: World Oil Consumption 1950-2005 http://www.worldwatch.org/global-fossil-fuel-consumption-surges

This huge exploitation took to the birth of new problems concerning energy production.

These problems have to do with fossil fuels themselves and we decided to classify them in three different categories:

- **Quantity of resources:** This consumption is clearly faster than the process of fossil fuel generation. The reserves to production ratio (R/P), defined as the availability over the consumption of the resource, indicates approximately the number of years for which the resource will be still present. Thinking about the oil we can see from the graph below [Figure 1-2] how, even if the ratio can change, there is a downward trend:

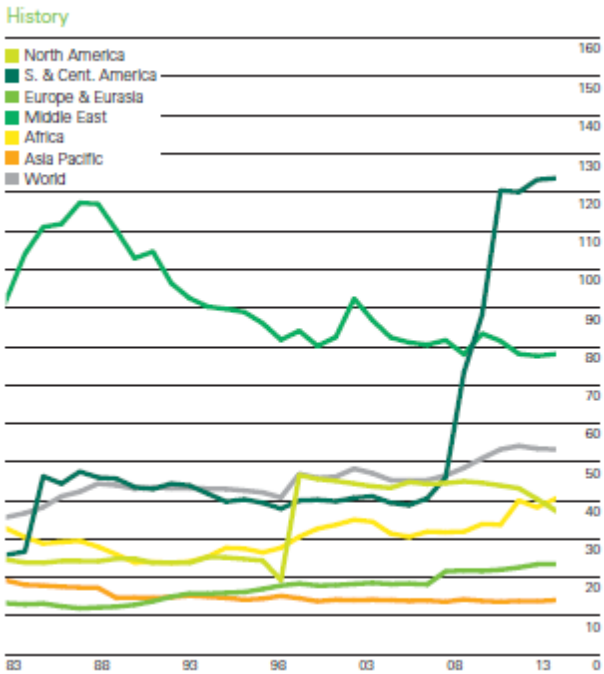

Figure 1-2 British Petroleum Report [1]

Considering these trends we will run out of oil in slightly more than 50 years. The other two fossil fuel resources, Natural Gas and Coal, are dealing with the same problem [Figure 1-3]: respectively they will be available for 55 and 113 years.

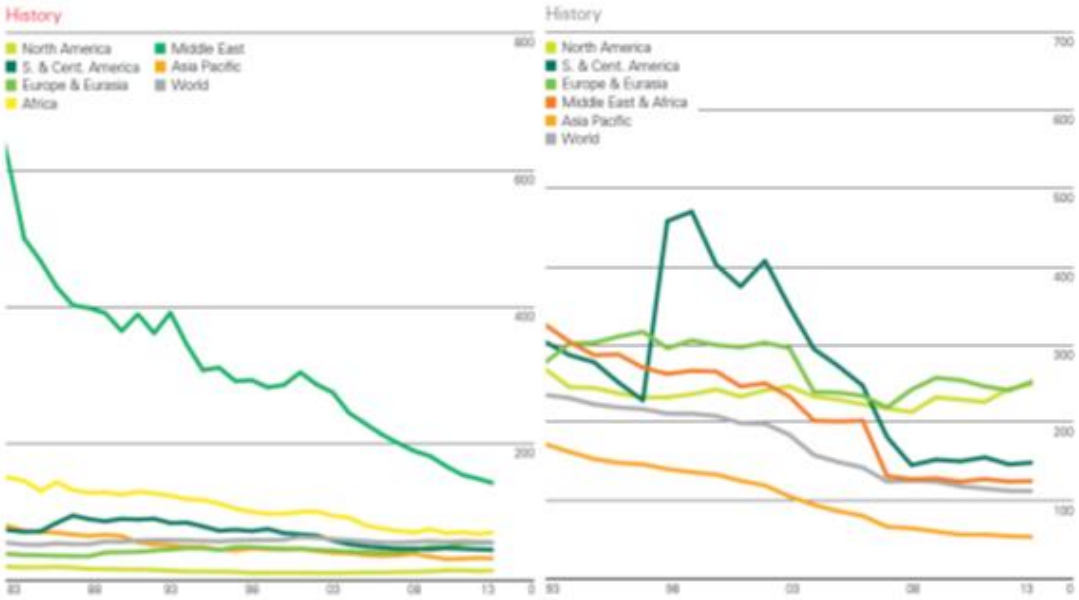

Figure 1-3 British Petroleum Report [1]

Even if the trend may of course change we can observe how the problem is serious and will get even worse in the recent future. This diminishing trend will reflect to the market as an increase of price.

- **Position of the deposits:** The most developed countries, which consume the fifty percent of the available resources, are the countries with less fossil fuel deposits. This problem regards above all natural gas and oil that are concentrated mainly in Middle East as can be seen in the two figures below, where is depicted the trade movements of these resources:

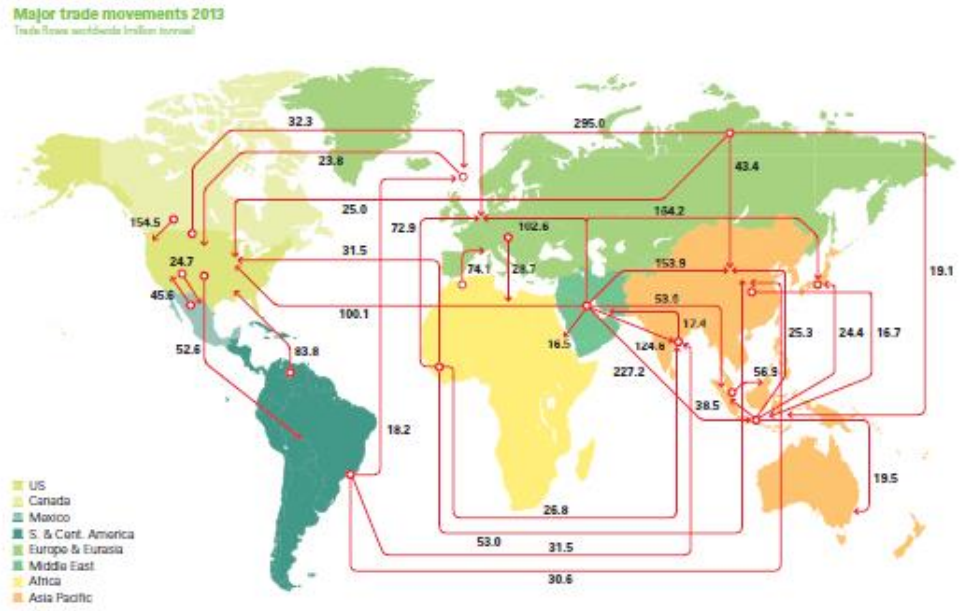

Figure 1-4: Oil trade movements British Petroleum Report [1]

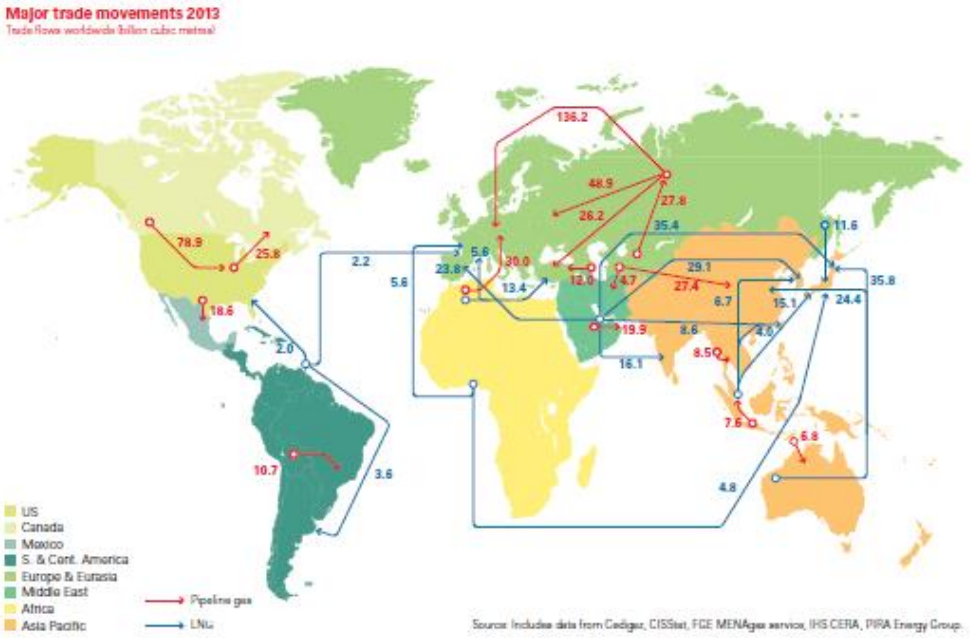

Figure 1-5: Natural Gas trade movements British Petroleum Report [1]

This induces on high economic dependence on others countries that are also politically unstable and can be seen as a threat from the world powers, creating not indifferent geo-political problems.

- **Effects of the usage**: Fossil fuel combustion releases products in the atmosphere which in part are toxic and in part are responsible of the greenhouse effect increase, mainly caused by the CO_2. The latter problem provokes a global warming: in the last hundred years an increase of the average temperature and of the sea level due to an improved thawing of the glaciers could have been observed. A first World reaction to the effects of fossil fuel can be found in the Kyoto Protocol where first long term objectives have been set. Europe set even a stricter objective that was recognized as the 20/20/20 objective since it foresees the achieving of three results by the 2020:
    1. 20% reduction of greenhouse gasses
    2. 20% renewable energy production
    3. 20% energy savings

    All the percentages are define with respect the 1990.

In view of these problems in the last years other means of production have been taken into account. The choice of the energetic source of a plant is not just an economical issue but also social and politic. The variables that drive a decision are not just cost and reliability of the plant but also availability of the resource and its environmental effect.

As underlined in the Kyoto protocol a way to fight the problems induced by fossil fuels is to exploit the production of energy by means of renewable sources. The definition of renewable energy is not trivial, to better define it we choose to use the definition adopted by the Texas Legislature:

> *"Renewable energy: Any energy resource that is naturally regenerated over a short time scale and derived directly from the sun (such as thermal, photochemical, and photoelectric), indirectly from the sun (such as wind, hydropower, and photosynthetic energy stored in biomass), or from other natural movements and mechanisms of the environment (such as geothermal and tidal energy). Renewable energy does not include energy resources derived from fossil fuels, waste products from fossil sources, or waste products from inorganic sources."*

We can notice how the number of technologies is consistent. Despite that, this field of study is still a challenge and above all the initial investment cost is still high. Anyway, we should always think about the future costs, as Nicholas Stern pointed out in [2]. In fact, according to his analysis, a future cost for solving the environmental damages due to fossil fuel abuse could amount up to the 20% of the world GDP while an investment in the renewable energies, now, could reduce the damage involving just the 1% of the GDP.

1.2 MARINE ENERGY, WHY WAVE ENERGY?

Our planet is for two third composed by water that actually is a huge tank of energy for now just slightly used. Quantitatively, as pointed out by the Marine Foresight Panel in a report, if we were able to exploit 0.1% of the renewable energy available from the ocean and convert it to electrical energy we would satisfy five times the world energetic requirements.

There are plenty of ways to exploit the intrinsic energy of the sea. We can divide these technologies in the following categories:

1. **Tide Energy:** The idea is to exploit the up-down movement of the tide due to the gravitational interaction between the water and the moon. The exploitation can be done by means of a dam that accumulates the water when the level is high. In this way, a geodetic head is obtained and can be exploited by a low head turbine connected to an electrical generator.

   Even if the geodetic head is not huge thanks to the volume of water and its density the amount of energy tends to be significant. The project of Tidalelectric would involve 60MW.

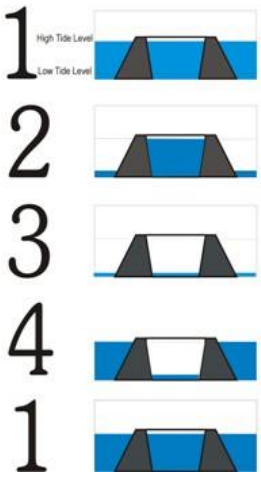

Figure 1-6 Tide energy principle

2. **Tidal Current:** The idea is to exploit the kinetic energy of the tidal movements inside the sea, this operation can be done by horizontal axis turbine, solution preferred for the constant current, or vertical axis turbine, preferred for the tidal current mainly because of the fact that the flow changes its direction of 180 degrees.

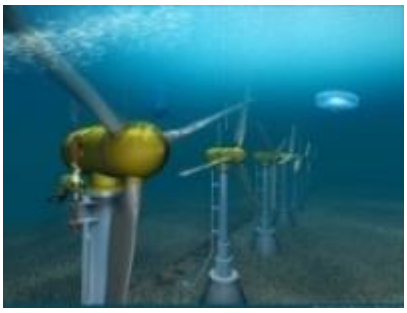

Figure 1-7 Tidal current axial turbines

3. **Ocean Thermal Energy Conversion:** The idea is to exploit the thermal difference between the sea surface which is warmed by the sun, 25/28 degree, and the bottom of sea which is colder, with significant depth 6/7 degree. This can create a thermodynamic cycle based on a low boiling point fluid as ammonia or fluorine. The difference in temperature should be at least around 20 degrees, so the depth jump should be consistence, around 600 m.

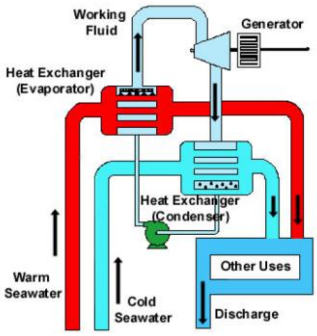

Figure 1-8 Thermal Plant Scheme

4. **Energy from the salinity gradient in the water:** the idea is to exploit the gradient of salt concentration between salty and sweet water, through a selectively permeable membrane. The energy comes from the difference of entropy between the salty and the sweet water. A steering process between the two waters, in fact, would release energy. In

particular, converting a salty water into a no-salty one, is an exothermic process, while passing from sweet to salty water is an endothermic. The way of producing energy can be done with two different technologies [3]:

- ***Pressure-Retarded Osmosis***: it aims to create a geodetic head by mean of the process of osmosis. The process consists in a transfer of water from a soft water tank to a salty water one, thanks to a selectively permeable membrane. This accumulation process generates a geodetic head that is then exploit to produce energy by means of traditional technologies.
- ***Reversed Electrodialisis:*** it aims to create a low voltage by means of migration of salt ions thanks to the osmosis process. It requires specific selectively permeable membranes.

5. **Energy from marine biomass:** the idea is to exploit the fact that the seaweed have a greater photosynthetic efficiency, with respect to the ground cultivations, and so they permit to generate more liter of bio-fuel that will be used to produce energy. The main advantage is that the production of the biomasses adsorb CO_2, as a secondary effect it can also reduce the greenhouse effect.

6. **Wave energy:** the idea is to exploit the movements of the waves so its mechanical energy (in various form) to generate energy. The technology adopted are of different kind and will be discussed in deep in the next section. Among these technologies the exploitation of wave energy is the better developed sector. In fact it has less location issues, since the waves

are present almost everywhere, and it has a lower implementation cost with respect to the energy density achievable as can be seen from this table took from [4] :

Resource	Power (TW)	Energy Density (m)	cost ($)
Ocean currents	**0.05**	**0.05**	**Medium**
tides	**0.03**	**10**	**High**
thermal gradient	**2**	**210**	**High**
Ocean waves	**2.7**	**1.5**	**Medium/High**
salinity gradient	**2.6**	**240**	**Very High**

Table 1-1 Marine energy cost/energy density

Wave energy can be considered as an indirect solar energy, since it derives from the wind action and the wind originates from the action of the sun. Despite wave energy is a product of solar energy, its energetic density, 2-3 kW/m^2, is greater than both solar, that has 0.2 kW/m^2, and wind energy, that has 0.002 kW/m^2. This can be attributed to the high density of the water particles and also from the fact that the generation of the wave is a process that involves a storage of wind energy. The waves in fact have been built up by the wind in a long period, and this is the cause of another advantage of the wave energy with respect to the wind energy. Waves, despite random as wind, have a more regular spectrum than the latter. This is possible because the waves can do long travels without significant losses. The main losses are due to the interaction with the sea bottom, so are stronger in seashore water [5]. Thanks to the storage effect, the production by wave energy is much more constant and available than wind and solar technology. It can reach a reliability of 90% versus a 20/30% of wind and solar energy. Moreover these plants do not have any

environmental impact and, differently by the wind turbine, wave power plant would not deface the landscape.

On the other side there are also drawbacks to deal with. In fact the waves as anticipated is a statistical phenomenon that is characterized by an energy spectrum, in particular a wave can have different phase, amplitude and frequency. Despite this variation is lower than the wind one, it is still difficult to design a system whose performances are great in all the condition. The control design mainly deals with this problem. Another difficulty in the controller design is given by the strong difference between the waves frequency, 0.1 Hz, and the required frequency of the grid, 50 Hz, (required for the best performance of the electrical machines). In addition to that, the environment where these plants are located is not favorable. Storms can highly solicit the structure, since the energy density can be up to 2000kW/m, so the infrastructure requires a greater investment cost. This is not the only higher cost, since in addition, in fact, we must consider the maintenance cost higher due to a corrosive environment and plant location (it might be offshore or underwater).

Summing up the pro and the cons of the wave technology are in the following table:

PRO	CONS
High Energy Density (2-3 kW/m^2)	Variable Phenomena
Higher Regularity Than Wind	High Investment Costs
Reliability UP to 90%	High Maintenance Cost
Low environmental impact and deface	Difficult Wave Grid Interaction

Table 1-2 Wave technology PRO and CONS

1.3 CLASSIFICATION OF WAVE ENERGY TECHNOLOGY:

We have seen what the pro are and cons of this kind of energy; let us now concentrate on its distribution around the world. When we talk about distribution we consider the power one, since it is an energy that comes directly from the nature and not from raw material. As we can observe in the map below [Figure 1-9] this distribution is inhomogeneous, the exploitable power hence is not the same in every seashore.

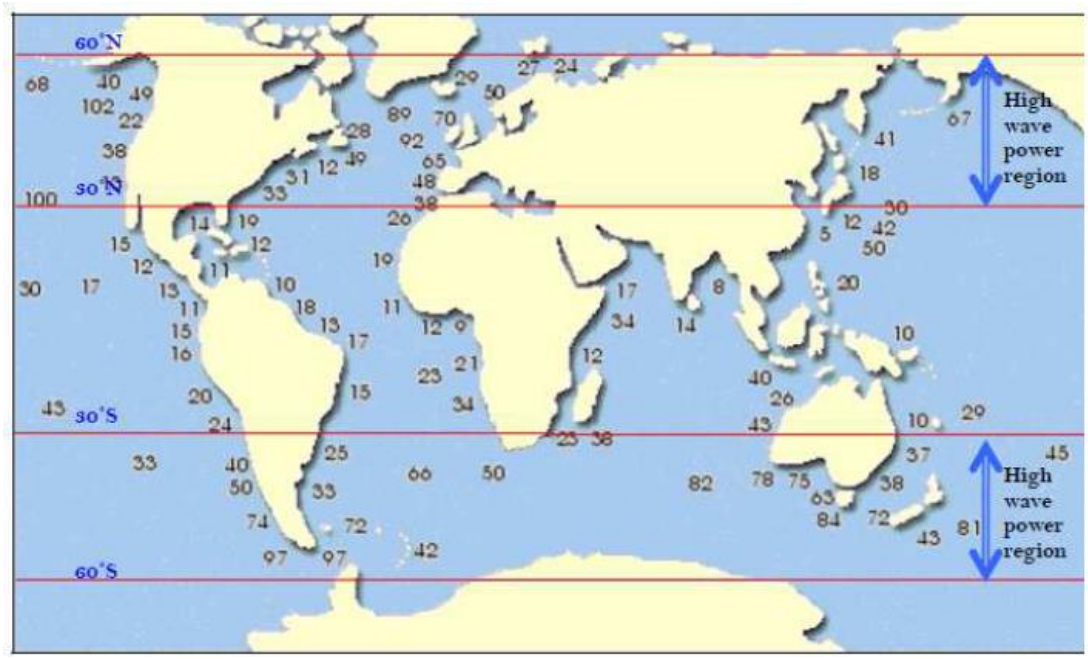

Figure 1-9: Power distribution at the global level (kW/m)

We can see how the most intense activity is concentrate in the zones between 30 and 60 degrees of latitude in both the hemispheres. This is due to the particular strong winds that blows from west in these areas. Intense activity can be seen nearby the New Zeland and South America and Antipode. Luckily

Europe shows in the North-West shoreline intensive activity, Especially in the coast of Ireland and Scotland where the density reach 75 kW/m, and Norway where it reach 30 kW/m. Going south considering so the Mediterranean sea we have activity that oscillates between 4 and 11 kW/m. In the southern point of Europe, Canarias Islands, we have a density of 25 kW/m. Considering all Europe we can estimate a total available power of 320GW.

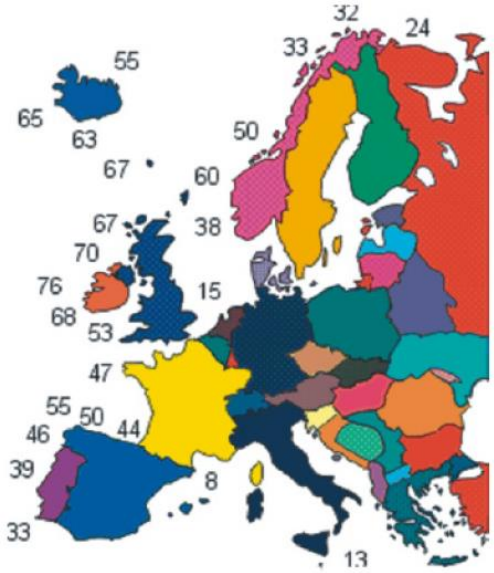

Figure 1-10 Power distribution at the European level (kW/m)

It is proved [6] that the linear power of the waves is proportional to the Time Period and to the square of the amplitude through the following formula:

$$P = \frac{\rho g^2 h^2 T}{32\pi} [W / m]$$

The plants that converts wave energy into electric energy are called Wave Energy Converters (WECs) systems. In order to do that, they always use a

Power Take Off (PTO) system which is the core device that accomplishes the conversion. It is possible to divide these technologies into spread categories; they can be divided not just on the type of PTO but also on location and kind of installation.

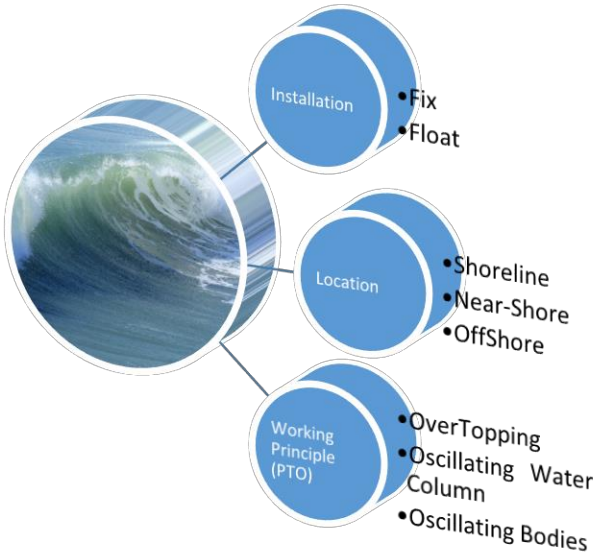

Figure 1-11 Technology Classification

Let's explain briefly the first whole classification:

- **Installation:** Installation indicate how the main moving part is connected to the ground, in fact we can have two different situations
    - ***FIXED:*** the main part of the plant is rigidly connected to the heart, this kind of plant are more common low depth water.
    - ***FLOATING:*** there is not rigid connection with the ground and the hydrodynamic force sustains the plant.

- **Location:** The location indicates the position of the plant with respect the shoreline. More a plant is distant higher will be the maintenance cost due to the needs of boats and deep water operation, in addition to that also the structural (investment) cost will be higher, in fact the distance from the shoreline is connected to the water depth, where, as stated before, extreme operation conditions might occur. The plant hence should be designed to face and withstand these conditions. On the other side the productivity of the plant will be higher.
    - ***SHORELINE:*** These plants are basically installed on the shoreline. Geological, geometrical and architectural consideration must be done in depth. However, these are the plants with less maintenance cost.
    - ***NEAR-SHORE:*** The power of these plants is still not the highest, they might be still fixed structure. A plant fall in this category if is not on the shore and if the fundal has depth less than a quarter of the wavelength.
    - ***OFFSHORE:*** These are the most energetic and expensive ones. They are always floating. To define an offshore plant we must watch at the depth of the water, the usual convention is given by a depth greater than 40m or of 1/3 of the wavelength.
- **Technology:** The classification is based on the how the wave energy is exploited in order to send the electric energy to the grid, is so based on the PTO. In general we will see that there are plants where there is a direct contact between the waves and the PTO and others in which there isn't. In the former the PTO itself may influence on the interaction with the water.

- ***Overtopping:*** These technologies aims at capturing the water in a reservoir in order to create a separate tank with a higher geodetic level. In this way, opening a channel with a low head turbine would permit an energy conversion. In addition to the reservoir that is connected to the water level through a slope (overcome by the wave inertia) there might be some reflector that helps conveying the water towards the slope. These plants may be fixed (Tapchan in Norway) or floating (Wave Dragon in Denmark).

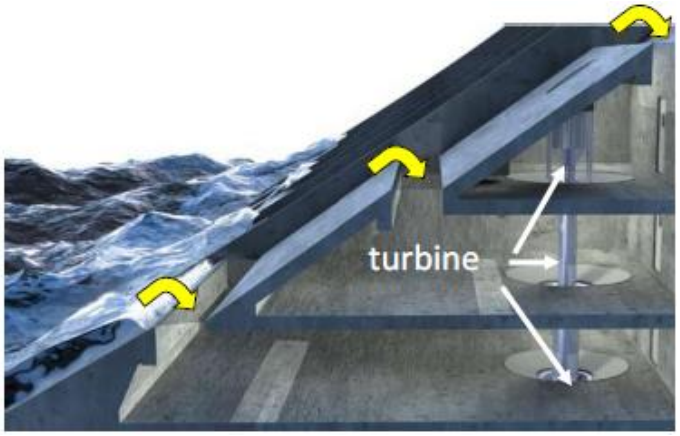

Figure 1-12 Tapchan Plant

Figure 1-13 Wave Dragon

The Tapchan plant consist on a reservoir on a cliff (is so a shoreline plant) 3 meters above the average see level. The project

started in 1985 from a prototype that produced 350kW, it presents a reflector that has an opening of 40 meters and a length of 170, the kinetic energy of the water overcomes the potential gradient and the almost null friction.

The Wave Dragon instead is an offshore floating plant, it also contains two reflector arms and in order to convert energy it uses Kaplan turbines. It has a low maintenance cost tanks to the intrinsic stability of the plant also in adverse condition but the construction and installation costs are high. The total weight is around 30 KTons and an installation of 7MW is foreseen.

- ***OWC:*** This technology exploit the movement of the water in order to create a flux of air through a channel with an air turbine installed. It's easy to understand the necessity of a special air turbine that spins always in the same direction despite the direction of the air (Wells turbine). These kind of plants can also be fixed or floating. We are going to provide two examples, one of each.

  An example of a fixed plant that actually is connected to the Spanish grid is the Mutriku Energy Plant.

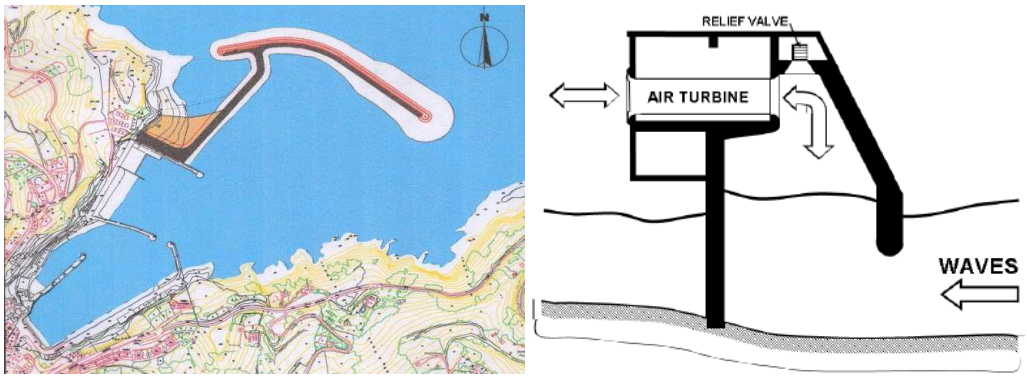

Figure 1-14 Mutriku Energy Plant

When the waves have a peak the air will be pushed to cross the turbine while a wave valley will recall the air back. The principal cost is due to the civil construction of the plant. Very often integrating the plant structure into a preexistent breakwater system permits to share the costs, both of maintenance and of installation. This cost optimization has been adopted in Mutriku that is actually a breakwater OWC with 16 chambers and 16 Wells turbine of 18.5 kW each.

An example of a floating plant is given by the Mighty Whale which was developed in Japan. A full size prototype was tested, the floating structure is 50m long 30m wide and 12 meter deep, It contains three air chambers connected to a Wells turbine. The total power of the prototype is 110 kW.

Figure 1-15 Might Whale Prototype

- ***OSCILLATING BODIES:*** As can be inferred from the name of the technology the idea is to use the movement of an oscillating body and convert it into electric energy. This conversion could be direct (Direct Drive) or can comprehend a hydraulic system as an intermediate medium. In the latter case the motion of the oscillating body is exploited to pump a fluid into a hydraulic motor which is connected to a generator. There must be systems either mechanical or electrical that manage to convert the slow frequency of the waves into the proper one. These devices are the most spread and studied among the WEC technology due to the simplicity of the concept that stands behind them.

  There are more kind of movements that can be exploited, as a rigid body the floating object has six degree of freedom whose names are shown in the picture below. The x axis usually is taken parallel to the main wave direction:

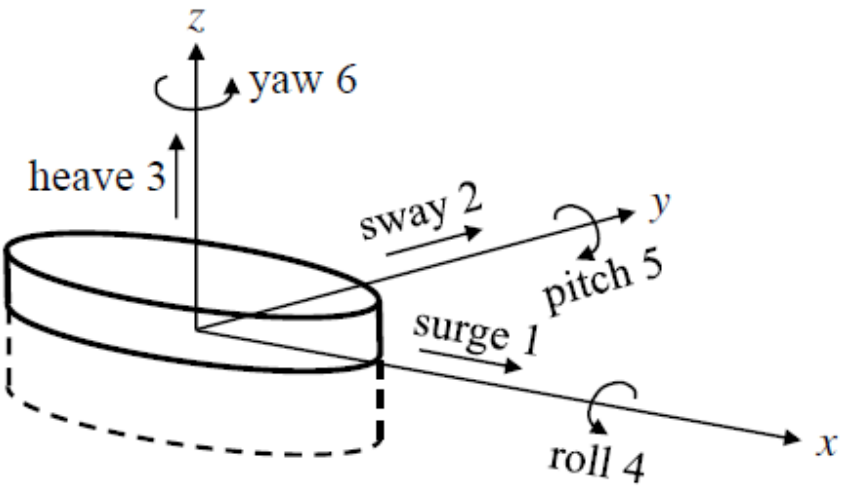

Figure 1-16 Degree of Freedom of a body in the sea

Differently from the other two technologies the classification is more diversified. Since we spoke about degrees of freedom we can create a classification based on the kind of motion that is exploited to produce energy. It might happen that more than one degree of freedom is exploited to generate energy, or that despite the body has more than one degree of freedom available, just one of these is effective for the generation. The three main ones are:

- *Heave:* This is the Up-Down movement with respect to the bottom of the sea, we will see that this kind of movement presents a phase delay with respect to the wave.

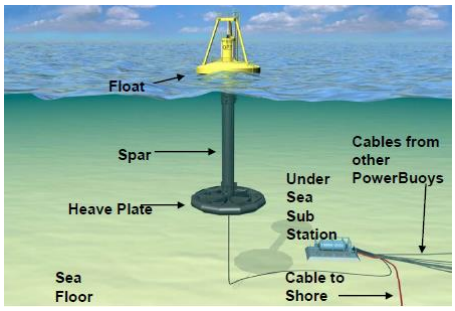

Figure 1-17 Reedsport OPT

There are plenty of plants based on this technology. The example we report is the Reedsport OPT wave park, developed in Oregon, USA, from the Ocean Power Technology company. This device exploit the heave motion of a float to pump oil into a hydraulic motor through a hydraulic cylinder. It produces 150kW.

- *Pitch-Surge:* Is the movement Backward-Forward following the main direction of the waves. This is achieved mainly through a pitching motion of the device which is hinged into the ground. An illustrative example is given by the Oyster plant in Scotland. A buoyant flap is hinged into the ground and through its oscillations activates hydraulic rams, which pump the fluids that will undergo a hydraulic circuit which is extended till onshore, where the same fluid hits an impulsive turbine (Pelton) connected to an asynchronous generator. A large prototype was built in 2009.

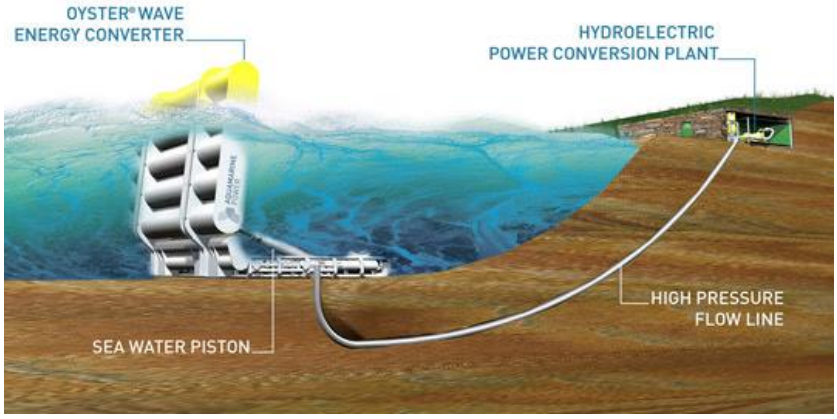

Figure 1-18 Oyster WEC

Another example of pitching motion (in this case pure pitching) is the Duck plant whose working principle will be described later, when we speak about the classification based on disposition of the plant with respect the wave direction.

All these device can exploit a relative or absolute motion, that's why we can divide them also in:

- *Single Body:* the energy comes from the absolute movement of one floating body with respect to the ground (it is so fixed). A significant example is the device developed by the Uppsala University, in Sweden, which exploits the heavy motion of a buoy to move a linear electric generator connected to the ground. We can observe from the image how the system works. The fact that there is no hydraulic circuit makes the system more efficient, since the flux of energy undergoes less conversion proecesses. This might be compared with the Archimede Wave Swing, which will be introduced later. For this kind of device the procedures to adjust the mechanical frequency to the electrical one must be more accurate and sophisticate, since it does not use hydraulic accumulator to regulate the flux of energy.

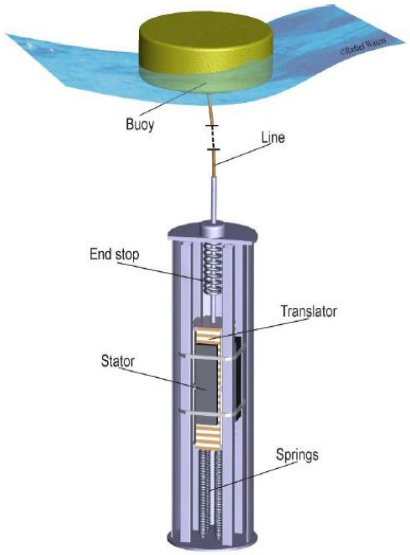

Figure 1-19 Uppsala Power-Buoy

- *Double Body:* the device exploits a relative motion between two floating bodies. There might be a body that is smaller

than the other and whose resonance frequency approaches the wave one. This body moves more than the bigger one and the energy is extracted from this movement. One example is the Acqua Buoy, which is an evolution of the IPS buoy, developed in Sweden by the company Interproject Service. The buoy is connected to a tube which is completely submerged under the water. The relative motion between the tube and the buoy drives a piston which pumps the water towards an onshore Pelton turbine.

After the description of this category we can conclude that floating plants always exploit relative motion (despite the motion can be approximated with the absolute motion of the absorber, which is smaller). The system though might have more bodies of the same dimension and exploit their relative motion (Wave Dragon or Salter's Duck, examples made later).

The classification carries on considering how these apparatuses are positioned with respect to the sea surface, they might be:

- *Submerged:* they are completely underwater, this means that they are connected to the ground and cannot be positioned offshore due to water depth. They suffer less extreme conditions being underwater. The working principle is mainly based on Stevin law: considering a point in deep

water the pressure will vary because of the changing amount of water above it. A significant example of these kind of plants is a project that was developed in Holland and that now is abandoned. The plant was the Archimede Wave Swing (AWS), and consists in two main structures: an oscillating upper part (connected to the floater) and a bottom fixed part (basement). The difference in pressure drives a linear electric generator which is set inside a cylinder which contains air whose pressure acts as a spring. The image below describe shows the structure.

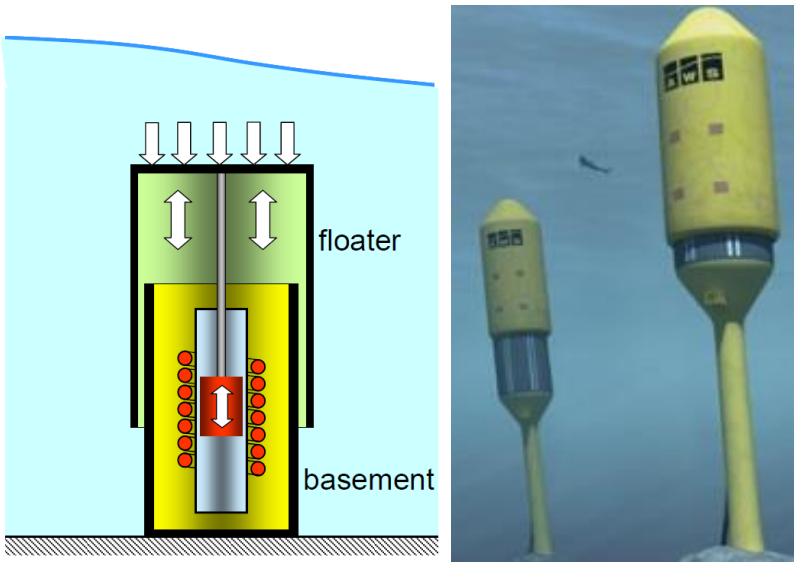

Figure 1-20: AWS structure and working principle

- *Floating:* These devices floats on the water and moves thanks to the waves kinetic energy. There are really plenty of

examples, and we have already introduced some of them (Reedsport, Uppsala Power Buoy, Oyster). To provide another example which is significant, we can introduce the plant that will be the center of our work. The plant is the Wave Star plant, and it's sending energy to the Danish grid, in the city of Nissum Bredning Fjord. We will deeply describe this plant and develop a model of it. For the time being we just classify it as a floating oscillating body technique, which uses a semi sphere shaped body to convert wave energy. This motion is used to pump oil through a piston into a hydraulic motor, which drives a generator.

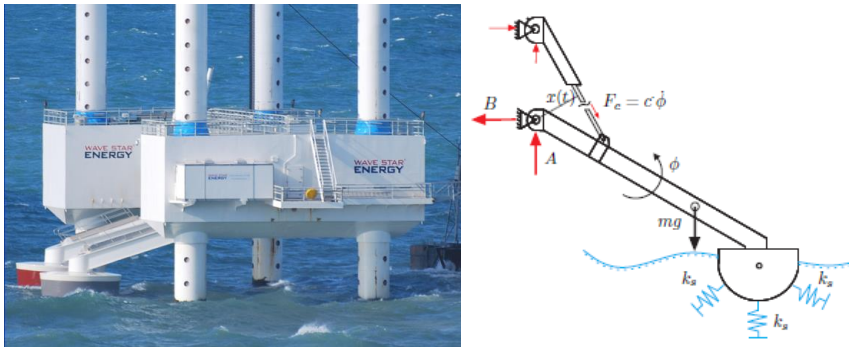

Figure 1-21: Wave Star Energy Plant

Another classification can be done looking at the disposition of the body with respect to the wave direction:

- *Attenuators:* the main direction of the waves is parallel to the main axis of the structure. One clear example of this technology is the Pelamis Plant, which is located in the

Portuguese cost and which was developed in UK. It consists in a series of 5 connected floaters, which through their movement activates the usual hydraulic circuit composed by a hydraulic piston, which absorb the curvature movements between the floating bodies, and a hydraulic motor, that aliments the generator. The plant as previously described extends perpendicularly to the main wave direction, for a length of 150m, and it produces 750kW. An image of the plant and of the connection between the bodies are provided below.

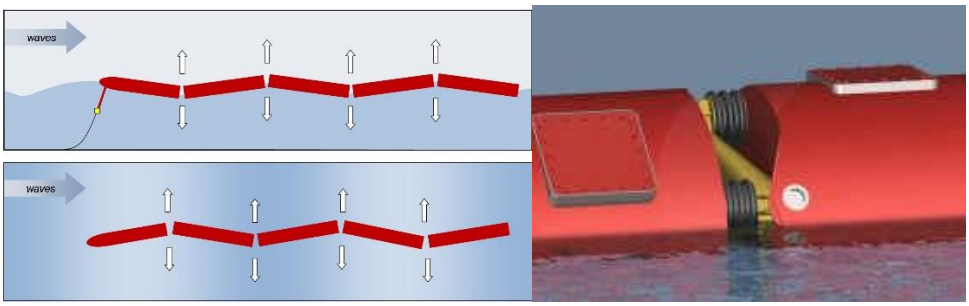

Figure 1-22: Pelamis Plant structure

- *Point Absorber:* the dimension of the body is smaller compared to the wave characteristic length, so all the direction of the waves produce an energy absorption. Most of the plant we introduced are point absorbers, like the Uppsala power buoy, the Reedsport wave power plant, and the same Wave Star Power Plant. We can provide another example that is the project of the company Ocean Power Technology, which was a Powerbuoy that was experimented at the US Marine Corps Base in the Hawaii. It has a 12 feet diameter and it's 55 feet long. The aim was to reduce the fossil fuel consumption at the Navy base and around it. The concept is the same: producing energy through the heave movement of a buoy. The plant is floating, and it was actually the first wave plant connected to the grid in USA.

Figure 1-23 OPT Powerbuoy

- *Terminator:* the main axis of the body is perpendicular to the wave direction. Due to their disposition, they act as breakwaters devices, so the waves by passing them loses almost all its energy. An example is given by the Salter's Duck buoy, a project developed by the University of Edinburg in Scotland. It consists in a string of ducks mounted in a line which is perpendicular to the main wave direction. The floating body are cam-like shaped, and their pitching motion is exploited to produce make four gyroscopes move and produce mechanical power directly available for a system of pump, which drives a hydraulic motor connected to a generator.

Figure 1-24 Salter's Duck buoy

1.4 DECISION PROCEDURE:

We have discussed the variety of technologies that can be used to produce energy by means of waves. Due to the financial crisis of the 2006 a lot of project were abandoned due to arise of founding problems. In fact, like all the

renewable energies wave energy requires high capitals to be invested in the R&D. Moreover, some projects are still prototypes that are subjected to basin tests or are even just subjected to the mathematical validation. Among all these projects, we had to decide where to apply our modeling and control design procedure.

Thanks to the U.S. Department of Energy and OpenEI [7] we were able to define, even if in an unassured way (as pointed out by OpenEI) which was the phase of the project. The phase of a project identifies the state of it: phase 0 means undeveloped while phase 4 means deployed. The table below precisely identifies the meaning of these phases. The graph instead tries to give a project distribution on the phases.

Phase	Definition according to [7]
Phase 0-Undeveloped	Projects that either had a specific site permitted or in the permitting process, but were later surrendered.
Phase 1-Siting/Planning	Projects and their respective companies' technologies that are not yet in the water, but may have applied for or already received a permit/license, or may be conducting environmental site assessments.
Phase 2-Site Development	Projects and their respective companies that have selected a site and begun site preparations (e.g., installation of a sub-sea cable).
Phase 3-Device Testing	Projects where devices are undergoing or have undergone testing/commissioning before deployment.
Phase4-Deployed	Commercial projects that have been completed with all device units in water, or past commercial projects that have had a removal of all devices and environmental remediation.

Table 1-3 Technology Phase

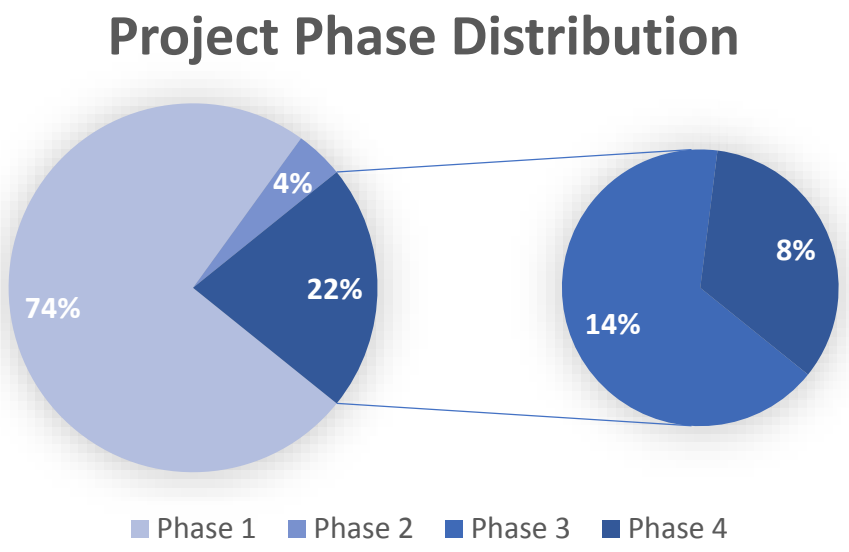

Figure 1-25 Actual Project Status

By this definition of phases we can immediately observe how the two main interesting phases are phase 3 and phase 4, in fact by choosing projects that appertain to these two phases we can produce a more useful analysis and design a controller that could be implemented on these devices.

Identified the phases that were more interesting in for our modeling and design purposes, we had to deeply analyze the database containing the project information trying to actualize them. We found a total of 330 projects among which to choose, but among those just 71 passed our first filter based on the phase. As we can see from the Graph above just the 22% of the projects passed the first filter. After that we applied this preliminary filter we decided to analyze the condition of the project. This phase consisted on validation of the data contained in the OpenEI database. Some of the information in the database, such as Company Name or even Location, were inaccurate or outdated. Moreover due

to the high investment done by some private organization, on some project, the information available to some of these projects were too limited and was impossible even to determine the basics information.

Applying this second filter we found out that of these 71 projects just 15 were active and at least slightly documented. Continuing the filtering of the projects we then concentrated on the quantity of documentation. We want in this project develop a model that given as an input a wave spectrum will give as output the energy produced by our system. This means that we must have the most of all the specific information about all the components. These lead us to decide among just 3 projects that will be described below.

In a graphic way our filtering reasoning can be represented by this graph:

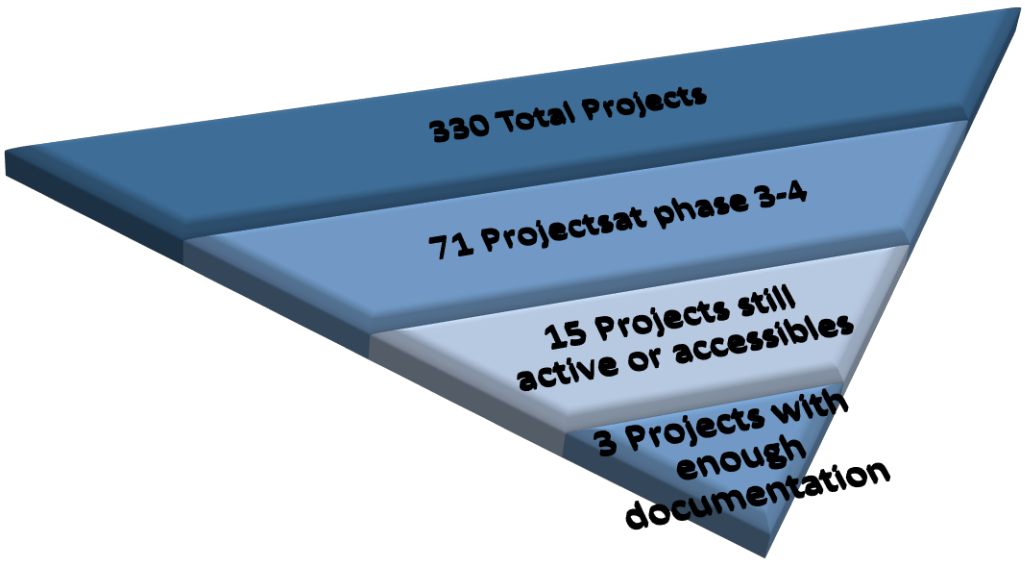

Figure 1-26 Selection of the Plant

1. ***REEDSPORT OPT WAVE PARK:*** This project is on phase 4 and is installed in Oregon (USA), it is characterized by the PowerBuoy technology and mainly founded by the Ocean Power Technologies. The technology consist in a floating point absorber that through the movement of the floating object pumps oil into a hydraulic motor. The latter is connected to the electrical generator that will transmit the created energy to a common transformer, for all the buoys, that makes possible the connection to the grid.
2. ***MUTRIKU WAVE ENERGY PLANT:*** As for the OPT Wave Park this project is on phase 4 and connected to the Spanish electrical grid. The project is based on OWC Breakwater technology. The presence of the breakwater made possible a lower impact on the cost of the plant. It uses 16 Wells turbine of 18.5 kW as maximum power to exploit the interaction between the water column and the air. The control mainly is done in order to avoid the stall of the Wells turbine while a AC/DC/AC conversion is done to take care of the different frequencies of the waves and the frequency required by the grid.
3. ***WAVE STAR ENERGY PLANT:*** This plant is on phase 3 but a phase 4 structure is ongoing building. The idea is simple: an arm with a buoy is floating into the sea and is connected to the fixed main structure. The relative motion between the two structures is used to pump the fluid into a hydraulic motor that is connected to a generator and will hence provide the energy conversion. The full size plant will have 20 floating arms and could reach a power generation of 640 kW with a conversion efficiency above 70%. Also here a AC/DC/AC conversion occurs.

Among these three project we decided to analyze and design a control for the Wave Star Energy Plant. This decision was taken thanks to the great availability of data[8] and a direct interaction between PTO and waves. Moreover we might be able after the modeling of the system and the design of the controller to verify the goodness of the model.

2 SECOND CHAPTER: MODELING AND MODEL VALIDATION

2.1 OVERVIEW OF THE WAVESTAR WEC:

The WaveStar C-concept is a multi-absorber WEC. It consist in semi-submerged hemispherical floats mounted on separate arms. These arms are hinged to the main structure that is resting on the sea bed through monopole foundations.

As was hint in the introduction an important characteristic of a WEC is given by the fact that it must resist unexpected and rare storms, that have an energy density much higher than the one in normal operational conditions, and that usually leads to an over dimensioning of the components. This characteristic is achieved in the WaveStar by the possibility of lifting out from the water the floats and in case of extreme condition the main platform body. This means that the PTO systems can be designed just for production stresses.

Figure 2-1 Wave Star in Production and Storm Protection

In view of the fact that waves frequency are very low the floating bodies can be filled with 15m^3 of water so that the natural frequency of the PTO system is inside the frequency band of the waves excitation, maximizing the energy production [3.1.2].

We can now model the PTO system that is composed by three main parts:

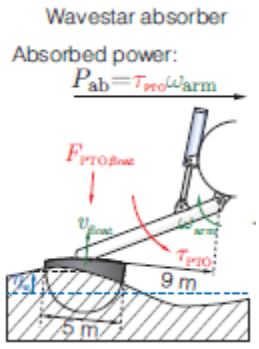

Figure 2-2 PTO Scheme

- The Waves by means of moving the floating body will induce a force on the Hydraulic Cylinder that will pump a low pressure fluid into an high pressure accumulator

- The high-pressure accumulator is connected through hoses and a hydraulic fixed displacement motor to the low-pressure accumulator. The hydraulic motor exploits the difference in the pressure head to produce a hydraulic torque.

- The Hydraulic torque is the exploited by the Electrical asynchronous generator connected to the grid through an inverter to produce energy.

We must then connect cinematically the movement of the floating body with the displacement of the cylinder; in fact, this relation will connect the input given by the waves with the hydraulic system, which is the responsible of the conversion of mechanical energy into hydraulic one.

2.2 SOLVING THE KINEMATIC:

An overview of the structure can be observed in the next figure. The Main Tube represents the fixed structure for the next generation prototype WaveStar C5 that is composed by 20 absorber. We can observe how the floats can be represented as a sphere with a truncated cone upper part. The sphere is of a glass-fiber structure that, as hinted before, will be filled with 15 m^3 of water when in energy production configuration, while will be emptied in storm protection. The PTO cylinder is characterized by a maximum 3 meters stroke, this means that approximately the power production configuration will be used just for sea states corresponding to a maximum significant wave height of 3 meters.

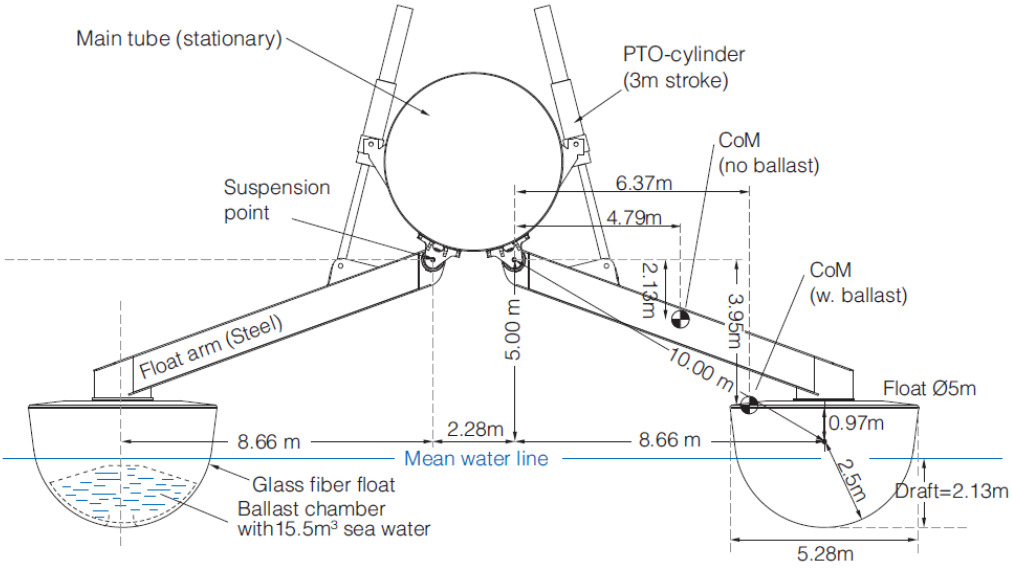

Figure 2-3 Mechanical System Layout Front View

Understood the main design we can proceed defining the reference frame that we are going to use to solve the kinematic. The angle ϑ_{arm} is defined as the

angle between the x axis of frame {A} and {B}. Frame {A} is rotating with the arm, while frame {B} is fixed and has the origin in the hinge. The ϑ_{arm} is defined positive counterclockwise (see next figures 2-4, 2-5) and will be null when the cylinder stroke is equal to $x_{c,0}$; that will be considered as the equilibrium position in this project. We can so define the link between the rotation of the arm and the cylinder stroke by considering the following links thanks to the Law of cosines, in fact given that when $\vartheta_{arm} = 0 \rightarrow x_c = x_{c,0}$ we can write:

$$\left.\begin{aligned} \left(x_{c,0}+c_c\right)^2 &= a_c^2+b_c^2-2a_cb_c\cos\left(\gamma_{c,\vartheta=0}\right) \\ \gamma_{c,\vartheta=0} &= \cos^{-1}\left(\frac{a_c^2+b_c^2-\left(x_{c,0}+c_c\right)^2}{2a_cb_c}\right) \end{aligned}\right\} \rightarrow x_c = -c_c+\sqrt{a_c^2+b_c^2-2a_cb_c\cos\left(\gamma_{c,\vartheta=0}-\vartheta_{arm}\right)}$$

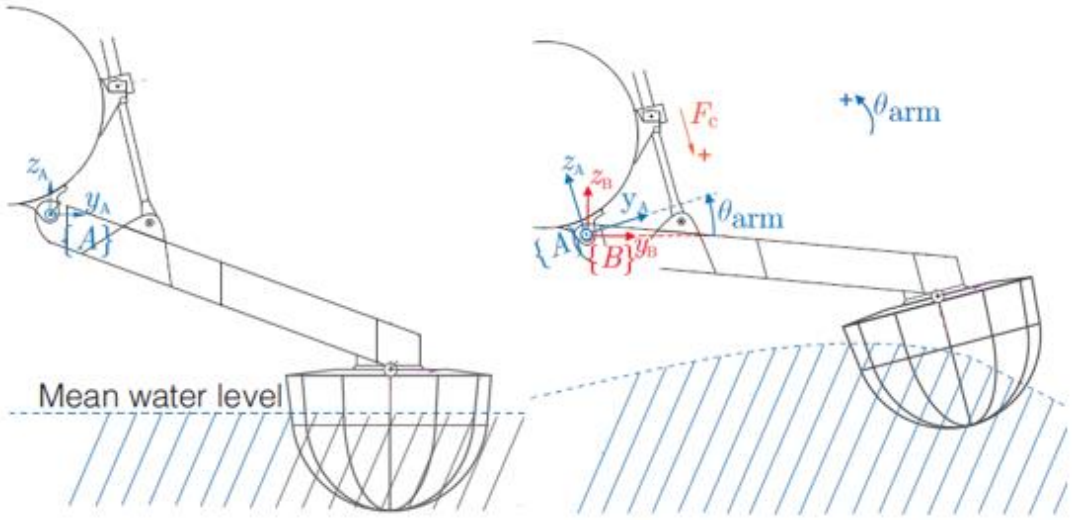

Figure 2-4 Frame definitions

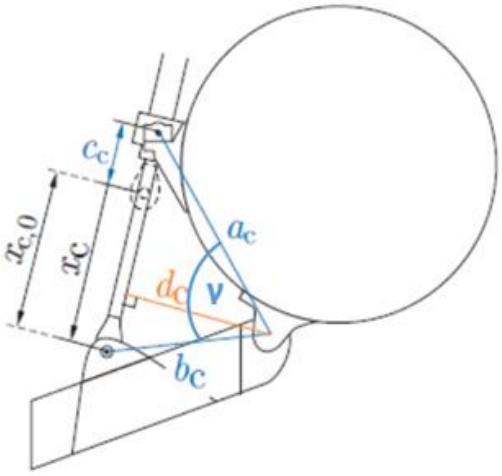

Figure 2-5 Crank and slotted link

Another important dimension to define is the cylinder's moment arm d_c, in fact it will be the necessary dynamical link between the PTO force and its torque.

The link is not difficult to find, in fact by considering the area equality:

$$d_c\left(x_c + c_c\right) = \frac{2a_c b_c \sin\left(\gamma_{c,\vartheta=0} - \vartheta_{arm}\right)}{2}$$

We obtain that:

$$d_c = \frac{a_c b_c \sin\left(\gamma_{c,\vartheta=0} - \vartheta_{arm}\right)}{\left(x_c + c_c\right)}$$

In paragraph [2.4] we are going to describe the dynamics in terms of the angle ϑ_{arm}, so it can be very important to achieve in this paragraph also some relations based on the time derivative of x_c and ϑ_{arm}.

As we will see in paragraph [2.5.2] we are going to neglect the inertia of the cylinder, this means that the driving equation of the cylinder dynamic is based just on the velocity $\dot{x}_c$ that will be achieved here:

$$\frac{dx_c}{dt} = \frac{d\left(f\left(\vartheta\right)\right)}{dt} = \frac{dx_c}{d\vartheta}\frac{d\vartheta}{dt} = \frac{-a_c b_c \sin\left(\gamma_{c,\vartheta=0} - \vartheta_{arm}\right)}{\sqrt{a_c^2 + b_c^2 - 2a_c b_c \cos\left(\gamma_{c,\vartheta=0} - \vartheta_{arm}\right)}}\dot{\vartheta}_{arm}$$

We have now all the kinematical link necessary to characterize our model.

2.3 WAVE MODEL:

The complex wave phenomena may be classified as stationary (within a certain time limit) and ergodic phenomena. This means that to characterize the phenomena we need to define a PSD (Power Spectrum Density function) that requires two inputs [9]:

- H_{m0}: *Significant wave height* that is defined as the average wave height of the one-third highest waves, is computed from wave through to wave crest.
- T_p: *Peak wave period* so the wave period where most energy is concentrated, considering that a period is computed as two zero down crossing of the mean water level.

The choice of the PSD is highly site dependent and may show changes, however two main spectrum are used in literature, the Pierson-Moskowitz (PM-Spectrum) and the JONSWAP Spectrum.

The PM spectrum describes a fully developed sea, so that the wind effect has reached a regime condition, it has blown long enough and on a large distance. The JONSWAP Spectrum instead was developed by the offshore industry the characterize waves in the North Sea. The North Sea being narrower than other seas gives shorter distance to the wind to fully develop a wind-wave equilibrium, it has so a peak-enhancement factor that concentrates energy in a narrower band.

The two spectrum can be mathematically represented as it follows [10]:

$$PSD(\omega) = H_{m0}{}^2 \alpha \left(\frac{\omega_p}{\omega_n}\right)^5 e^{-\frac{5}{4}\left(\frac{\omega_p}{\omega_n}\right)^4} \gamma^{\beta}$$

where:

$\omega_p = 2\pi / T_p$ $\omega_n =$ general pulsation

$$\alpha = \frac{0.0624}{0.23 + 0.0334\gamma - \frac{0.185}{1.9+\gamma}} \qquad \beta = e^{-\frac{\left(\omega_n/\omega_p - 1\right)^2}{2\sigma^2}}$$

$\sigma = 0.07$ for $\omega_n < \omega_p$ $\sigma = 0.09$ for $\omega_n < \omega_p$

$\gamma = 1$ PM-Spectrum γ=3.3 JONSWAP

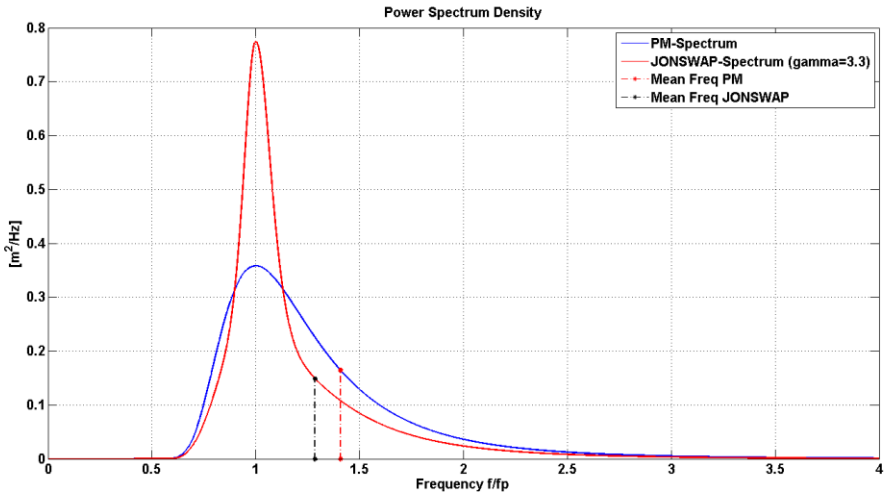

Figure 2-6 Different Wave PSD

We can observe by plotting the two spectrum that the JONSWAP has a narrower peak band as said before. This means that since the final objective of this final work is to design a controller for the WaveStar WEC we can use the PM

spectrum, in fact it will require a higher flexibility of the control strategy to ensure an optimal energy extraction.

Once we have characterized the type of spectrum that we are going to use we must also define how to use it to create random waves conditions.

2.3.1 Random Phase Method:

A straightforward method can be implemented thinking about the definition of the power density spectrum. In fact, the power density spectrum identifies the power associated to a frequency band equal to the frequency resolution. This means that given a sinusoidal signal of amplitude A sampled with a resolution Δf the Power density spectrum is defined as:

$$PSD = \frac{S_{AA}}{\Delta f}$$

Where S_{AA} is the auto spectrum of the signal. The auto spectrum however considers also negative frequencies, we need to get rid of it. To do that we can double the power associated with the positive frequencies (except at 0 where the power associated is correct).

The auto spectrum of a simple sinusoidal signal $A(f) = C\cos(2\pi f\ \mathrm{t}) = \frac{C}{2}e^{i\omega_n} + \frac{C}{2}e^{-i\omega_n}$ can be computed as:

$$S_{AA} = A^*(f)A(f) = \frac{C}{2}e^{-i\omega_n}\frac{C}{2}e^{i\omega_n} = \frac{C^2}{4}$$ for both positive and negative frequencies.

This means that the amplitude of the sinusoidal wave can be represented as:

$$\left|\eta_{w,i}\right| = \sqrt{2S_{PM}\left(f_i\right)*\Delta f} \rightarrow \eta_{w,i}(t) = \sqrt{2S_{PM}\left(f_i\right)*\Delta f}\,\sin\left(2\pi f_i t + \delta_{rand,i}\right)$$

As we can observe the phase is random and is computed for each frequency taken into account, while the amplitude is defined in order to respect the Spectral power of the PM spectrum. By plotting the results:

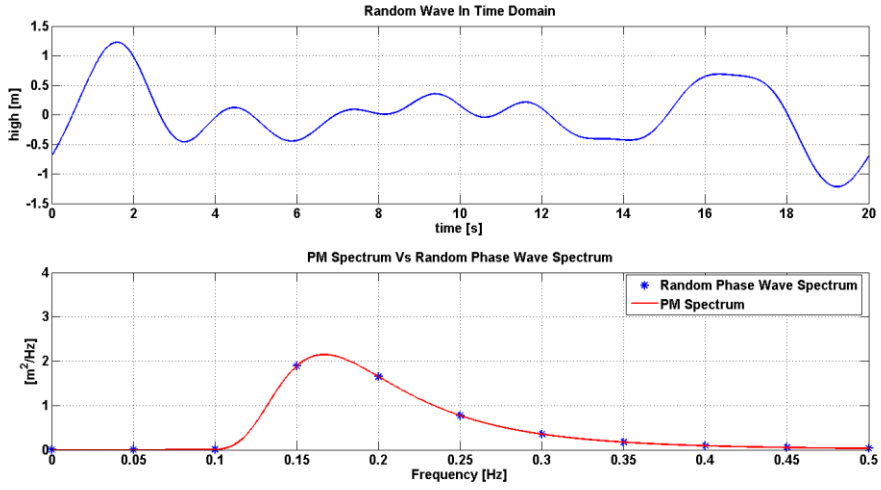

Figure 2-7 generated wave and wave spectrum

As we can observe from the above figure, the PSD of the random phase wave, after transforming again, respects exactly the PM Spectrum.

This method can be sufficient to compute the average power absorption as shown in [11], while does not reproduce wave grouping and is not able to show fluctuation around the target spectrum as observed in the reality.

However for our control purposes, we are mainly interested to the power production, which implies that this model is satisfactory.

2.4 CHARACTERIZING THE DYNAMIC OF A SINGLE ARM:

Let's firstly just consider the dynamic of a single arm, the incoming wave forces will act on an application point that is the origin of the frame that is placed in the barycenter of the floating object. The angular displacement of the arm will be affected by three mains torques, in fact the arm will produce a torque due to the gravity field, a torque due to the presence of the PTO and finally the "driving" torque given by the wave/body interaction. This can be graphically represented as it follows:

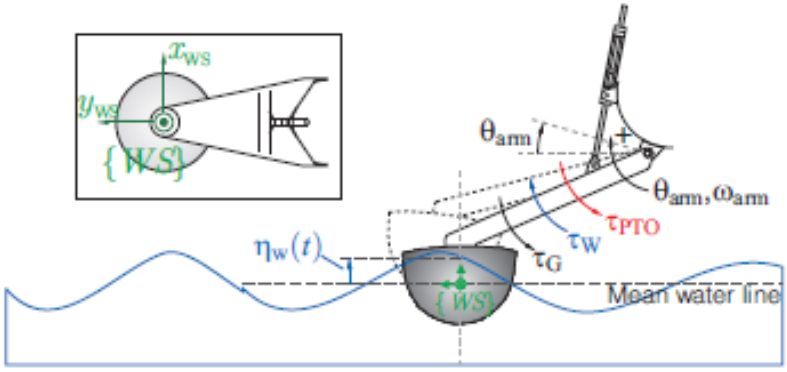

Figure 2-8 Graphical Representation of the Buoy

The dynamical equilibrium will be so given by:

$$J_{mech}\ddot{\vartheta}_{arm} = \tau_{wave} - \tau_{gravity} - \tau_{PTO}$$

The τ_{wave} will be obtained considering the linear wave theory, this theory is valid for gravity waves, so waves induced by the action of the wind blowing

over the water surface and in which the restoring force is given only by the gravity field. This theory holds under some specific assumptions in fact we consider that:

- The viscous forces and other are negligible
- The flux is irrotational
- The fluid is incompressible

Given these three assumptions and by means of the mass conservation we can conclude that the motion of the particles must satisfy the Laplace Equation:

$$\frac{\partial^2 \Phi}{\partial x^2} + \frac{\partial^2 \Phi}{\partial y^2} = 0$$

That can be solved adding conditions such as:

- Particle velocity at the surface must be equal to the free surface velocity
- Particles must have a normal velocity with respect to the ground and to the buoy null (impermeability condition)
- Pressure at the surface must be equal to the atmospheric one

The linear wave theory has limitation, in fact is valid just when the presence of the body doesn't induce diffraction and does not alter the wave propagation in a significant way. Two ratios are mainly used to understand if the linear wave theory can be used to predict the behavior of the body, in fact the theory is valid if:

- $\frac{2\pi a}{\lambda} \approx 1$ where a identify the characteristic body dimension and λ the wave length. This ratio identifies the effect of the body on the wave. By asking that the dimension of the body to be similar to the wave length we are asking that the body doesn't affect the wave pattern too significantly.
- $\frac{\eta_w}{a} << 1$ This requirement asks the wave amplitude to be much smaller than the body dimension, this is not always true in extreme sea condition and could lead to an overestimation of the power generated. However for a WEC in production the motion between waves and absorber are moderate and so a linearized model can be used; just in case of largest production waves we must ensure that the wave power production is not exaggerated due to a violation of the latter condition.

The solution of the Laplace equation will be done by means of numerical tools, in fact the linear wave theory has a great advantage, it allows to superimpose the various effect so that is possible to divide the wave torque into three components:

- *Exciting wave torque* τ_{exc} : it consider the interaction between the body and the waves, the diffraction will be also considered, in fact we are not in the case in which $\frac{2\pi a}{\lambda} << 1$ so where the diffraction cannot be neglected.
- *Radiated wave torque* τ_{rad} : is the torque due to the movement of the body inside of the water that radiates waves, will be discussed in paragraph [2.4.3]

- *Archimedes torque* τ_{arch} : is the torque due to the fact that the movement of the body will change the buoyancy.

  So we may write that:

$$\tau_{wave} = \tau_{exc} + \tau_{rad} + \tau_{arch}$$

Thanks to the linear wave theory, we can deal with each of the torque separately and then superimpose the effects. The torques will be computed giving the best boundary condition. It means that we will find the effect of the radiation torque for a mass-less float moved in calm water, the effect of the buoyancy force when the float is displaced in calm water without considering the radiation. The exciting wave torque instead will be computed considering the body fixed.

2.4.1 Exciting Wave Torque:

The exciting wave torque depends just on the body shape and on the wave field. Given the body shape, in fact, we can achieve through the usage of ANSYS AQWA the spectrum of the exciting force normalized on the wave amplitude. The problem hence could be divided in two parts:

2.4.1.1 Wave generation:

Like discussed before it depends on the spectrum we choose to represent the wave field. We will use the PM spectrum due to its higher variance of the distribution around its peak. This will lead to a more difficult control design. In

order to generate from the spectrum the waves we will use the random phase method, since the PM is a PSD. See section [2.4.1.1]

2.4.1.2 Force spectrum on wave high:

Is the result of the simulation through ANSYS AQWA, the report is on (APPENDIX A), and allow us to generate the force input to our system. We are going however to discuss how for the shape of a body is possible to achieve the force spectrum. The excitation force is a dynamic force meaning that is due to the velocity of the water around the body. In particular, it can be expressed like an integral of the dynamic part of the pressure created on the immerged surface of the body. In other words, considering just the heave motion, we can write:

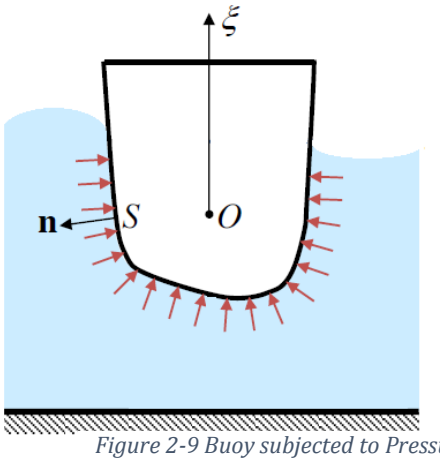

Figure 2-9 Buoy subjected to Pressure Distribution

$$f_e\left(\omega, H_{wave}\right) = -\int_S n_\xi p_e\left(\omega, H_{wave}\right) dS \rightarrow \tau_{ext} = f_e\left(\omega, \eta_{wave}\right) d_{arm}$$

Where n_z is the projection of the normal vector of the surface on the ξ direction and $p_e\left(\omega, \eta_{wave}\right)$ is the variation of the pressure around the equilibrium depending on the wave field.

The resulting force spectrum is shown in the following figure:

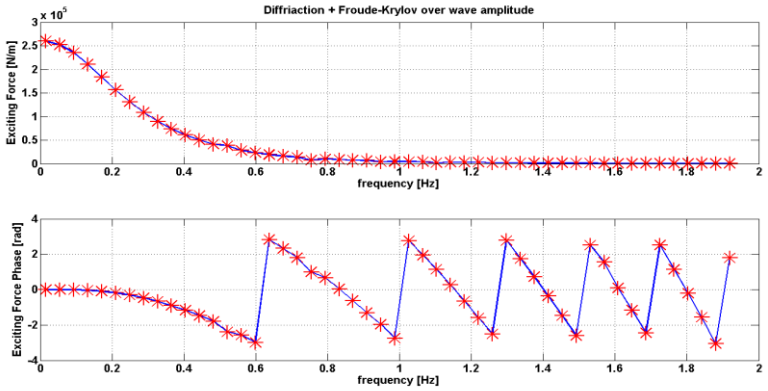

Figure 2-10 Exiting Wave Force over Amplitude Spectrum

This spectrum is defined point wise since is achieved through an FEM method: we can observe how we have not multiplied yet the wave amplitude. To achieve the final force spectrum we have to take into account the random part of the process that is given by the wave generation. This means that we have to multiply the force spectrum and the wave amplitude spectrum defined as $|\eta_{wave}| = \sqrt{2S_{PM}(f_i) * \Delta f}$, $\measuredangle \eta_{wave} = \delta_{rand,i}$ so this means that the force spectrum will be given by:

$$|f_{ext}| = \left|\frac{f_{ext}}{\eta_{wave}}\right| |\eta_{wave}|, \quad \measuredangle f_{ext} = \measuredangle \frac{f_{ext}}{\eta_{wave}} + \measuredangle f_{wave}$$

Resulting in the following plot:

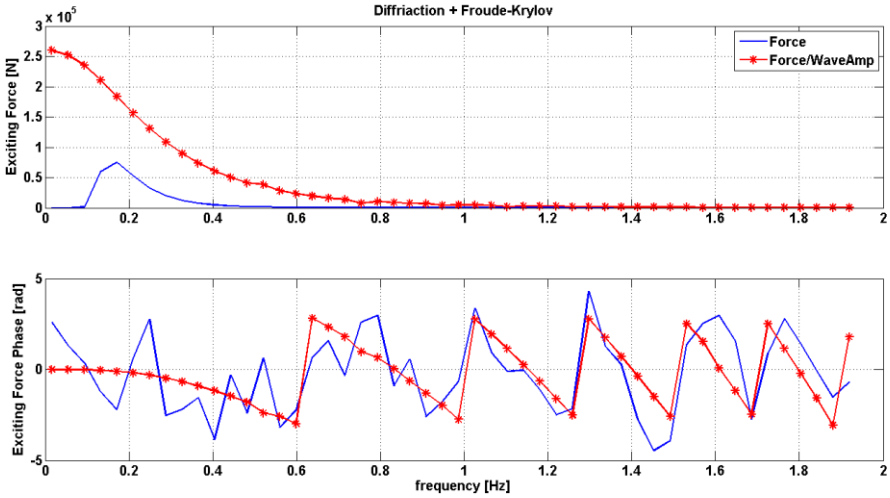

Figure 2-11 Exiting Wave Force over Amplitude and Exiting Wave Force Spectra

We can now achieve the time story of the force by antitrasform the spectrum, we are going obviously to consider just the real part since the final resulting force must be real so:

$$f_{ext}(t) = \sum_i \left| f_{ext}(f_i) \right| \cos\left(2\pi f_i t + \measuredangle f_{ext}(f_i)\right)$$

As said before we need to achieve the final torque and so:

$$\tau_{ext} = f_e(t)\, d_{arm}$$

Obtaining for the latter spectrum the following time history:

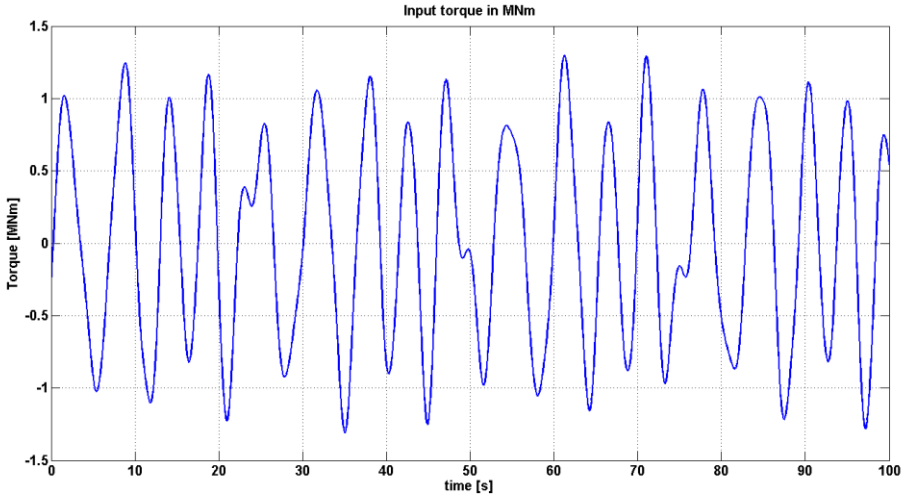

Figure 2-12 Exiting Wave Torque

We have so defined the input for our system.

2.4.2 Archimedes and Gravity Torque:

We can define a total torque that depends on both the gravity that is acting on the arm and the buoyancy that the floating object is experiencing.

So we can define:

$$\tau_{elastic} = \tau_{archimedes} - \tau_{gravity} = V_{sub}\left(\vartheta_{arm}\right)\rho_{water} g d_{arm}\left(\vartheta_{arm}\right) - m_{mech} g d_{mecc}\left(\vartheta_{arm}\right)$$

Where d_{arm} and d_{mecc} are the arm from the hinge to the application point of the force. However by considering the small displacements imposed by the linear wave theory we can linearize the above expression:

$$\tau_{elastic} = \underbrace{\tau_{archimedes}\Big|_{\vartheta_{arm}=\vartheta_{arm_{eq}}} - \tau_{gravity}\Big|_{\vartheta_{arm}=\vartheta_{arm_{eq}}}}_{\text{will be null when added to the } \tau_{PTO} \text{ at equilibrium}} + \frac{\partial \tau_{elastic}}{\partial \vartheta_{arm}}\Bigg|_{\vartheta_{arm}=\vartheta_{arm_{eq}}} \left(\vartheta_{arm} - \vartheta_{arm_{eq}}\right)$$

$$\tau_{elastic} = \left.\frac{\partial \tau_{elastic}}{\partial \vartheta_{arm}}\right|_{\vartheta_{arm}=\vartheta_{arm_{eq}}} \left(\vartheta_{arm} - \vartheta_{arm_{eq}}\right) = -k_{elastic}\vartheta_{arm} + k_{elastic}\vartheta_{arm_{eq}}$$

Considering our situation, so the fact that at $\vartheta_{arm} = 0$, we can simplify immediately the expression writing that:

$$\tau_{elastic} = \tau_{delta}\big|_{\vartheta_{arm}=0} + \left.\frac{\partial \tau_{elastic}}{\partial \vartheta_{arm}}\right|_{\vartheta_{arm}=0} \left(\vartheta_{arm}\right) = \tau_{delta}\big|_{\vartheta_{arm}=0} - k_{elastic}\vartheta_{arm}$$

Let's now write the buoyancy expression in function of the position of the floating hemisphere. For sake of simplicity, we decided to consider the buoyancy force associated just with the hemisphere and not with the cone; moreover, we are also considering the fact that the hemisphere is hinged with the arm and so will remain perpendicular to the mean water level. We will observe, however, how by means of the linearization this consideration will not affect the calculation:

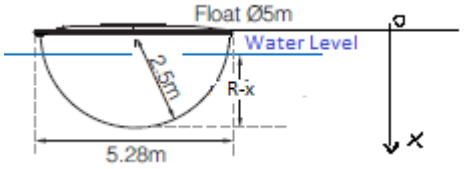

Figure 2-13Buoy Reference System

$$F_{buoyancy} = \rho g \int_{x}^{R} \pi\left(R^2 - x^2\right)dx = \rho g\left(\frac{2}{3}\pi R^3 - \pi R^2 x + \frac{\pi x^3}{3}\right)$$

We now have to connect the water level with the theta angle looking at the following figure the link is immediate:

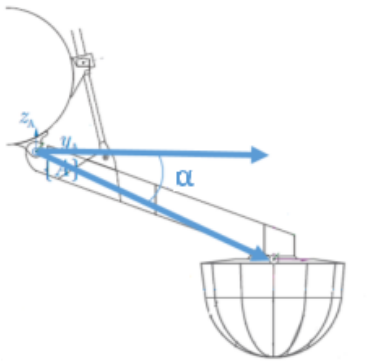

Figure 2-14 Arm-Buoy reference system

$$x = d_{arm}\sin(\alpha) - d_{arm}\sin(\alpha - \vartheta)$$

So the buoyancy torque in function of theta will be given by:

$$\tau_{Archimede} = \rho g\left(\frac{2}{3}\pi R^3 - \pi R^2 x + \frac{\pi x^3}{3}\right) d_{arm}\cos(\alpha - \vartheta)$$

While the gravitational torque will be given by:

$$\tau_{gravity} = m_{mecch} d_{mecc}\, g\cos(\alpha - \vartheta)$$

We can now linearize the expression so:

$$\frac{\partial \tau_{arch}}{\partial \vartheta} = \rho g \frac{\partial\left(\frac{2}{3}\pi R^3 - \pi R^2\left(d_{arm}\sin(\alpha) - d_{arm}\sin(\alpha - \vartheta)\right) + \frac{\pi\left(d_{arm}\sin(\alpha) - d_{arm}\sin(\alpha - \vartheta)\right)^3}{3}\right) d_{arm}\cos(\alpha - \vartheta)}{\partial \vartheta} =$$

$$= \rho g\left[\begin{array}{l}\frac{2}{3}\pi R^3 d_{arm}\sin(\alpha - \vartheta) - \pi R^2\sin(\alpha)\, {d_{arm}}^2\sin(\alpha - \vartheta) - \pi R^2 {d_{arm}}^2\cos(2\alpha - 2\vartheta) + \\ + \frac{\pi {d_{arm}}^4}{3}\left[\left(\sin(\alpha) - \sin(\alpha - \vartheta)\right)^2\left(\sin(\alpha)\sin(\alpha - \vartheta) + 2\cos\left(2(\alpha - \vartheta)\right) + 1\right)\right]\end{array}\right]$$

$$\frac{\partial \tau_{gravity}}{\partial \vartheta} = m_{mecch} d_{mecc}\sin(\alpha - \vartheta)$$

This means that the slope of the linearized expression for the hydrostatic restoring torque will be given by:

$$-k_{elastic}=\left.\frac{\partial\tau_{elastic}}{\partial\vartheta_{arm}}\right|_{\vartheta_{arm}=0}=\rho g\left[\frac{2}{3}\pi R^3 d_{arm}\sin(\alpha)-\pi R^2\sin(\alpha)^2\,d_{arm}{}^2-\pi R^2 d_{arm}{}^2\cos(\alpha)\right]+m_{mecch}d_{mecc}\sin(\alpha)$$

This equation as suggested by [9] can be approximated as:

$$-k_{elastic}=\left.\frac{\partial\tau_{elastic}}{\partial\vartheta_{arm}}\right|_{\vartheta_{arm}=0}\approx\rho g A_w d_{arm}$$

with A_w the crossectional area of the float at the draft line

The difference will be minimal as can be seen by this plot:

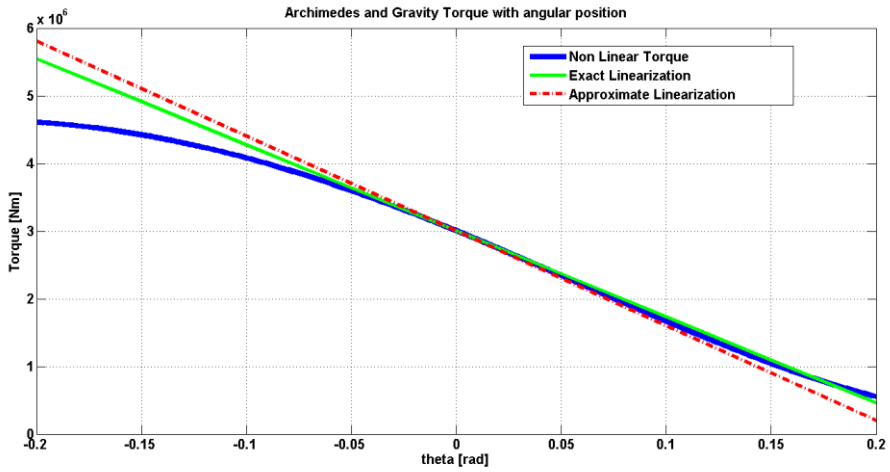

Figure 2-15 Static Torque

2.4.3 Radiated Wave Torque:

The radiated waves are waves produced by the motion of a floating body in a calm water condition. It can be observed that by moving an object into a calm water the object will produce waves that propagates far away. The waves will persist even if the body ceases to move, it should move forever if no damping

is considered. This will so produce a force on the body surface that depends on the previous motion of the body. The radiation torque is composed by two main factors, the added mass (in this case inertial moment) and the radiation damping coefficient. The added mass represent the mass of the surrounding water that is dragged by the body in its motion, it's a function of the frequency and it's not zero at infinite frequency. For this reason, we can "extract" the infinite frequency coefficient.

To obtain their value in frequency domain we must use a commercial code that once given the geometry of the buoy computes the coefficients.

The radiation torque, in case of regular waves, can be written as:

$$\tau_{rad}(t) = -J_{add}(\omega_w)\ddot{\vartheta}_{arm}(t) - B_{hyd}(\omega_w)\dot{\vartheta}_{arm}(t)$$

With $B_{hyd}(\omega_w)$ the value of the radiation damping and $J_{add}(\omega_w)$ the added mass.

When we perform a time domain simulation, we can use the general expression of this torque, which is valid for irregular wave too. We can write that:

$$\tau_{rad}(t) = -J_{add,\infty}\ddot{\vartheta}_{arm}(t) - \mathrm{k}_r(t) * \dot{\vartheta}_{arm}(t) = -J_{add,\infty}\ddot{\vartheta}_{arm}(t) - \int_{-\infty}^{t} \mathrm{k}_r(t-s)\dot{\vartheta}_{arm}(\mathrm{s})ds$$

The $J_{add,\infty}$ represents the added inertial moment at infinite high frequency. The function $\mathrm{k}_r(t)$ convolved with the velocity takes into account the memory effect given by the radiation term.

A relation between the radiation damping or the added mass and the k_r radiation-force impulse-response function can be found [12]. In fact let's consider a simple sinusoidal motion (produced by a regular wave) of the body so:

$$\begin{cases} \vartheta = \Theta e^{i\omega t} \\ \dot{\vartheta} = i\omega\Theta e^{i\omega t} \\ \ddot{\vartheta} = -\omega^2\Theta e^{i\omega t} \end{cases} \rightarrow \tau_{rad} = \left(\omega^2 J_{add}(\omega) - i\omega B_{hyd}(\omega)\right)\Theta e^{i\omega t}$$

This means that we can write:

$$\left(\omega^2\left(J_{add}(\omega)\right) - i\omega B_{hyd}(\omega)\right)\Theta e^{i\omega t} = J_{add,\infty}\omega^2\Theta e^{i\omega t} - \int_{-\infty}^{t} k_r(t-s)\, i\omega\Theta e^{i\omega t} ds$$

$$\left(\omega^2\left(J_{add}(\omega) - J_{add,\infty}\right) - i\omega B_{hyd}(\omega)\right)\Theta e^{i\omega t} = -i\omega\Theta\int_{-\infty}^{t} k_r(t-s)\, e^{i\omega s} ds$$

$$\left(i\omega\left(J_{add}(\omega) - J_{add,\infty}\right) + B_{hyd}(\omega)\right)e^{i\omega t} = \int_{-\infty}^{t} k_r(t-s)\, e^{i\omega s} ds$$

Now by applying a change of variable in the integral forms to z=t-s:

$$\left(i\omega\left(J_{add}(\omega) - J_{add,\infty}\right) + B_{hyd}(\omega)\right)e^{i\omega t} = \int_{\infty}^{0} k_r(z)\, e^{i\omega(t-z)}(-dz)$$

So at the end:

$$i\omega\left(J_{add}(\omega) - J_{add,\infty}\right) + B_{hyd}(\omega) = \int_{0}^{\infty} k_r(z)\, e^{-i\omega z} dz$$

We may so express the $-j\omega\left(J_{add}\left(\omega\right)-J_{add,\infty}\right)-B_{hyd}\left(\omega\right)$ as a Fourier transform of the impulse response $\mathrm{k}_r\left(t\right)$, this means that the equation above describes a frequency response function that relates the angular velocity to the radiated wave torque.

This observation can lead to the opposite relation so by means of the inverse Fourier transform [13]:

$$\mathrm{k}_r\left(t\right)=-\int_{-\infty}^{\infty}\left(i\omega\left(J_{add}\left(\omega\right)-J_{add,\infty}\right)+B_{hyd}\left(\omega\right)\right)e^{i\omega t}d\omega=-\frac{2}{pi}\int_{0}^{\infty}B_{hyd}\left(\omega\right)\cos\left(\omega t\right)d\omega$$

The latter equality can be written since the Fourier transform is complex conjugate with respect the 0 frequency axis.

This can led us compute the time domain function to be convolved starting from the Frequency domain expression of the radiation damping and added inertia.

We know that every scalar impulse response represents a SISO system. If the system is linear or linearized, as in our case, it is also represented by its FRF, its transfer function in the Laplace domain, and by a linear state-space realization. There is a link between all these 4 kinds of representation, meaning that having one of them, we have characterized the system, and we can achieve the others through mathematical medium.

From ANSYS AQWA we obtain the discrete values of $J_{add}(\omega)$ and $B_{hyd}(\omega)$ We have so the FRF, decomposed in its real part ($B_{hyd}(\omega)$) and its imaginary part $A_{hyd}(\omega) = \omega\left(J_{add}(\omega) - J_{add,\infty}\right)$.

Starting form this point, we have different ways to achieve a transfer function which represent the link between the radial torque and the angular velocity in the Laplace domain (thanks to the convolution properties), meaning:

$$\tau_{rad}(s) = -J_{add,\infty}\ddot{\vartheta}_{arm}(t) - \mathrm{k}_r(t) * \dot{\vartheta}_{arm}(t) \; -> \; \frac{\tau_{rad}(s)}{\vartheta(s)} = -J_{add,\infty}s^2 - \mathcal{L}\left(k_r(t)\right)s = -J_{add,\infty}s^2 - K_r(s)s$$

The following table can represent two different paths:

1	$B_{hyd}(\omega)$	→	$k_r(t)$	→	$\hat{K}_r(s)$
2	$A_{hyd}(\omega)$ $B_{hyd}(\omega)$	→	$K_r(j\omega)$	→	$\hat{K}_r(s)$

2.4.3.1 Method 1:

To achieve the impulse response function from FRF, we simply need the real part of it, as described before:

$$\mathrm{k}_r(t) = -\frac{2}{pi}\int_0^{\infty} B_{hyd}(\omega)\cos(\omega t)\,d\omega$$

Since we don't have a continuous spectrum, to integrate we will have to use a numerical integration (like the trapezoid method). We will obtain a time series representing the impulse response. To have a better representation we

took out some outbound value of the FRF caused by numerical errors accomplished by ANSYS AQWA. The resulting impulse response is:

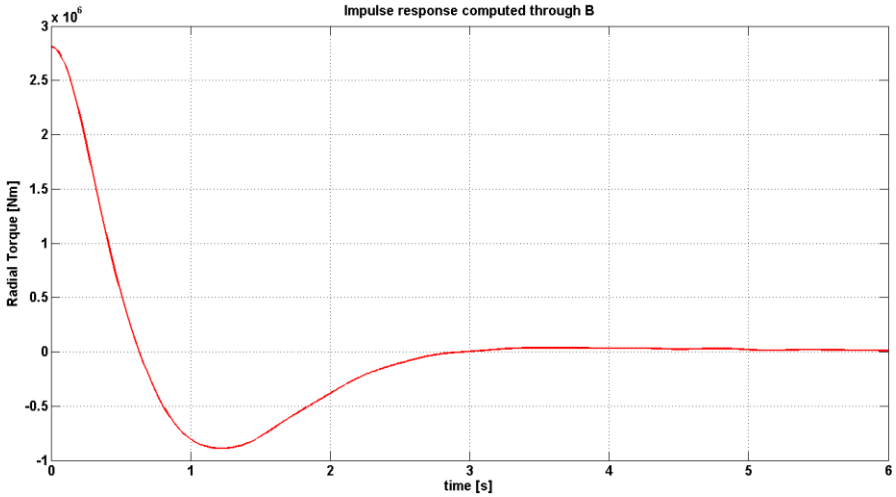

Figure 2-16 Impulse Response of the Vertical Displacement due to Radiative Force

Once we have the previous time series, by means of the Matlab function *imp2ss* we obtain a state space realization, which though contains many unnecessary state variables. The truncation technique exploits the SVD method, and is implemented through the Matlab function *balmr*. The final degree of the system is chosen as input equal to 3.

Given the state space realization, we can obtain the Laplace transfer function through the common procedure of antitrasform:

$$\hat{K}_r(s) = C(sI - A)^{-1} B + D = \frac{N(s)}{D(s)}$$

To arrive at the final result, some approximation has been done in the passage impulse response-state space realization. We can notice it by recalculating the impulse response from the transfer function we obtained (Figure 2-17).

Even if this method approximates well the original impulse response has some intrinsic problems. In fact let's look to some properties that the radial force should have [14]:

1. **Low-frequency Asymptotic Value:** this property establishes a null static value of the transfer function. In fact a body moving at 0 frequency can't produce the oscillating radial force. By looking at the frequency response function we can observe that:

$$\lim_{\omega\to 0}\left(K_r\left(j\omega\right)\right)=\lim_{\omega\to 0}\left(B_{hyd}\left(j\omega\right)+j\omega\left(J_{add}\left(\omega\right)-J_{add,\infty}\right)\right)=B_{hyd}\left(0\right)\triangleq 0$$

   This means that the equivalent transfer function must have a zero in 0.

2. **High-frequency Asymptotic Value:** this property establishes that the transfer function has to tend to zero at infinite frequency. In other words we are asking that:

$$\lim_{\omega\to\infty}\left(K_r\left(j\omega\right)\right)=\lim_{\omega\to\infty}\left(B_{hyd}\left(j\omega\right)+j\omega\left(J_{add}\left(\omega\right)-J_{add,\infty}\right)\right)=\lim_{\omega\to\infty}\omega\left(J_{add}\left(\omega\right)-J_{add,\infty}\right)=0$$

   This means that the transfer function must be strictly proper.

3. **Initial-Time Value:** this property implies a different from zero initial value of the impulse response so mathematically:

$$\int_0^\infty B\left(\omega\right)d\omega\neq 0\rightarrow\frac{2}{\pi}\int_0^\infty B\left(\omega\right)d\omega=\lim_{t\to 0^+}k_r\left(t\right)\neq 0$$

The first inequality is easily understandable from the properties of the spectrum of B, in fact B assumes in every frequency positive values [6] being a dissipative force (see also the discussion about passivity).

Since before we have defined that the transfer function must be proper, it means that the relative degree should be one. Given that:

$$\lim_{t\to 0^+} k_r(t) = \lim_{s\to\infty} sK_r(s) \neq 0 \rightarrow \deg\left(N(s)\right) = \deg\left(D(s)\right) - 1$$

This equivalence between Laplace and time domain cannot be extended to not strictly proper transfer function. For a simply proper function, though, we may use the state space representation to calculate the initial value.

$$\lim_{t\to 0^+} k_r(t) = \lim_{t\to 0^+} \left(Ce^{At}B + D\right) = CB + D$$

4. **Final-Time Value:** this property represent the stability of the system. A stable system in fact has an impulse response that has the following characteristic:

$$\lim_{t\to\infty} k_r(t) = \lim_{t\to\infty} \frac{2}{\pi}\int_0^\infty B(\omega)\cos(\omega t)\,d\omega = 0$$

5. **Passivity:** Considering the physics of the radiation process, we can infer that this is a passive process meaning that it has the property of passivity. This property implies that at every time interval the stored energy is less than the energy absorbed (from the environment). In others words there is a global dissipation in the process. If the system can be represented by a transfer function (so it's linear and time invariant) the passivity in time domain can be expressed in frequency domain as positive realness of the transfer function. Mathematically $\mathrm{Re}\left\{K_r(j\omega)\right\} \geq 0$.

Having summarized all these properties we can verify which of them are respected by this first method. Our resulting transfer function is:

$$\hat{K}_{r,3}(s) = \frac{1.407s^3 + 293.4s^2 + 2061s - 47.07}{s^3 + 7.187s^2 + 16.95s + 17.83} 10^4$$

We can immediately see how the properties 1 and 2 are not respected since the relative degree is zero and there is no zero in 0. From this result we can achieve back the Radiation Damping associated to it in fact:

$$\hat{K}_{r,3}(j\omega) = \lim_{s \to j\omega} \hat{K}_{r,3}(s), \quad \hat{B}(\omega) = \mathrm{Re}\left[\hat{K}_{r,3}(j\omega)\right].$$

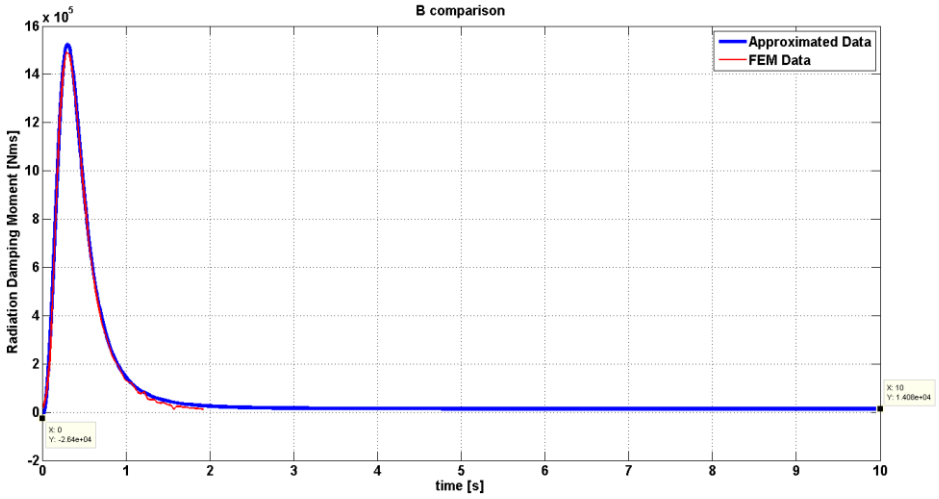

Figure 2-17 FRF achieved with FEM compared with FRF approximated

As we can see from the plot above and as well from the mathematical expression of the transfer function not only the properties 1,2 but also property 5 is not respected.

With this method there is no way to impose some constrain to the approximation. The whole approximation is good but at very low and very high frequency, the results differ from the reality. This won't provoke bad results in the simulations since the wave power is mainly concentrated in a range of frequency where the fit is good. Despite that we tried to overcome these problems with method 2 that allows us to impose some constrains.

2.4.3.2 Method 2:

Starting for the FRF, we can obtain directly the approximate transfer function through the Matlab function *invfreqs,* which exploits a minimization algorithm in order to achieve the coefficients of transfer function numerator and denominator by means of Levy algorithm [15]. As inputs of this function we can give the degree of the numerator and the denominator, and this makes us understand how immediately problems 2 and 3 unsolved with method one could be overcome.

We can prevail problem 1 by mean of a mathematical trick, which is searching for an approximating transfer function of our original FRF divided by $j\omega$. It means that we are searching for a transfer function $\hat{K}_{r,\text{int}}(s)$ such that minimize the following scalar value:

$$\vartheta = \arg\min_{\vartheta} \sum_{l} \left| \frac{K_r(j\omega_l)}{j\omega_l} - \hat{K}_{r,\text{int}}(j\omega_l, \vartheta) \right|^2$$

Where ϑ is a vector containing the numerator and the denominator coefficients of the transfer function $\hat{K}_{r,\text{int}}$, which, as we can understand, is not the direct approximation of our original FRF K_r but the approximation of $\frac{K_r(j\omega_l)}{j\omega_l}$. In order to achieve the real approximation we have just to multiply the final results by s. In this way we also obtain a zero at s=0, meaning we solve problem 1:

$$\hat{K}_{r,3}(s) = s\hat{K}_{r,\text{int}}(s) = \frac{3.42s^2 + 19.14s}{s^3 + 7.539s^2 + 15.82s + 18.14}10^6$$

The algorithm automatically uses a technique that avoids approximating the FRF with a function with positive poles (property 4 is respected, how we will see from the impulse response below). Both from the graph and from the mathematical expression of the transfer function we can see how the damping ratio now is 0 at null frequency and tends to 0 infinite frequency.

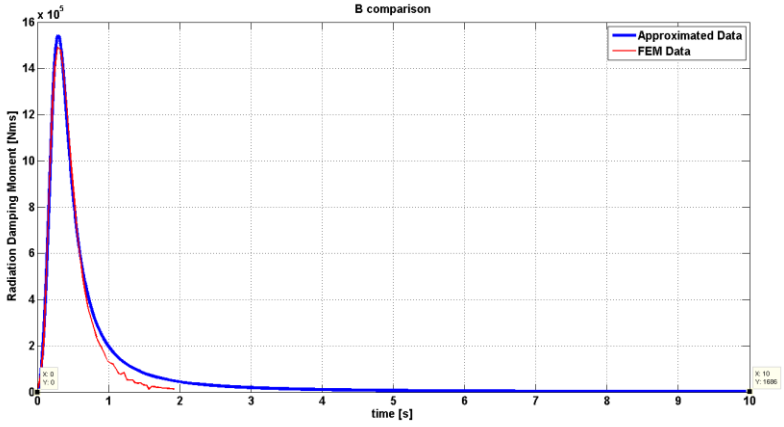

Figure 2-18 FRF achieved with FEM compared with FRF approximated

Since the damping coefficient is always greater or equal to 0, we can conclude that also property 5 is respected.

We can now compare the approximated impulse responses and FRF achieved with the two methods:

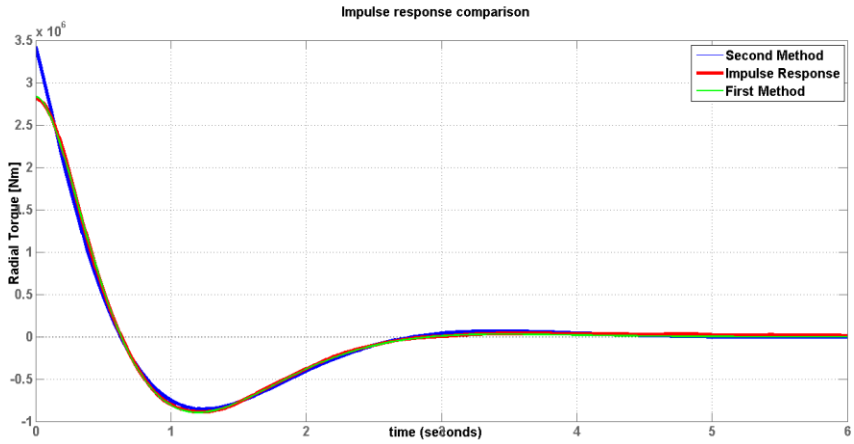

Figure 2-19 Impulse Responses Compared

Impulse response with method 2 is slightly less precise above all at the beginning. Since the transfer function achieved with method 1 is not proper, we cannot use the initial value theorem, as explained above. However, the differences for the rest of the time history are negligible.

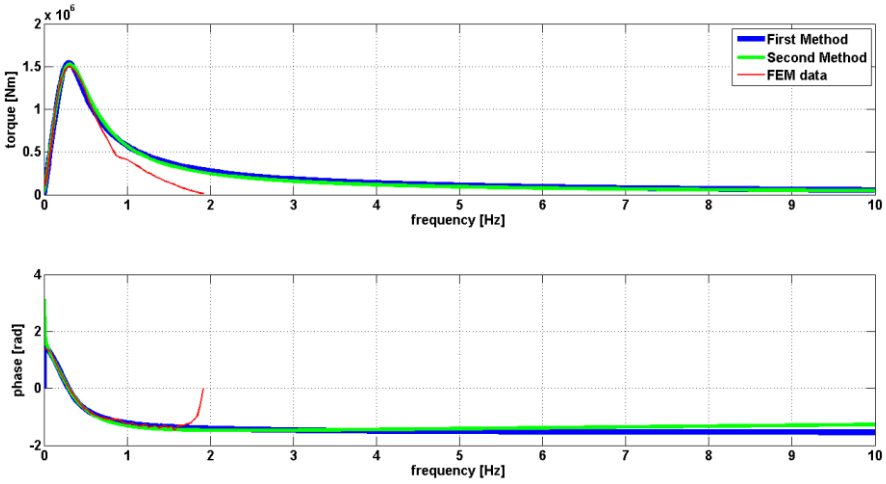

Figure 2-20 FRF compared

From the FRF comparison we can see how the superimposition is not perfect, but it's really good for the range of frequency we are going to deal with in our simulations. Wave forces, in fact, mostly excited frequencies in between 0.1Hz and 0.6Hz.

2.4.4 Equation of motion for a single arm:

By rearranging the linearized expression of the dynamical equilibrium we can write that:

$$J_{mech}\ddot{\vartheta}_{arm} = -k_{elastic}\vartheta_{arm} + k_{elastic}\vartheta_{arm_{eq}} - J_{add,\infty}\ddot{\vartheta}_{arm}(t) - \mathrm{k}_r * \dot{\vartheta}_{arm}(t) + \tau_{exc} - \tau_{PTO}$$

And so that:

$$\left(J_{mech} + J_{add,\infty}\right)\ddot{\vartheta}_{arm} = -k_{elastic}\vartheta_{arm} - \mathrm{k}_r * \dot{\vartheta}_{arm}(t) + \tau_{exc} - \tau_{PTO} \underbrace{-\tau_{PTO}\big|_{eq} + \tau_{delta}\big|_{\vartheta_{arm}=0}}_{0 \text{ by definition of equilibrium position}}$$

$$\left(J_{mech}+J_{add,\infty}\right)\ddot{\vartheta}_{arm}+k_{elastic}\vartheta_{arm}+\mathrm{k}_r*\dot{\vartheta}_{arm}(t)=\tau_{exc}-\tau_{PTO}$$

Due to the fact that this express a linear model for the arm dynamic we can pass in Laplace domain and write that:

$$\frac{\Theta(s)}{\tau_{exc}-\tau_{PTO}}=\frac{1}{\left(J_{mech}+J_{add,\infty}\right)s^2+\hat{K}_r(s)s+k_{res}}$$

In order to create a faster mechanical block in Simulink, we can pass from the Laplace representation to a global state space realization. This passage is done through the function *tf2ss*. We obtain a realization described by 5 state variables (2 mechanicals and 3 related to the radial force), and a mechanical system described by the usual linear state space equation:

$$\left[\begin{array}{c|c} A_{tot} & B_{tot} \\ \hline C_{tot} & 0 \end{array}\right]\rightarrow\begin{cases}\dot{X}=A_{tot}X+B_{tot}u(t)\\ Y=C_{tot}X\end{cases}$$

Where $Y=\begin{bmatrix}\vartheta\\ \dot{\vartheta}\end{bmatrix}$ and $u(t)=\tau_{exc}(t)-\tau_{PTO}\left(P_{cyl}\right)$, where the torque given by the PTO is function of pressure in the cylinder that is itself function of the other state variables.

2.5 CHARACTERIZING THE HYDRAULIC SYSTEM:

Once we have dealt with the dynamic of the floating object and linked it with the displacement of the cylinder we can start analyzing the hydraulic part of the PTO. The hydraulic system is the interface between the wave power extraction and the power generation, and an optimization procedure will be

studied for it in order to maximize the extraction, which is the main aim of our project.

The hydraulic system can be schematized as it follows:

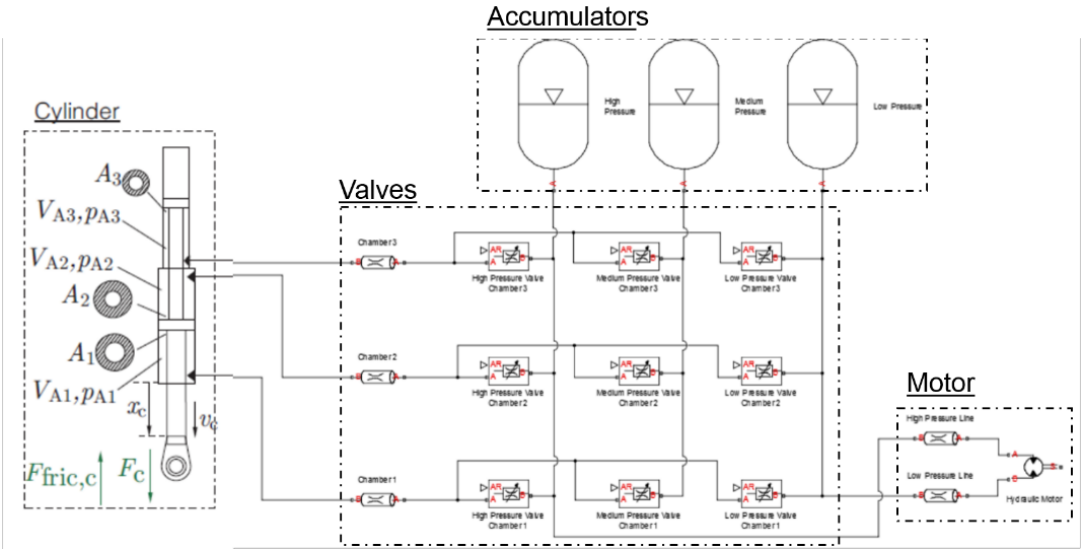

Figure 2-21 Plant layout

The system is so composed by 4 main components:

- *The Cylinder*: it is actually the component that is connected directly with the arm of the floating part, we have already discussed the connection of the dynamics. It's the link between the wave power extraction and the hydraulic power generation.
- *The Valves Manifold*: it is composed by a set of nine valves that connects the three accumulators and the three chambers of the cylinder. Each valve is driven electronically, and the signal will lead their opening and closing.

- *The Accumulators*: they are responsible for the smoothing of the incoming wave power. There are three accumulators systems, high pressure, low pressure and medium pressure. The energy conversion is driven just by the high and low pressure ones. The medium pressure can be used as an "emergency storage" and it's useful in order to reduce the losses in the cylinder due to the difference in pressure of the chambers. The compressibility losses in the cylinder, in fact, is relative to a pressure shift and is proportional to the square of it. Moreover, we will see how it will give a better performance at the system once we introduce our control strategy.

- *Motor*: it is the last part of the hydraulic system, it is connected to the high and low pressure accumulators and it will provide the torque to the electrical generator.

We have so to determine the dynamic of these system, and each of these 4 main parts will be discussed separately. The connections will not be considered as ideal, since we are going to consider also the losses in the pipes. An entire paragraph will be dedicated to the pipes and how we manage the internal dynamic.

We are going now to analyze in deep each subsystem.

2.5.1 Pipes connections:

Hydraulic pipes provide the connections between the hydraulic elements. In our model, we won't consider ideal hoses, since we are aware that the losses due to compressibility of the fluid and the losses due to the interaction between the tube and the fluid, influence on the whole performance of the

system. The extracted energy from the cylinder will be greater than the energy that feeds the hydraulic motor.

The losses along the tube can be divided in concentrated losses, due to sudden changes of the geometry of the tube, and distributed losses, which are due to the interaction between the surfaces of the tube with a viscous fluid.

2.5.1.1 Distributed and Concentrated Losses:

If we consider a pipe with a flux running through it, we can consider a constant rate of loss of energy. We know that the three main kinds of energy of a stationary fluid (for the time being let's avoid the local inertia term) are the pressure energy, the kinetic energy, and the potential energy. If we consider the total amount of energy we can write:

$$H = \frac{v_m^{\,2}}{2g} + h = \frac{v_m^{\,2}}{2g} + \frac{P}{\rho\gamma} + z \text{ [m]}$$

Where h indicates the piezometric or hydraulic head, constant for each section of the tube, since the fluid threats are parallel to each other (Bernoulli equation in normal direction). For the conservation of the mass, the flow rate, so the velocity in a constant section tube, is constant along the pipe. Due to losses and due to the latter consideration we can write:

$$\frac{dH}{ds} = \frac{dh}{ds} = -J$$

Where J is a measure of the strength of the losses and it's non-dimensional. Let's reason over this term: in order to get it, we can think about the variables which influence on the strength of the losses. Surely influence is

given by the velocity of the fluid, its viscosity, its density, the geometry of the pipe and the roughness of the surface. The latter parameter for us will be consider null, since we deal, inside our hypothesis, with smooth tubes. Anyway, for the generic introduction to the problem, we consider it.

We indicate, hence, five dimensional parameters. Since we are dealing with a mechanical problem (no temperature involved in first approximation), through the usage of the non-dimensional analysis we know that the dimension of the base of the system is 3 (length, mass and time), and J is hence influenced by two non-dimensional parameters. These relations are proved (experimentally and sometimes analytically), and the parameters are the Reynolds number and the non-dimensional roughness:

$$J = f\left(\mathrm{Re} = \frac{\rho \mathrm{vD}}{\upsilon}, \frac{r}{D}\right)$$

Since we are dealing with smooth tubes, we will neglect the influence given by the roughness, and we will concentrate just on the Reynolds number. What is proved is that, after a transition number which depends mainly on the geometry of the system, the functional link between J and Re drastically changes. This is physically due to the change of motion, from laminar to turbulent. The relation between J and Re is described by the following equations:

$$J = \lambda \frac{v_m^{\ 2}}{2gD}$$

$$\text{laminar flow: } \lambda = \frac{64}{\mathrm{Re}}$$

$$\text{turbolent flow: } \lambda = \frac{0.316}{\mathrm{Re}^{0.25}}$$

Where the latter is the Blasius equation, which we adopt to avoid the usage of implicit equation like the Prandtl one.

We want now to bring all of this in our equations. Since we are writing the equilibrium in term of force, we can transform the energy loss in an equivalent pressure that multiplies the area of the tube. To find the equivalent pressure (which will go always against the direction of the fluid) we just have to adjust dimensionally all the terms:

$$JL = [m] - - > JL\rho g = [Pa] = P_{loss}$$

$$\upsilon = \frac{\mu}{\rho} \text{ (kinematic viscosity) } v = \frac{4Q}{\pi D^2}$$

$$P_{loss,lam} = \lambda_{lam} \frac{v_m^{\ 2}}{2gD} L\rho g = \frac{64 v \upsilon L \rho}{D} = \frac{128 \rho \upsilon Q L}{\pi D^4}$$

$$P_{loss,turb} = \lambda_{tur} \frac{v_m^{\ 2}}{2gD} L\rho g = \frac{0.316}{\mathrm{Re}^{0.25}} \frac{v_m^{\ 2}}{2gD} L\rho g = \frac{0.316}{\mathrm{Re}^{0.25}} \frac{Q^2}{2D\left(\frac{\pi D^2}{4}\right)^2} L\rho$$

We will use these expressions to express an equivalent braking force given by the losses. Since the expression are different and we don't want any discontinuity, we create a unique expression trough the hyperbolic tangents, which acts as filters. The border of the filter is the Reynolds transition number (2300 for our structure).

$$P_{loss} = \underbrace{\left(\frac{1}{2}+\frac{1}{2}\tanh\left(\frac{2300-\mathrm{Re}}{100}\right)\right)*\frac{128\rho\upsilon QL}{\pi D^4}}_{\text{Laminar Component}\approx 0 \text{ for Re}>2400} + \underbrace{\left(\frac{1}{2}+\frac{1}{2}\tanh\left(\frac{-2300+\mathrm{Re}}{100}\right)\right)*\frac{0.316}{\mathrm{Re}^{0.25}}\frac{Q^2}{2D\left(\frac{\pi D^2}{4}\right)^2}L\rho}_{\text{Turbolent Component}\approx 0 \text{ for Re}<2400}$$

In addition to the distributed losses we have to consider, as anticipated, also the concentrated ones. Since these are localized losses, the length of the tube and its hypothetic roughness do not influence the phenomenon. These losses, instead are proved to be depended from the square of the velocity, through a proportionality coefficient that depends on the shape of the geometry variation. We are given the coefficients in [8]. They are provided such that they give an equivalent pressure through the following expression:

$$P_{loss,conc} = \frac{\varepsilon * \rho}{2} * \left(\frac{4Q}{\pi D}\right)^2$$

Where ε is the fitting loss coefficient. The total loss, hence, will be express by the sum of the effects:

$$P_{loss,tot} = P_{loss,\mathrm{lam}} + P_{loss,\mathrm{dis}}$$

2.5.1.2 Inertial terms:

We can consider now the whole equation of the hydraulic hose. If the pressure difference across the tube is imposed from outside and it is consistent, we can't neglect the energy related to the inertia of the fluid. Since we have all the equations in terms of pressure, writing the equation of the hose becomes a matter of writing a force equilibrium.

Let's consider a small piece of a constant area hose, find the differential equilibrium and let's integrate over the length of the tube. We neglect the local

variation of the density with the time, and so we can write the differential inertia force like:

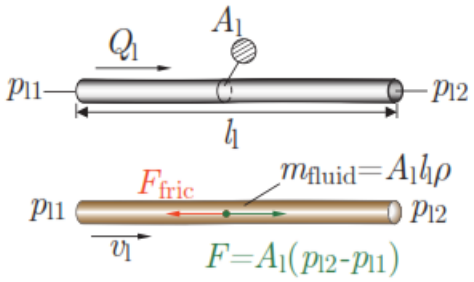

Figure 2-22 Inertia in the tubes

$$\frac{dQ_m}{dt}ds = \left(\underbrace{vA\frac{d\rho(s)}{dt}}_{\text{negligible}} + \rho(s)A\frac{dv}{dt} \right) ds = \left(P(s) - P(s+ds) - P_{loss/length}(s)ds \right) A =$$

$$\frac{dQ_m}{dt}ds = \left(-\frac{\delta P(s)}{\delta s}ds - P_{loss/length}ds \right) A$$

Integrating, knowing that the mass flow rate and its rate of change are constant along the tube:

$$\int_s \frac{dQ_m}{dt}ds = \frac{dQ_m}{dt}l = A\int_s \left(-\frac{\delta P(s)}{\delta s}ds - P_{loss/length}ds \right) = A(P_{11} - P_{12} - P_{loss,tot})$$

$$\frac{dQ_m}{dt} = \frac{A}{l}\left(P_{11} - P_{12} - P_{loss,tot} \right)$$

Where the loss in the tube depend on the flow rate as well. We wrote finally the differential equation of the tube. Observing the equation above, we can consider negligible the dynamic of the fluid when the length of the tube

increases. For this reason, this equation will not be used to represent the behavior of the fluid between the valves and the accumulators.

2.5.2 Discrete Displacement Cylinder:

First of all we must determine the reference system for the cylinder. We will consider positive displacement and velocity associated to a negative theta, this means that we are respecting the link obtained from the cinematic. The three chambers, which can be seen in the figure, have different area and acts in different ways. We can observe how chamber 1 and 3 acts negatively and chamber 2 positively. The flow rate is positive when exiting from the chamber.

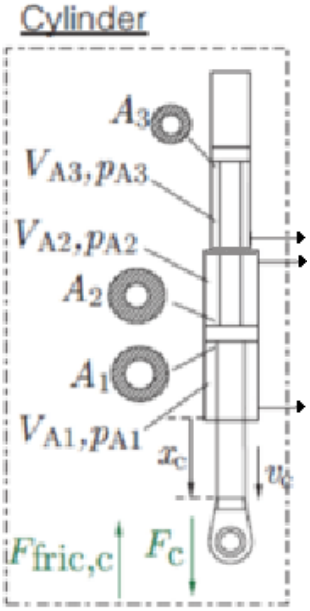

Figure 2-23 Cylinder layout

Given the main references for the physical quantities used in the model of the cylinder we can start writing the equation. Let's start writing the definition of the bulk modulus of oil [16]:

$$\beta = \rho \frac{dP}{d\rho} \rightarrow d\rho = \frac{\rho}{\beta} dP$$

Applying now the mass balance inside a chamber:

$$M_{in} - M_{out} = \frac{d(\rho V)}{dt} = \rho \frac{dV}{dt} + V \frac{d\rho}{dt} = \rho \frac{dV}{dt} + \frac{\rho V}{\beta} \frac{dP}{dt}$$

That can be written with our convention and neglecting the leakage inside the cylinder chamber. This cylinder, in fact, uses appropriate gasket inside the cylinder leading to a negligible leakage phenomena:

$$\rho Q_{in} = \rho \frac{dV}{dt} + \frac{\rho V}{\beta}\frac{dP}{dt} \rightarrow \frac{\rho V}{\beta}\frac{dP}{dt} = \rho Q_{in} - \rho \frac{dV}{dt}$$

In other words:

$$\dot{P} = \beta(P)\frac{\left(-Q_{in} - \dot{V}\right)}{V}$$

We have so defined the driving differential equation for a generic chamber of the cylinder. We will have three differential equation in pressure for the three chambers:

$$\begin{cases} \dot{P}_1 = \beta(P)\dfrac{\left(-Q_{A1} + \dot{x}_c A_1\right)}{\left(V_{0,A1} + A_1\left(x_{c,\max} - x_c\right)\right)} \\ \dot{P}_2 = \beta(P)\dfrac{\left(-Q_{A2} - \dot{x}_c A_1\right)}{\left(V_{0,A2} + A_2 x_c\right)} \\ \dot{P}_3 = \beta(P)\dfrac{\left(-Q_{A3} + \dot{x}_c A_3\right)}{\left(V_{0,A3} + A_3\left(x_{c,\max} - x_c\right)\right)} \end{cases}$$

Some observation can be done about these equations:

- We consider a variable bulk modulus with pressure, this is a realistic case where there is presence of air in the fluid (we consider a 0.5% of trapped air). The bulk modulus equation is given by [17]:

$$\beta(\mathrm{P}) = \beta_0 \frac{1+\alpha\left(\frac{p_a}{p_a+p}\right)^{1/\gamma}}{1+\alpha\frac{p_a^{1/\gamma}}{\gamma\left(p_a+p\right)^{\frac{\gamma+1}{\gamma}}}\beta_0}$$

Where β_0 is the bulk modulus without trapped air, γ is the gas specific heat ratio, α is the percentage of trapped air and $p_a + p$ is the absolute pressure.

- The equilibrium condition, so the condition with $\vartheta_{arm} = 0$ and calm water, is a condition where

$$x_c = x_{c,0}$$

We have written the equation in terms of volumetric flow rate, this choice has been done in order to be free to consider or not the compressibility of the oil in the rest of the plant. In fact, as it will be shown, there are components where the compressibility can be neglected in order to speed up the simulation.

This means that is important however to connect the density with the pressure so that we can pass from volumetric flow rate to mass flow rate where there is no conservation for the former.

In fact in a compressible fluid $\dot{M}_{in} = \dot{M}_{out} \not\Rightarrow \dot{V}_{in} = \dot{V}_{out}$.

Let's so find a relation between density and pressure, and again we can use the definition of the bulk modulus:

$$\beta(P)=\rho\frac{dP}{d\rho}\rightarrow\frac{1}{\rho}d\rho=\frac{dP}{\beta(P)}$$

This is a first order differential equation with separable variables; this means that can be solved by means of integration:

$$\int_{\rho_0}^{\rho}\frac{d\rho}{\rho}=\int_{0}^{P}\left[\frac{1}{\beta_0+\beta_0\alpha\left(\frac{p_a}{p_a+p}\right)^{1/\gamma}}+\frac{\alpha\,p_a^{\,1/\gamma}}{\gamma\left(p_a+p\right)^{\frac{\gamma+1}{\gamma}}+\alpha\left(p_a+p\right)^{\frac{\gamma+1}{\gamma}}\left(\frac{p_a}{p_a+p}\right)^{1/\gamma}}\right]dP$$

Considering an atmospheric pressure of 1 bar we can simplify the expression as:

$$\int_{\rho_0}^{\rho}\frac{d\rho}{\rho}=\int_{0}^{P}\left[\frac{1}{\beta_0+\beta_0\alpha\left(\frac{1}{1+p}\right)^{1/\gamma}}+\frac{\alpha}{\gamma\left(1+p\right)^{\frac{\gamma+1}{\gamma}}+\alpha\left(1+p\right)}\right]dP$$

The expression on the left hand side can be solved while the one on the right hand side due to the presence of the integral of $\frac{1}{\beta_0+\beta_0\alpha\left(\frac{1}{1+p}\right)^{1/\gamma}}$ cannot be solved analytically if not by using hypergeometric functions that would lead to a slowdown of the simulation.

This means that the final solution will be achieved by numerically integrate the right hand side obtaining a function evaluated in some points, which will then be used in Matlab Simulink to create a lookup table where the

value of density for a given pressure will be find by linear interpolation of the them. In other words we are going to compute $\rho(P) = \rho_{0,\text{with gas}} e^{\int_0^P \frac{dP}{\beta(P)}} \approx \left(1 - \frac{\alpha}{1-\alpha}\right) \rho_0 e^{\int_0^P \frac{dP}{\beta(P)}}$ for different values of pressures.

The numerical integration will be done by means of the Gauss-Legendre quadrature weights and nodes. We are going to use 500 nodes.

The resulting plot can be observed here where we consider our working fluid (oil) with a starting density of 900 $\left[kg / m^3\right]$

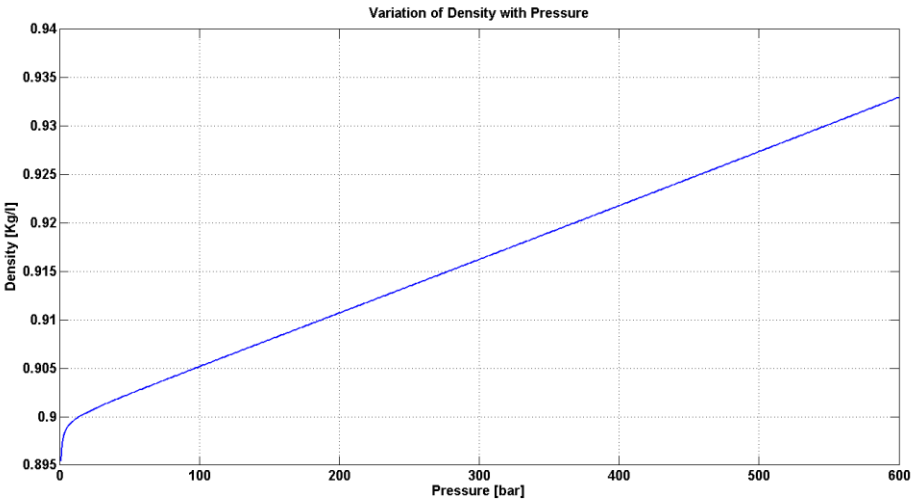

Figure 2-24 Density variation with pressure

Having a link between density and pressure we can pass from mass flow rate to volumetric flow rate in an algebraic way $\dot{M} = \rho(P)\dot{V}$

The cylinder dynamics however must consider also the friction force that the cylinder will sustain. The static friction model, is a classical model that consist in the modeling of the 4 main components of the friction such as Breakaway friction, Stribeak friction, Coulomb friction and Viscous Friction [18],[19].

2.5.2.1 Static friction model:

Static friction as said before is composed by three main components, each of them that represent a different physical interaction between the piston and the chamber:

- *Coulomb Friction:* Is a component proportional to the normal force that is exchanged between two bodies. Its sign depends just on the sign of the velocity, but its amplitude is not affected by it. Its mathematical representation is given by:

  $F_c = \mu |F_N| sign(v_p)$ for velocities that are different from 0.

- *Viscous friction:* This component takes into account the viscosity of the lubricants, this component has to be added when the system is characterized by rapid changes in velocity. This component depends on the velocity and it increase its magnitude with it:

  $F_v = k_v |v|^{\delta_v} sign(v_p)$ where k_v is the viscosity of the oil and δ_v is the nonlinear coefficient that relates the viscous friction to the velocity.

- *Stiction and Stribeck friction:* When a body is at rest it will encounter a higher value of friction due to the static cohesion. The striction component is defined just for zero velocity and represent the minimum force to obtain motion. According then to the work of Stribeck it is

possible to observe a decrease of the friction once the body is moving that is not discontinuous, this means that the regime value of the coulomb friction will be obtained by means of an exponential decay. In other words we can describe these two components as:

$\left(F_{Stiction} - F_{Coulomb}\right) e^{-\left|\frac{v_p}{v_\sigma}\right|^{\delta_\sigma}}$ where v_σ is the Stribeck velocity and δ_σ is the gradient of friction decay. While $F_{Stiction}$ and v_σ are defined experimentally, the gradient of the friction decay is described usually by $\delta_\sigma = 2$

By superimposition of the three components we can obtain the final friction force as:

$$F = \left(F_C + \left(F_S - F_C\right) e^{-\left|\frac{v_p}{v_\sigma}\right|^{\delta_\sigma}} + k_v \left|v\right|^{\delta_v} \right) sign\left(v_p\right)$$

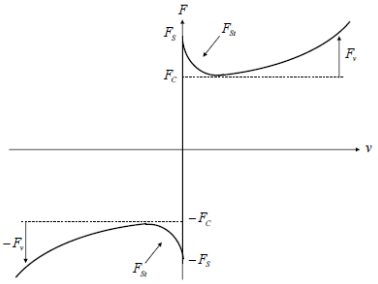

Figure 2-25 Friction with velocity

We can observe how this function presents a discontinuity at 0 velocity, this can create problems during the simulation. For this reason we decided to solve the discontinuity problem. We used the hyperbolic tangent:

$$F_{fric} = \left(F_C + \left(F_S - F_C\right) e^{-\left|\frac{v_p}{v_\sigma}\right|^{\delta_\sigma}} + k_v \left|v\right|^{\delta_v} \right) \tanh\left(a v_p\right)$$

Where α is the slope value for the hyperbolic tangent, bigger is it better will be approximated the ideal friction behavior

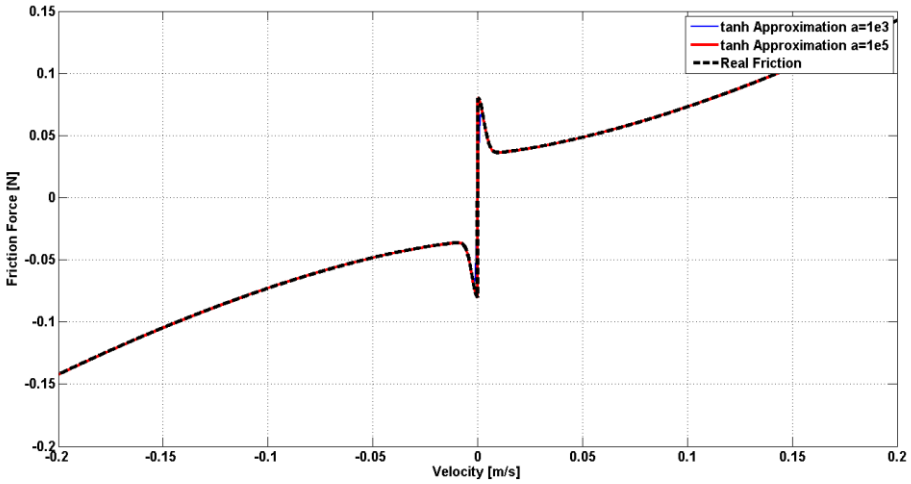

Figure 2-26 Comparison of friction behavior with different slopes

2.5.2.2 Comparison with Simscape model:

In order to check that the model designed is working properly we decided to compare the results with a cylinder designed by means of the Matlab-Simscape predefined blocks. The comparison is done by considering just an imposed displacement of the piston in both of the cylinders; we are not going to test the friction model. This decision was made because we are using the same model used by Simulink in the translational friction Simscape block. We can so observe the results given for an extreme displacement of 10 cm:

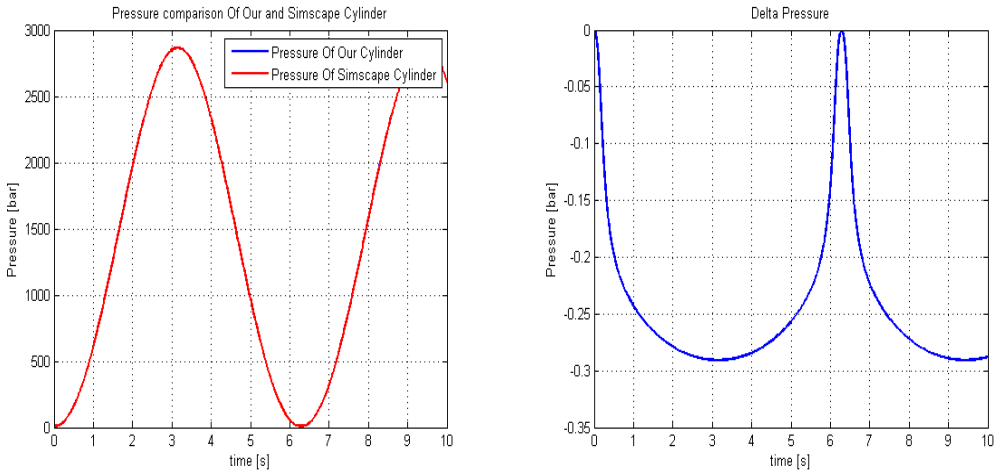

Figure 2-27 Error comparison on cylinder chamber pressure

We can observe how the error done is minimal and can be attributed to a different model of the bulk modulus variation with pressure. We provide also a graph in which we compare two different displacement:

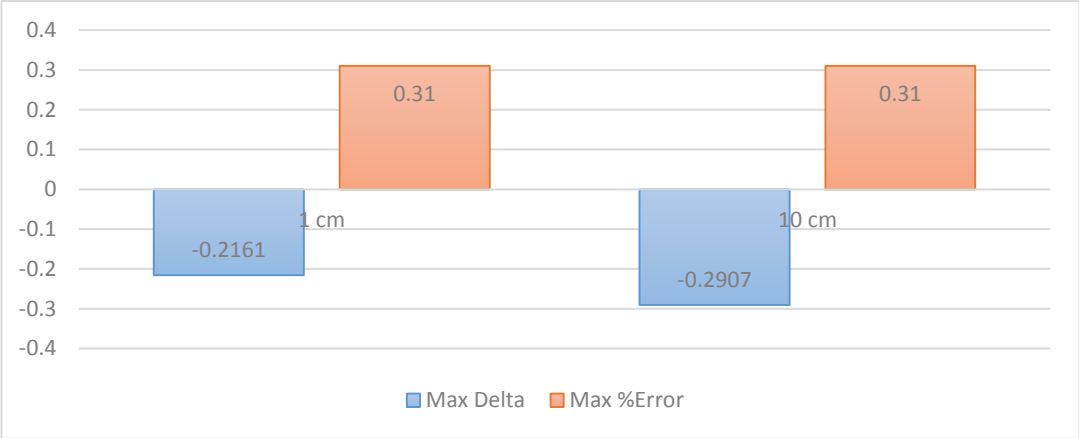

Figure 2-28 Error with different displacements

We can immediately see that the error committed increases with the pressure at which the fluid in the cylinder is subjected (that is related to the

displacement imposed), however the relative error is smaller than 1% and so the model of the cylinder model can be validated.

2.5.3 Valves Manifold:

The valves are the responsible for the flow rate in and out of the cylinders. These electrical commanded valves receive as input a voltage that can be used in two different ways: as a single bit signal that indicates just the open or close configuration, or as a 8 bit signal that identify 256 different configurations. However the signal considered is, we can model the valve as a variable area orifice. We can sketch the valve as it follows:

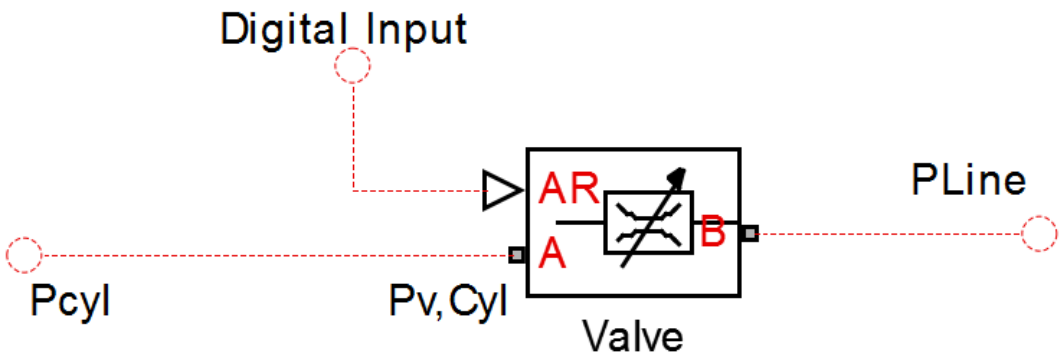

Figure 2-29 Valve as a variable orifice

We decided to avoid the simulation of the fast dynamics of the internal fluid of the valve; this can be done because the volume of the fluid "trapped" in the valve is small compared to the length of the pipes that connect the valve to the cylinder. By mean of this approximation the flow rate relation will connect algebraically the $P_{v,Cyl}$ with P_{Line} as it follows:

$$P_{v,Cyl} = P_{line} - \left(\frac{Q_v}{C_d A_v(\alpha_v)} \right)^2 \frac{\rho}{2} = P_{line} - \left(\frac{Q_{m,v}}{C_d A_v(\alpha_v)} \right)^2$$

Where C_d is the discharge coefficient and $A_v(\alpha_v)$ is the area dimension in function of the input and of the dynamic of the valve opening. We can observe how we are not using a compressibility model to describe the pressure drop across the valve. This decision has been done because the Mac number can be neglected thanks to the dimensioning of the valve. The expression of the density change in the valve can be written as [20]:

$$\frac{\rho_0}{\rho} = \left(1 + \frac{\gamma - 1}{2} M^2 \right)^{-(\gamma-1)} \approx 1 + \frac{1}{2} M^2$$

This means that we are entitled to use the Bernoulli's theorem for incompressible fluid without committing big errors. We are using this approximation just in the valve that has a limited amount of fluid while we will consider the variation of the density within the pipes.

Once we have defined the $P_{v,Cyl}$ as function of the flow rate we can impose the differential equation that connects the difference of pressure between cylinder and valves to the mass flow rate in fact:

$$\dot{Q}_{m,v} = \frac{\left(P_{v,Cyl} - P_{cyl} \right) A_{tube} - P_{losses}(Q_v) A_{tube}}{l_{tube}}$$

As we can see we have the usual pipes dynamics and losses as described in section [2.5.1], obviously we must consider also the concentrated losses due to the discharge of the fluid in the cylinder and the pipe fittings.

We are considering also the time necessary to open and close the valve chamber. In fact, this time is not negligible if we want to develop a good model. The opening and closing of the valve can be described by a step function considering the single bit input:

$$A_v(\alpha_v) = \alpha_v A_0 \quad \text{where } A_0 \text{ is the fully opened valve}$$

With the dynamic of α_v defined by:

$$\dot{\alpha}_v = \begin{cases} \frac{1}{t_v};\ \alpha_v < 1 \wedge u_v = 1 \\ -\frac{1}{t_v};\ \alpha_v > 0.005 \wedge u_v = 0 \\ 0;\ \text{else} \end{cases}$$

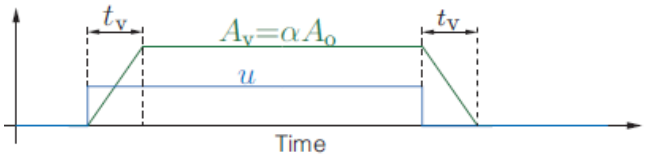

Figure 2-30 Valve Opening and closing behavior

We can observe how we have limited the value of α_v to a 0.5%, this is to avoid the infinite pressure resistance that would mathematically arise with a null area.

2.5.3.1 Comparison with the Simscape model:

We must test if the valves have a behavior that is comparable to the Simscape model. In Simscape we selected the valve as a variable orifice valve. We have then imposed values of pressures in the cylinder chamber and in the pressure line. The resulting flow rates as we can observe are similar and the error committed is negligible. The graph shown is for a pressure gap of 140 bar:

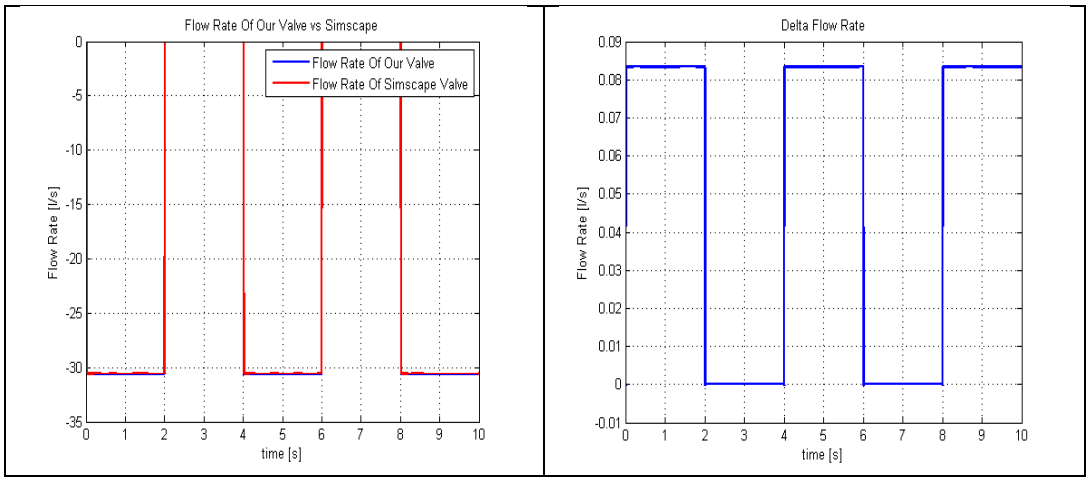

Figure 2-31 Comparison on the flow rate

As for the cylinder we will define the relative error and the maximum difference in the flow rate in two different delta pressure conditions:

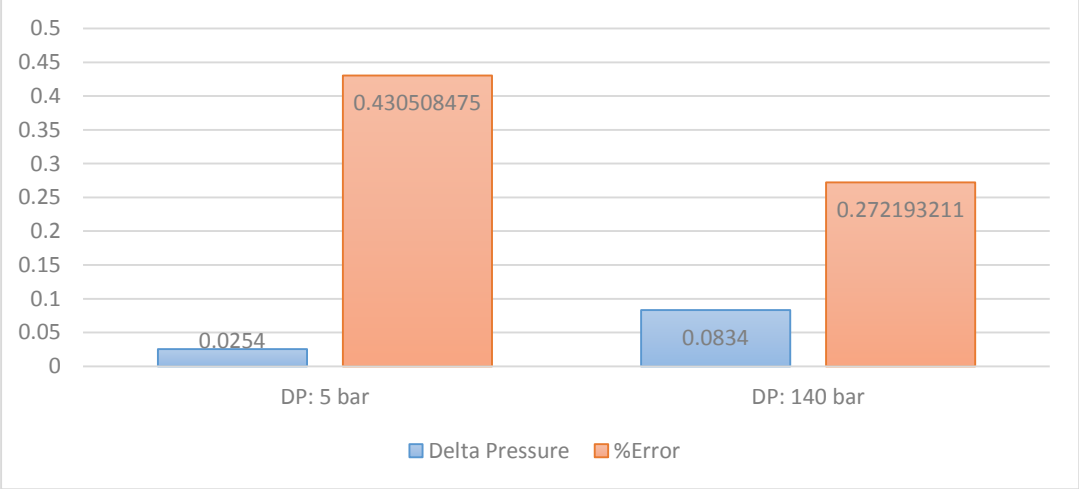

Figure 2-32 Error with different DP

We can observe how the percentage error is contained. This difference is mainly due to a different model of the pipe losses.

2.5.4 The Accumulators:

The generation of energy through waves is, as anticipated, really irregular, while the frequency of the grid requires a regularity. This is achieved through the usage of inverters, which through the conversion AC-DC-AC manage to achieve a regular frequency. Despite their presence, a battery of accumulator is very useful to regularize the working condition of the hydraulic motor. When the system is pumping more fluid than required, this will be stored inside the accumulator, which vice versa will release fluid as soon as the production is less than the requirement.

The accumulator can be modelled in different ways, depending on the hypothesis we are setting. Our accumulators are provided of a sack where inside there is a gas, which pressurizes the fluid. In this way air and fluid do not mixture. Considering the same pressure and temperature of the gas and of the fluid, we will have two degrees of freedom of the system (given all the extensive parameters), so two differential equations describing the system. In order to know the state of our accumulator, we have to know the values of pressure and temperature. The volume, like every state variable, will be a consequence of them.

We will develop three models of the accumulator, in particular we will find out the equations of:

Acc_1: accumulator with an heat exchange and compressibility taken into account

Acc_2: adiabatic accumulator with compressibility taken into account

Acc_3: adiabatic accumulators without compressibility

These kinds of accumulators show different behaviors. In fact, while the first one will experience losses due to heat exchange, the latter won't experience the variation of pressure due to the exchange with the external world. This means that the adiabatic accumulators are more efficient (if we consider, reasonably, that the temperature inside the accumulator will always be greater than the external one). Simulink library uses accumulators which are of kind 3, and these considerations will be needed to justify our different choice.

About the difference between the last two accumulators, when we consider the compressibility of the fluid and we perform a thermodynamic cycle, we have like a spring in our system. The fluid compresses during compression and expand during expansion, like the gas. This will show different thermodynamic processes but we will see that it won't influence the efficiency of the accumulator (the spring is a storage of energy).

Let's consider a heat exchange and the first law of thermodynamics. The gas inside the accumulator in fact is a closed system, and it will respect the following:

$$\frac{dU}{dt} = \frac{dQ}{dt} + \frac{dL}{dt}$$

$$m_g c_v \frac{dT_g}{dt} = kA(T_w - T_g) - P_g \frac{dV_g}{dt}$$

$$\frac{dT_g}{dt} = \frac{1}{\tau_a}(T_w - T_g) - \frac{R_g T_g}{c_v v_g}\frac{dv_g}{dt} = \frac{1}{\tau_a}(T_w - T_g) - \frac{R_g T_g}{c_v V_g}\frac{dV_g}{dt}$$

Where τ_a is the thermal time constant, and it's related to the dynamicity of the heat exchange in the system [21]. If the value is high, it means that the process of heat exchange is slow.

In the equations we used also the gas law in specific terms:

$$P_g v_g = R_g T_g$$

We now consider both the state equation of the gas and of the fluid, written in differential way:

$$\frac{dP_f}{dt} = \frac{\beta}{V_f}\frac{dV_f}{dt}$$

$$\frac{dv_g}{dt} = \frac{dv_g}{dP_g}\frac{dP_g}{dt} + \frac{dv_g}{dT_g}\frac{dT_g}{dt} = \frac{-R_g T_g}{P_g^{\,2}}\frac{dP_g}{dt} + \frac{R_g}{P_g}\frac{dT_g}{dt} = \frac{-v_g}{P_g}\frac{dP_g}{dt} + \frac{v_g}{T_g}\frac{dT_g}{dt}$$

$$T_g = T_f \qquad \mathrm{P}_g = P_f \qquad V_g = V_{acc} - V_f - V_{ext}$$

Where we set also the relations between the gas state variables and the fluid ones. The external volume is considered to take into account a part of the volume of the fluid outside the accumulator. This volume belongs to the system we are considering.

If now we analyze what is the rate of change of the volume of fluid inside the accumulator:

$$\frac{dV_f}{dt} = Q_a + \frac{dV_g}{dt}$$

With all these set we can write two differential equations in terms of T,P and their derivatives, since we can express the volume of the gas and its rate of change in terms of them.

$$\begin{cases} \dfrac{dT}{dt} = f_1\left(\dfrac{dP}{dt}, P, T\right) = \dfrac{1}{1+\dfrac{R_g}{c_v}}\left(\dfrac{1}{\tau_a}\left(T_w - T\right) + \dfrac{R_g T}{c_v P}\dfrac{dP}{dt}\right) \\ \dfrac{dP}{dt} = f_1\left(\dfrac{dT}{dt}, P, T, Q\right) = \dfrac{1}{1+\dfrac{V_g \beta}{V_{liq} P}}\left(\dfrac{V_g \beta \dfrac{dT}{dt}}{V_{liq} T} + \dfrac{\beta Q}{V_{liq}}\right) \end{cases}$$

$$P(0) = P_{in}$$
$$T(0) = T_{in}$$
$$V_g = \frac{R_g T}{P_g}$$

To carry out an accumulator that is adiabatic and considers the compressibility, we simply have to put the time constant equal to infinite. This correspond to multiply the first term of the right hand side of the temperature differential equation with zero.

$$\frac{dT_g}{dt} = -\frac{R_g T_g}{c_v V_g}\frac{dV_g}{dt}$$

The differential equation of the pressure remains the same. What we get integrating the equation above, are the usual relationship between the variables in an adiabatic process.

$$\mathrm{T}\, v^{\gamma-1} = \mathrm{cost} \qquad Pv^{\gamma} = \mathrm{cost} \qquad P^{1-\gamma}T^{\gamma} = \mathrm{cost}$$

If we want to develop the third model of the accumulators described above, we have to apply another consideration. If there is no compressibility, in fact, it means that the flow rate of the water equals the rate of change of the volume of gas with time:

$$Q = -\frac{dV_g}{dt}$$

In this case we lose one differential equation, and we keep the differential equation of the temperature.

$$\frac{dT_g}{dt} = -\frac{R_g T_g}{c_v V_g}\frac{dV_g}{dt} = -\frac{R_g T_g}{c_v \int_t Q} Q$$

The equation can be as well transformed in a system of the differential equation, but one of this is a simple integrator between the volume of gas and the input, that is the flow rate.

Solving the only equation we have, we get immediately to the result, which is, like before, the relationship between variables in an adiabatic process, commanded by the input directly connected to the volume;

$$\mathrm{T}\, v^{\gamma-1} = \mathrm{cost} \qquad Pv^{\gamma} = \mathrm{cost} \qquad P^{1-\gamma}T^{\gamma} = \mathrm{cost}$$

Despite the relationship between the variables remains the same, their time history changes between case 2 and 3. In the second case, in fact, we have another differential equation that rules the trend of pressure.

Let's briefly analyze the differences performing firstly a thermodynamic cycle.

The data of the simulation are:

$$P_{acc,empty=}40bar \qquad T_{acc,empty} = 20C \qquad V_{acc,empty} = 50l \qquad \tau_a = 200$$

And the results are the following graphs:

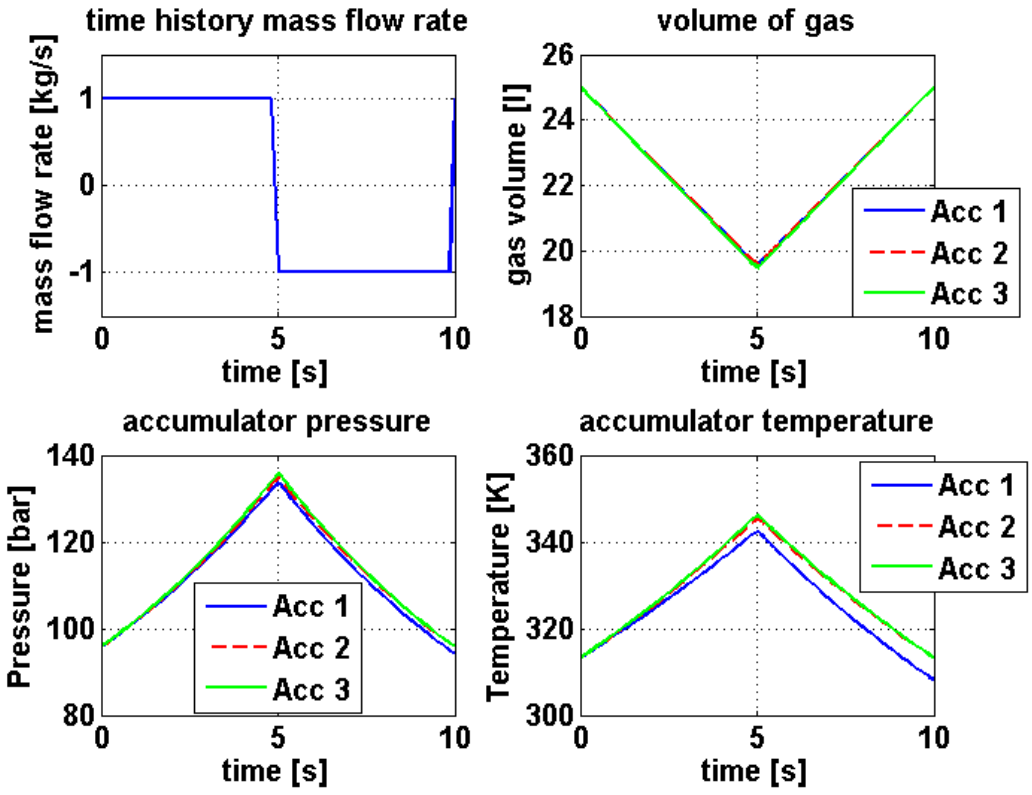

Figure 2-33 Accumulators Variables Trend

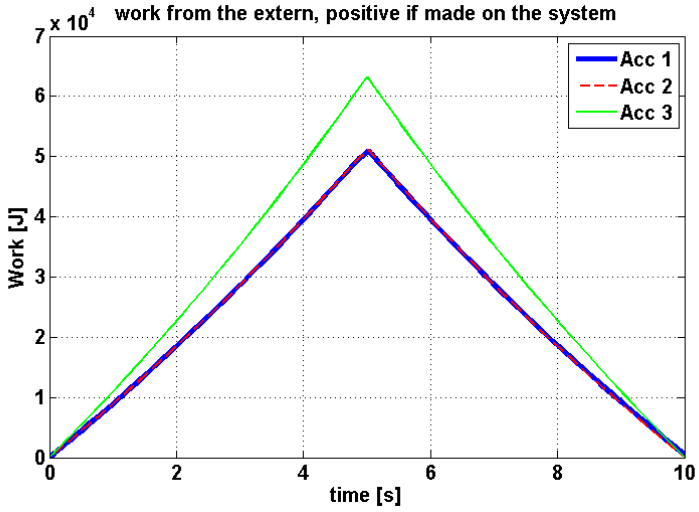

Figure 2-34 Work inside the Accumulator

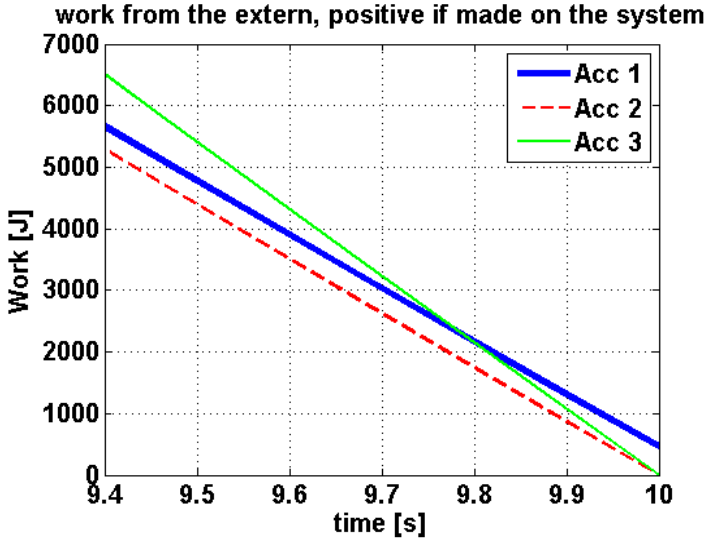

Figure 2-35 Work inside the Accumulator Zoom of the last second

This cycle is simply an imposition of mass flow rate inside the three accumulators. We can see how the initial point equals the final point for accumulators 2 and 3, while for accumulator 1, which experienced a loss of

energy, the final point does not equal the initial point. Moreover, if we make a calculation of the total work, it turns out that is null for cases 2 and 3 (we were given back what we gave), while it is greater than zero for case 1 (we lost some power during the storage time, due to the heat exchange).

We can see how, despite the two adiabatic accumulators give backs the same energy that they received, their behavior in the middle of the cycle is different. The drop of pressures in the uncompressible case are bigger, because all the energy we provide is used to compress just the gas, and not also the fluid. At equal flow rate and time (equal inner mass of fluid), we are able to store more energy in case 3.

2.5.4.1 Comparison with the Simscape model:

Let's now do a last simulation for the single accumulators. We just fill the accumulators with a flow rate of 0.25l/s for 10 seconds, and we check the relationship between the state variables. We can see how the stories are equal between cases two and Simscape (case 3), despite the final point of the dynamic process is different. We finally remember that we are considering ideal adiabatic processes, meaning isentropic.

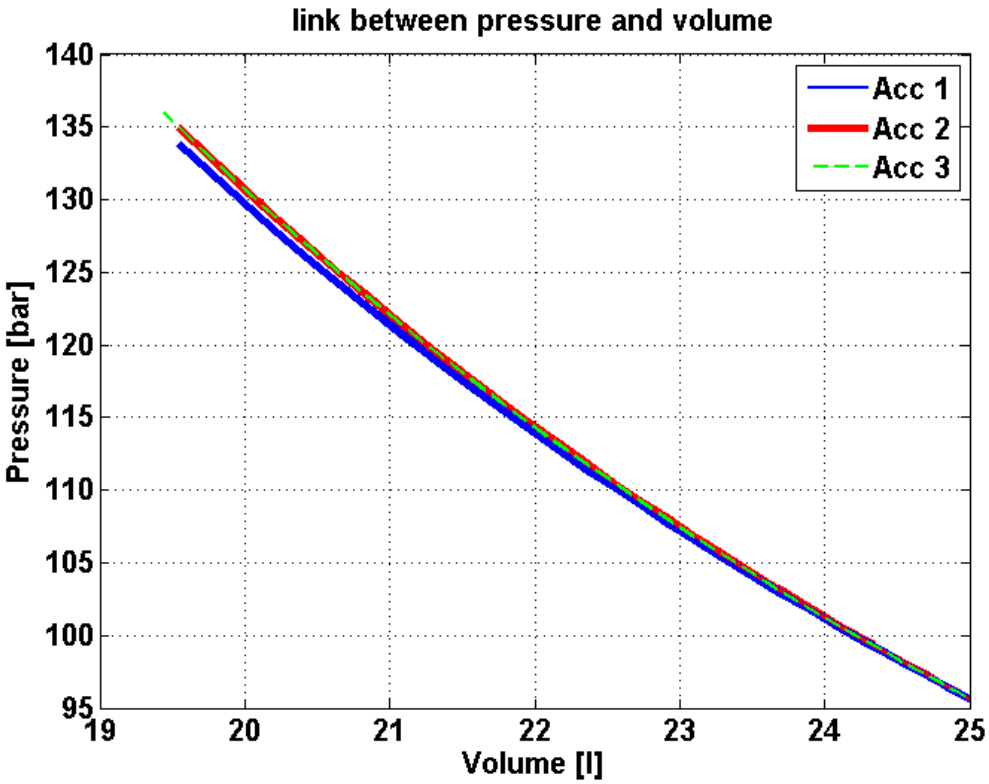

Figure 2-36 P-v plane

We can see from the figure above that the initial points, on the right of the graph, coincide. We started with the accumulator half full of water. Since the models are different, computing the relative errors does not have sense and utility. Accumulator number three instead, shows a relative error equal to 0 with respect its relative Simulink block.

The connection between the hoses and the accumulators is made by a valve. This means that the pressure in the accumulator is not exactly equal to the pressure upstream of it. The relation is algebraic, and it involve the equation of the orifice:

$$P_{acc,upstream} = P_{acc} + sign(Q_{acc})\frac{\rho Q_{acc}^{\ 2}}{2A_a}$$

Where the flow rate if the accumulator is positive if the flow enters. In this case we have a pressure inside the accumulator less than the one upstream.

The pressure just outside the accumulator will influence the behavior of the valve.

2.5.5 Hydraulic motor and generator:

The final step of the power take off system is the conversion of the hydraulic energy into the electrical one, which is sent to the grid. The hydraulic motor is a hydraulic machine that converts hydraulic energy into mechanical, and a result of the process is the rotation of the shaft. In the same shaft the electric machine is keyed, and it works as a generator, converting the mechanical energy into electrical. As we can see this conversion has some steps, each of which contribute to determine the total efficiency [2.8].

Let's firstly describe the hydraulic motor, and the conversion from hydraulic into mechanical energy.

2.5.5.1 Hydraulic into mechanical energy conversion:

The fundamental variables which describes the working principle and the conversion of the energy are the flow rate, the angular velocity, the torque and the pressure head. If we consider an ideal case we can achieve the relation between the flow rate and the angular velocity:

$$Q = cil[m^3] * \frac{rpm}{60} = cil[m^3] * \frac{w}{2\pi} = D_w w$$

If we consider an ideal transmission, without any mechanical loss, we can write that the hydraulic power equals the mechanical one:

$$P_{hyd} = Q\Delta P = P_{mech} = Cw$$

$$P_{hyd} = Q\Delta P = D_w w\Delta P = Cw \rightarrow C = D_w \Delta P$$

And we achieve that the torque is proportional to the hydraulic head.

We don't deal with an ideal case, but with a real one, that undergo a loss of energy inside the motor, expressed by a hydraulic efficiency and a mechanical one. The hydraulic efficiency is due to the leakage losses, and acts hence as a loss of hydraulic power. To give the same angular velocity, a greater flow rate is required. The mechanical efficiency, instead, acts at the output shaft. We achieve less power output than in the ideal case. The latter considerations explains the position of the efficiency terms in the real equations:

$$Q = \frac{D_w w}{\eta_{hyd}}$$

$$C = D_w \Delta P \eta_{mech}$$

$$P_{hyd} = Q\Delta P \neq P_{mech} = Cw = \left(D_w \Delta P \eta_{mech}\right)\left(\eta_{hyd} \frac{Q}{D_w}\right) = Q\Delta P \eta_{mech}\eta_{hyd} = \eta_{mech}\eta_{hyd} P_{hyd}$$

Where we put into evidence the losses due to the conversion process inside the motor. These efficiency are not constant, but they depend on the

working condition of the motor. Following partly [8], we can express the real value of flow rate and torque in the following way:

$$\eta_{hyd} = 1 - \left(C_{h1} + C_{h2}\Delta P + C_{h3} w \right) < 1$$

$$\eta_{mech} = 1 - \frac{\left(C_{t1} + C_{t2}\Delta P + C_{t3} w + C_{t4} w^2 \right)}{D_w \Delta P} < 1$$

Searching hydraulic motors from [22], we can find the curves that describe the two efficiency of the motor, selecting a stroke of 50cc for our final system. We doing a best fit with these curves in order to find the coefficient that best approximate them. The algorithm used exploit the minimum square error method. We can then easily write, for our hydraulic motor:

$$Q = \frac{D_w w}{1 - \left(C_{h1} + C_{h2}\Delta P + C_{h3} w \right)}$$

$$C = D_w \Delta P - \left(C_{t1} + C_{t2}\Delta P + C_{t3} w + C_{t4} w^2 \right)$$

We now give some consideration about the model we will adopt.

1) The volumetric flow rate is not equal at the inlet and outlet of the motor. In our model, the coefficient of proportionality express the relation between the angular speed and the inlet flow rate. Since we are having an expansion within the motor, the outlet flow rate will be greater than the input one. This drove us to consider a proportionality between the angular velocity and the mass flow rate, instead of with the volume flow rate (which is not unique across the motor). We scale the stroke

coefficient in an appropriate way to achieve that (dividing it by the density at the inlet conditions).

2) The shape of the curve has been made with trials in order to achieve a good fit, and some coefficient might be negative, as the case of C_{h3}, since the hydraulic efficiency increases with the angular speed (less leakage).
3) To implement a faster system, we will consider for the losses the drop of pressure equal to the difference of pressure between the high and the low accumulators.

We have now the expression of the torque, and we can hence obtain the torque curve C (w). This curve will have an intersection point with the generator curve. This point will give the operational condition when the transients are over.

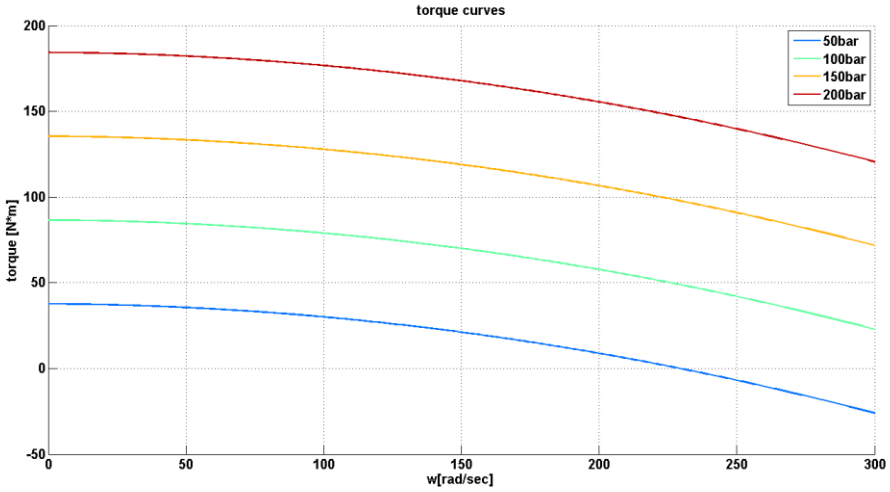

Figure 2-37 Motor Curves

2.5.5.2 Mechanical into electrical energy conversion

We now start considering the conversion from mechanical into electrical energy [23].

The machine responsible for this is the asynchronous machine, which can work both as a motor and as a generator. This machine has a curve that pass through different areas, and each area corresponds to a different operational condition of the machine (motor, generator, brake).

To understand how we can achieve this curve we briefly describe the machine. We will avoid the description of the transient, coherently with our implementation in Simulink. The transient is, instead, modelled within the Simulink block "asynchronous machine", but it's very fast compared to our dynamicity. This justifies our choice.

A rotor and a stator compose the machine. The stator has 3 windings, one for each phase, and it is connected to the grid in order to get reactive power. This power is used to generate a rotating magnetic field. The rotor is composed by the same number of windings short-circuited, which experience across them a variation of flux of magnetic field. Differently from the DC machine, whose working principle is based on the Ampere law (Lorentz force), to understand the working principle of the AC machine we have to base on the Faraday law (that's why the machine is also called the induction machine). This variation of flux produces a current in the rotor windings. The rotation of the magnetic field is connected to the frequency of alimentation through the couple of poles of the machine. Its velocity of rotation is called the synchronous velocity.

$$w_s[rpm] = 60\frac{f}{p}$$

The magnetic axis of the rotor field tends to align with the stator rotating magnetic axis. This is achieved by a generation of a motor torque that balances the inertia, and, if there were no external torque, the rotor would accelerate till the synchronous velocity, and when it reaches it there won't be any motor torque (equilibrium final condition, in an ideal case without any disturbance and friction).

If there is external torque, there must be motor torque also at the regime condition. This is created by a shift between the rotor angular speed and the synchronous speed. This difference produce the torque. The magnetic field of the rotor, though, rotates at the same velocity of the stator magnetic field, but it has a relative velocity with respect the rotor different from zero. The induced frequency in the rotor is:

$$f_{B,rot} = \frac{n_0 - n}{60} p = \left(\frac{n_0 - n}{n_0}\right)\left(\frac{pn_0}{60}\right) = sf_{B,stat} = sf$$

n_0 = syncronous speed [rpm]

n=rotor speed [rpm]

p=number of poles couples

Where s is define as the rotor slip. When the rotor is still (w=0) this value is equal to 1. When the rotor is spinning with zero external torque, the speed equal the synchronous one and the slip is 0.

This means that all the rotor electrical variables have a frequency equal to $f_{B,rot}$, as seen by the rotor relative frame. This turns to be useful when we build the equivalent circuit. If the motor spins at the synchronous velocity, we don't have any induction, and, hence, any torque.

To build the model, we start from the fact that when the rotor is open (not short-circuited) the machine acts like a transformer. If k=1, the exact voltage is transmitted to the rotor open cage (losses neglected).

If we close the rotor circuit, we induce a current and a torque. The equivalent circuit of one phase could be seen like the following.

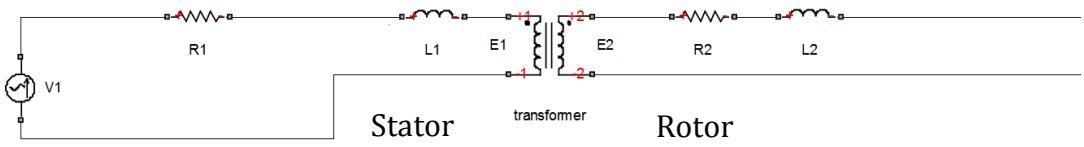

Figure 2-38 Schematic Structure for the Asynchronous Generator

For how the machine works, both the magnitude and the frequency of the voltage in the rotor depend proportionally to the motor slip. This happens because, if k=1, the voltage magnitude in the stator and in the rotor can be written as:

$$V_{stat} = 2K\phi f_{stat} N = V_1$$

$$V_{rot} = 2K\phi f_{rot} N = 2K\phi f_{stat} Ns = V_{stat} f = V_2$$

K : constant of the motor

N:number of conductors of one phase

If we write the equation of the equivalent circuit, we know that we can work with complex vectors, and we can write the following:

$$Z_1 = R_1 + jw_s L_1$$

$$Z_2 = R_2 + jw_r L_2 = R_2 + jsw_s L_2$$

$$w_s = w_0$$

$$I_2 = \frac{sE_1}{R_2 + jL_2 sw_0} = \frac{E_1}{\frac{R_2}{s} + jL_2 w_0} = \frac{E_1}{R_2 + jL_2 w_0 + \frac{R_2(1-s)}{s}}$$

This circuit can be represented by a constant inductance and a variable resistance with s.

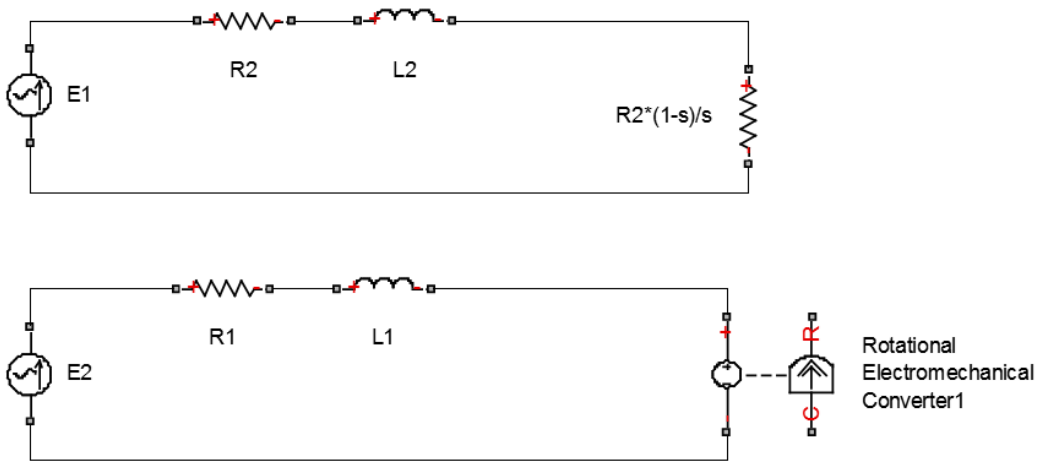

Figure 2-39 Equivalent Circuits for the Asynchronous Generator

The variable resistance converts the electric energy into the mechanical one. To do all the calculation, we have firstly to build the whole circuit, considering the stator as well. We want, in fact, to achieve expressions as function of the input, which is the stator voltage. We decide to bring everything to the rotor side, but being k=1 this won't provoke any change in the parameters.

The total equivalent circuit is the following, where we take in account even magnetic and electrical losses through a parallel impedance, but for the calculation of the current and the torque they won't have any influence as can be seen from the circuit below here. They influence the total efficiency of the system.

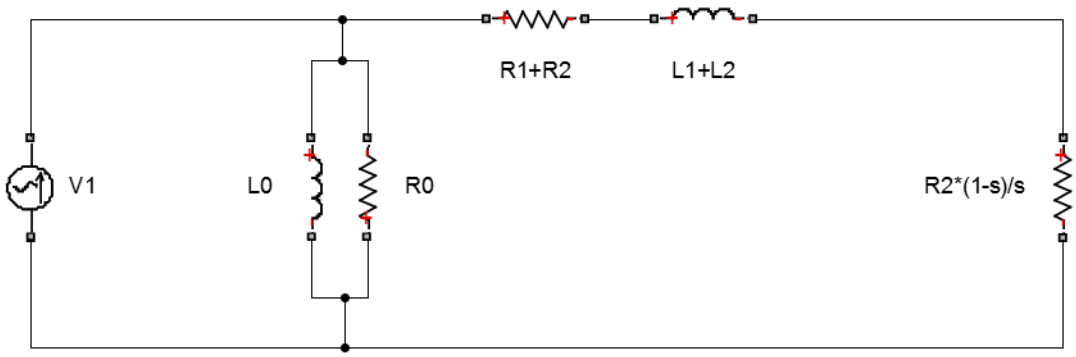

Figure 2-40 Equivalent Circuit for the Asynchronous Generator

We can now carry out all the calculations:

$$I_{12} = \frac{V_1}{\sqrt{\left(R_1 + \frac{R_2}{s}\right)^2 + \left(w_0\left(L_1 + L_2\right)\right)^2}} = \frac{V_{rms}}{\sqrt{\left(R_1 + \frac{R_2}{s}\right)^2 + \left(w_0\left(L_1 + L_2\right)\right)^2}}$$

$$P_{el} = 3\left(R_1 + \frac{R_2}{s} \right) {I_{12}}^2$$

$$P_{ep} = P_{ep1} + P_{ep2} = 3(R_1 + R_2){I_{12}}^2$$

$$P_t = 3\frac{R_2}{s}{I_{12}}^2$$

$$P_m = 3R_2\frac{(1-s){I_{12}}^2}{s} = P_t - P_{ep2} = P_{el} - P_{ep}$$

$$P_m = Cw_{rot}$$

$$C = \frac{P_m}{w_{rot}} = 3R_2\frac{(1-s){I_{12}}^2}{(w_0(1-s))s} = 3R_2\frac{{I_{12}}^2}{sw_0} = 3R_2\frac{1}{sw_0}\frac{{V_{rms}}^2}{\left(R_1 + \frac{R_2}{s} \right)^2 + \left(w_0(L_1 + L_2) \right)^2} = f(s)$$

$$s = \frac{w_0 - w}{w_0}$$

P_{el} = electric power

P_{ep} = electric lost power

P_t = electromagnetic power

P_m = mechanical power

We can plot the curve of the motor torque. The slip can go between minus infinite to infinite, since a priori the rotor can rotate at any speed. To plot the diagram, we use the data we have.

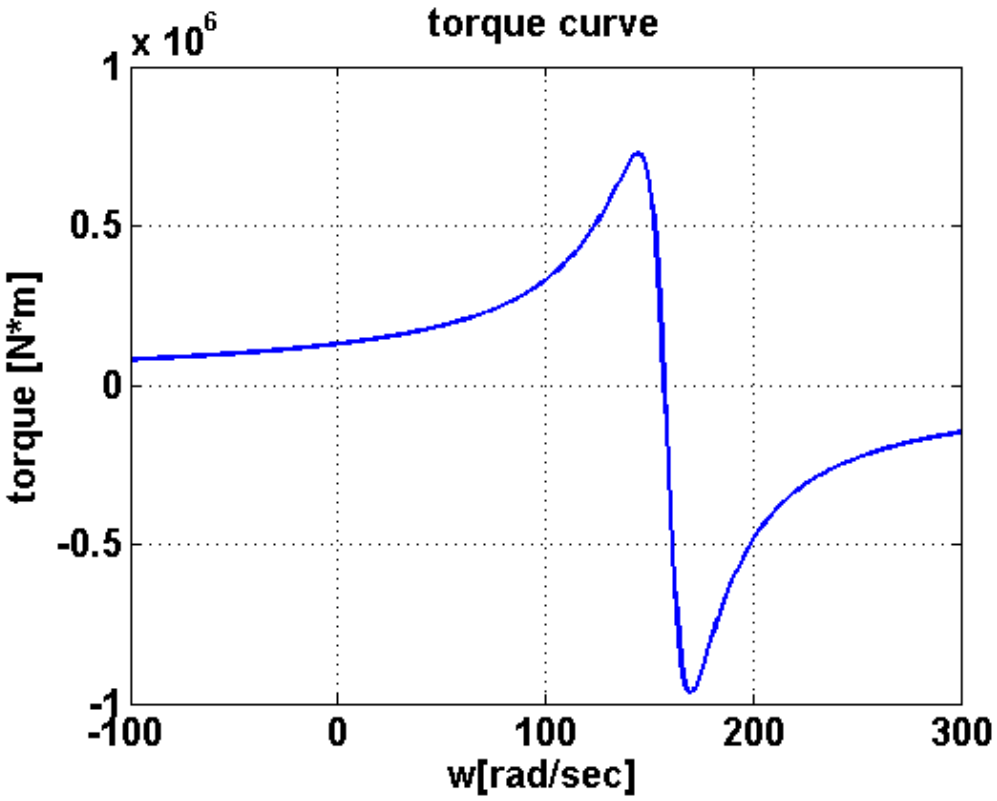

Figure 2-41 Asynchronous Motor Curve

Corresponding to the different regions the machine works differently. If the torque and the angular velocity has different signs, in fact, the machine work as a generator (or just as brake if the power available is not enough to win the

internal losses). The behavior is exactly the same, the only difference is that the rotor spins faster than the stator magnetic field, and so the direction of the magnetic field generated by the rotor is opposite with respect its source. This implies a negative torque, which must be balanced by a positive torque outside, which must be also greater to the one necessary to win just the internal losses. To define the operational regime point of the system, we spill the curve of the generator, since we are looking at it from the user point of view. We scaled the electrical torque since the two curves cover values different between each other and the graph would not be readable.

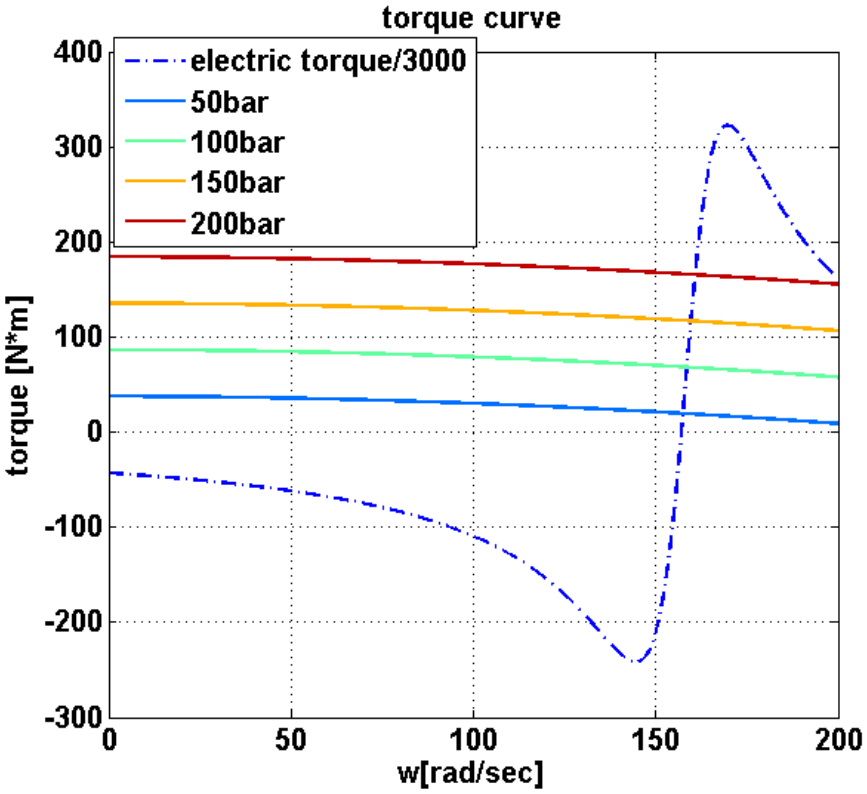

Figure 2-42 Intersection between Hydraulic Motor and Asynchronous Generator

We can see how the equilibrium point is stable, and how the velocity in the operational point is almost constant regardless the gradient of pressure across the motor. This is due to the very steep gradient of the generator curve, and it makes the regulation of the velocity really easier. The transient will be finally descripted by the dynamic equilibrium equation:

$$\frac{dw}{dt} = \frac{1}{\left(J_{mot} + J_{gen}\right)}\left(C_{mot} - C_{gen} - Fw\right)$$

Where the last term takes into account the mechanical losses due to the friction that acts on the generator (the one of the motor are already taken into account through the efficiency)

We now connect the system hydraulic motor-generator to the whole system. As usual, to connect the elements in the hydraulic circuit we need hoses. Since we are coupling the equation of the hoses with the one achieved before, we will write the equation that rules the behavior of the part of the system composed by the high pressure hose, the motor, the generator and the low pressure hose.

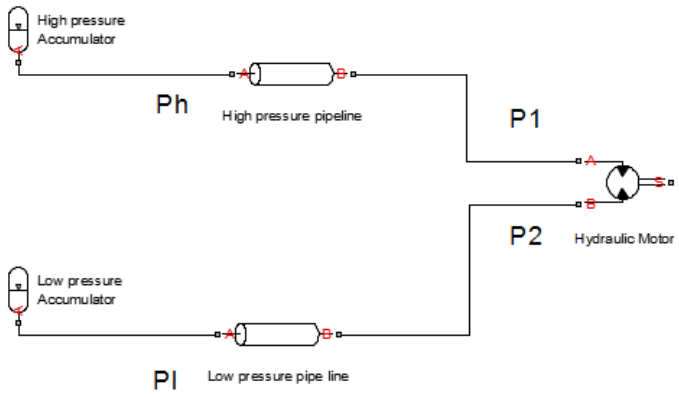

Figure 2-43 Scheme of the Pressure Lines Connected with the Hydraulic Motor

We consider that the mass flow rate and its rate of change are the same in the high pressure hose and in the low pressure one:

$$\frac{dQ_m}{dt} = \frac{A}{l}\left(P_H - P_1 - P_{loss,tot}(Q_1)\right) = \frac{A}{l}\left(P_2 - P_L - P_{loss,tot}(Q_2)\right)$$

P_H = pressure just nearby the entrance of the high pressure accumulator

P_L = pressure just nearby the entrance of the high pressure accumulator

P_1 = pressure just nearby the inlet of the motor

P_H = pressure just nearby the outlet of the motor

Where we pointed out how the volume flow rates changes from the top to the bottom of the motor, since an expansion occurs. Anyway, for the little weight that the losses have in our system, considering the same volume flow rate to calculate the losses in both tubes will take to an error equal almost to zero, and to a better simplicity of representation through the block diagrams

(given as single input the inlet flow rate, we have all the losses in one calculation).

We can now couple all the equations, and we achieve at the end the final result:

$$Q_m = \rho_{in} D_w w$$

$$\rho_{in} = \rho_0 e^{\int_{P_{atm}}^{P_{in}} \frac{dP}{\beta(P)}}$$

$$\frac{dQ_m}{dt} = \frac{A}{l}\left(P_H - P_1 - P_{loss1,tot}(Q_1)\right) = \frac{A}{l}\left(P_2 - P_L - P_{loss2,tot}(Q_2)\right)$$

$$P_1 = P_H - P_{loss1,tot}(Q_1) - \frac{l}{A}\frac{dQ_m}{dt}$$

$$P_2 = P_L + P_{loss2,tot}(Q_2) + \frac{l}{A}\frac{dQ_m}{dt}$$

$$P_1 - P_2 = \Delta P_{mot} = P_H - P_L - P_{loss1,tot}(Q_m) - P_{loss2,tot}(Q_m) - 2\frac{l}{A}\frac{dQ_m}{dt} = \Delta P_{mot}\left(Q_m, \frac{dQ_m}{dt}\right) = \Delta P_{mot}\left(\mathrm{w}, \frac{dw}{dt}\right)$$

$$C_{mot} = D_w \Delta P_{mot}\left(\mathrm{w}, \frac{dw}{dt}, P_H, \mathrm{P}_L\right) - \left(C_{t1} + C_{t2}\Delta P_{mot}\left(\mathrm{w}, \frac{dw}{dt}, P_H, \mathrm{P}_L\right) + C_{t3}w + C_{t4}w^2\right)$$

The final equation is definitely the following one:

$$\frac{dw}{dt} = \frac{1}{\left(J_{mot} + J_{gen}\right)}\left(C_{mot}\left(\mathrm{w}, \frac{dw}{dt}, P_H, \mathrm{P}_L\right) - C_{gen}\left(w\right) - Fw\right)$$

Where everything appears as a function of w and its rate of change. We can see how the hydraulic system adds an inertia to the motor, that anyway is really small compared to the preexistent one.

In the latter equation the input are the two pressures at the bottom of the accumulators. We can singularly test our motor imposing for example a constant difference of pressure. The result is the velocity (or the flow rate) of the motor.

2.5.5.3 Comparison with the Simscape model:

Let's now perform a simulation, comparing the results of our model with the one made with Simscape. As input of both systems we give a head of 100 bars, and we can compare the output in terms of inlet flow rate.

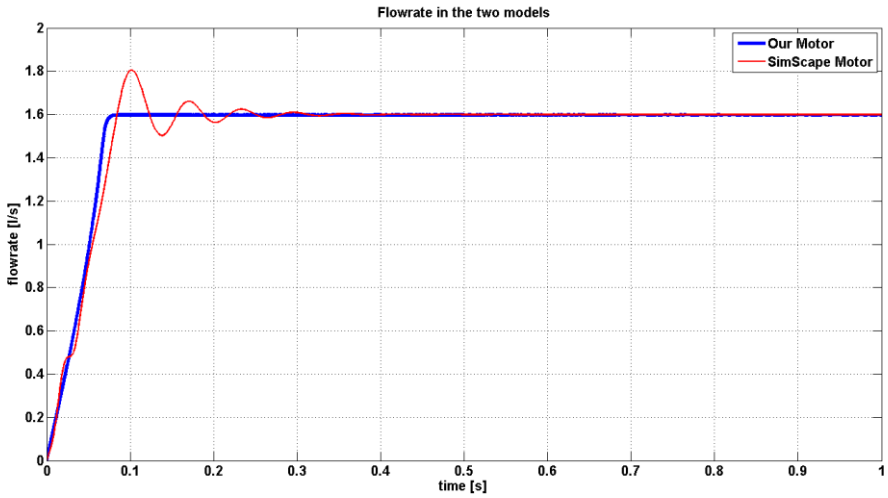

Figure 2-44 Angular Speed with Time

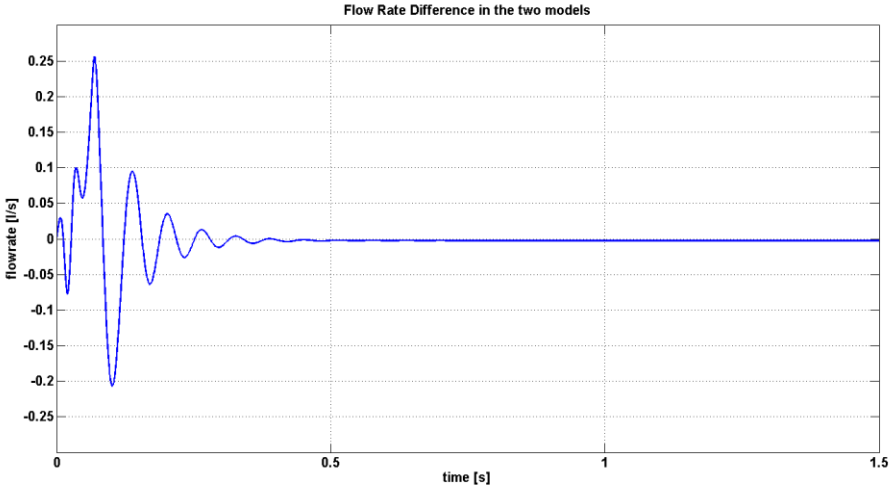

Figure 2-45 Difference Between the Angular Speeds with Time

We can see how the regime value of the flow rate is the same, while we deal with differences when we look at the transient. In fact, since the Simulink blocks have implemented the transient effects, we decided to skip this part and implement a first order model. The dynamic of our system, in fact, is really much slower than the dynamic of the electrical poles, which are responsible of the higher order effect that could be observed just during the transient. In addition to it, we will have a faster model, which will be positive once we connect all the parts together. These considerations justifies our choice.

2.6 MODEL VALIDATION: COMPLETE SYSTEM

Having modeled all the parts of the system we can now proceed to the assembling and run the whole system checking the differences and trying to justify them.

We are going to do two different comparisons between the Simscape Model and Our model since the accumulators give the greatest difference. We are going so to test two different accumulators:

- Simscape Model vs Our Model with adiabatic accumulators that also does not consider the compressibility of the fluid (in the accumulators).
- Simscape Model vs Our Model with real accumulators where we consider the heat exchange and the compressibility.

We will observe how the differences are small enough to validate the model.

The comparison between the models will be carried out using sinusoidal input instead of the random one. This is done in order to see how the system with this kind of input finds a regime dynamic condition.

Before implementing the simulation, we have to be aware that this system can't survive without a basic control that opens and closes the valves in a logical way. Despite it won't be already the optimized one we are setting an easy initial control strategy that will allows to compare our model against the one designed through Simscape.

The basic control that we thought is based on the comparison between the pressure in the cylinder chamber and the pressure in the accumulators. The same strategy has been adopted for the valves that connects the accumulators of high and low pressure. The medium pressure accumulator is not yet connected but it will be used for the optimization strategy.

The idea is to open the high pressure valve when the pressure in the connected chamber is higher of a certain amount with respect the one of the high pressure accumulator. Vice versa, we open the low pressure valve when the pressure in its relative chamber is smaller of a certain amount than the one of the low pressure accumulator. In the other situations, that is when the pressure in the chambers are in between the pressure of the two accumulators, the valves are closed so that we can exploit the compressibility of the fluid. The pumping process occurs mainly in the latter situation.

For the comparison we are going to look at some significant physical quantities:

- Pressure in chamber one
- Volume of water in high and low pressure accumulators
- Pressure in high and low accumulators
- Hydraulic and electrical torque

2.6.1 Comparison 1:

We are going to compare our model with accumulators equal to the Simulink ones with the whole Simulink simulation.

Pressure in chamber one

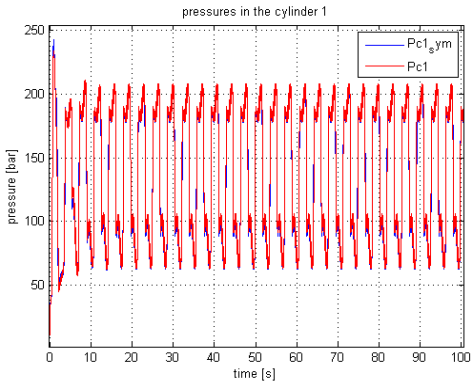

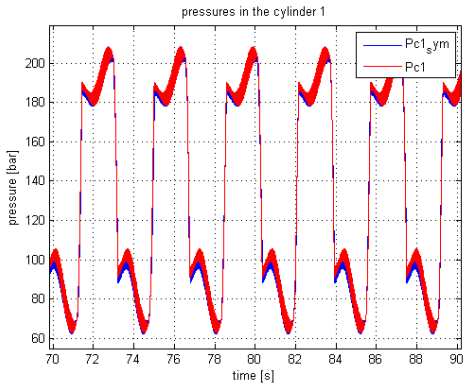

The greatest differences are at the beginning during the transient, while at regime condition the differences are almost negligible.

Volume of water in the high/low pressure accumulator

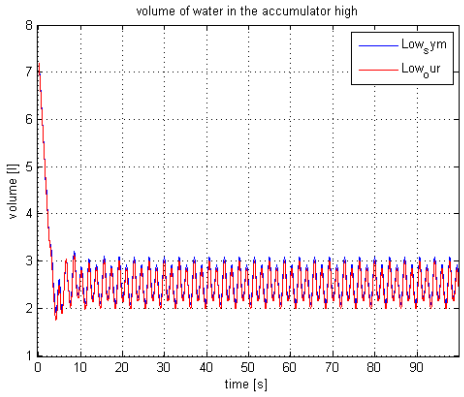

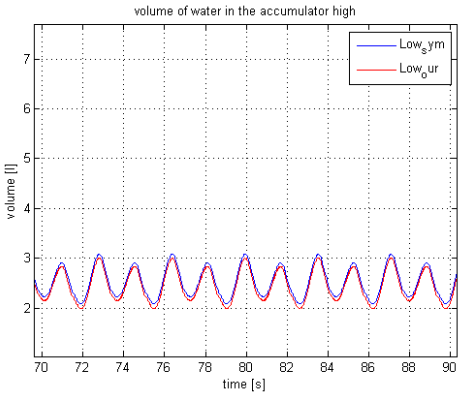

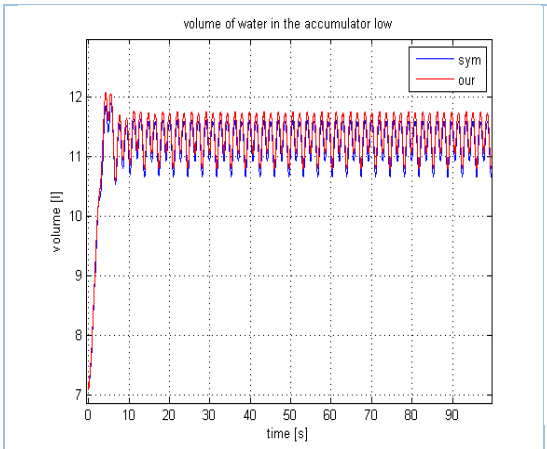

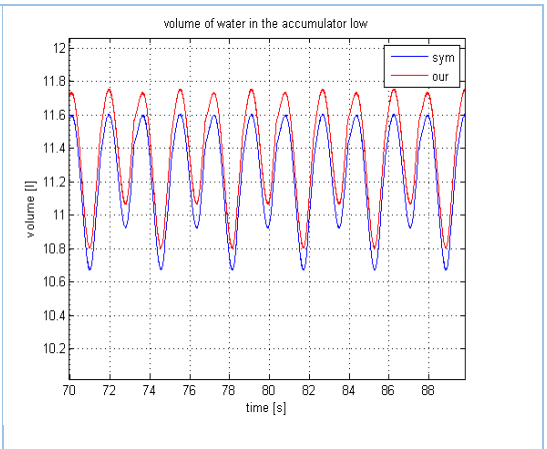

From the accumulator volumes we can see how our model has average volume greater in the low pressure accumulator while is lower in the high pressure one. The difference is almost around 0.1 liter and it keeps constant. This is mainly due to the motor and different opening times of the valves, caused by the differences in the pressures. Our motor, since is not modelled taking into account the electromagnetic poles, requires a different amount of flow rate at the beginning, that averagely is greater. If we integrate the flow rate on time we observe the volume passed through the motor at time T, since the beginning of the simulation. The difference arrived to an asymptotic value, since the derivatives (the flow rates) behaves almost immediately equally. This value partly justify the constant difference between the volumes.

Pressure in the high/low pressure accumulator

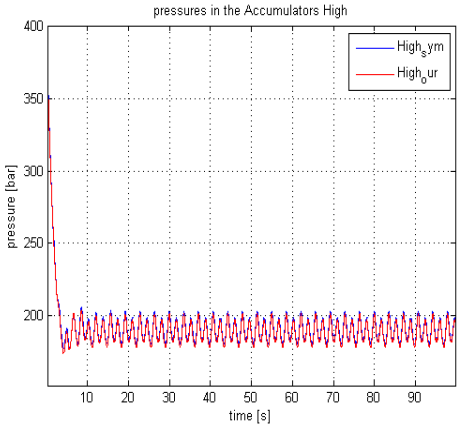

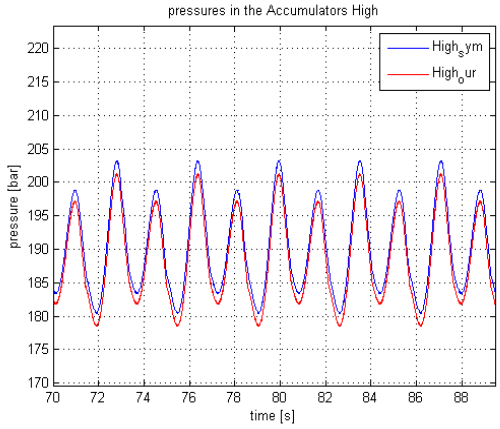

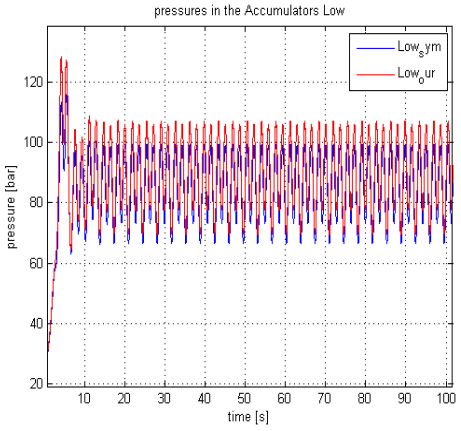

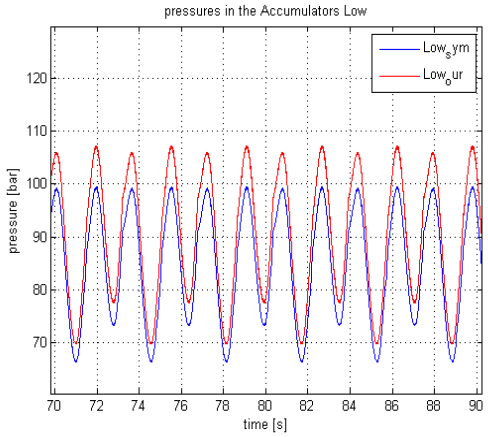

A difference in volume provokes a different pressure. This difference, though, is also due to a different model of losses. Our system has a different model of the losses in the tubes, which are more severe.

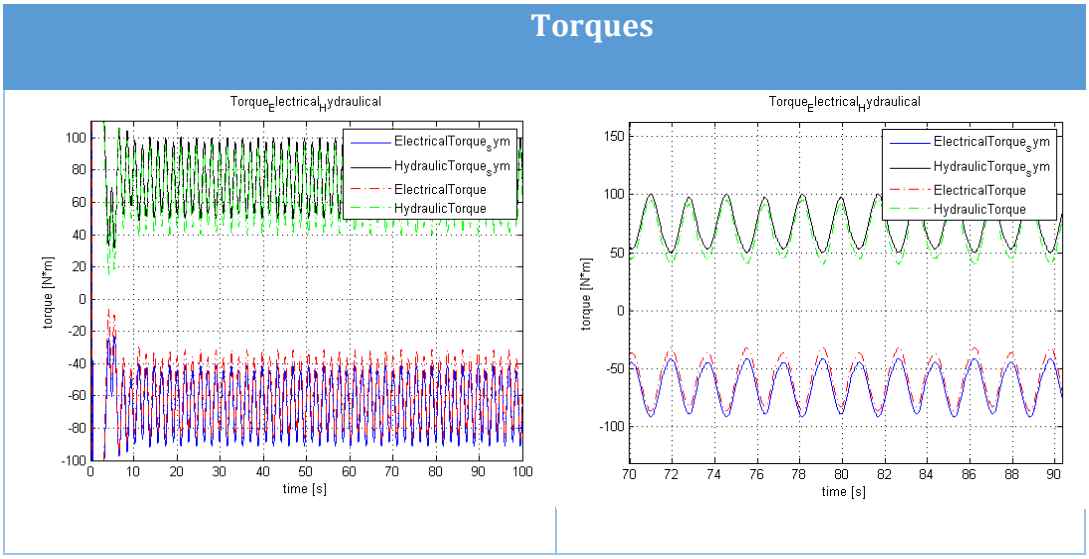

Our electrical torque is smaller than Simulink one, and it means that our efficiency will be less.

2.6.2 Comparison 2:

We are going to compare the model we will definitely adopt, with the Simulink one. We are showing the simulation up to 250 seconds, to put in evidence the thermic transient, which is really slow. The thermodynamic state variables reach a regime value quite different from the Simulink one.

Pressure in chamber one

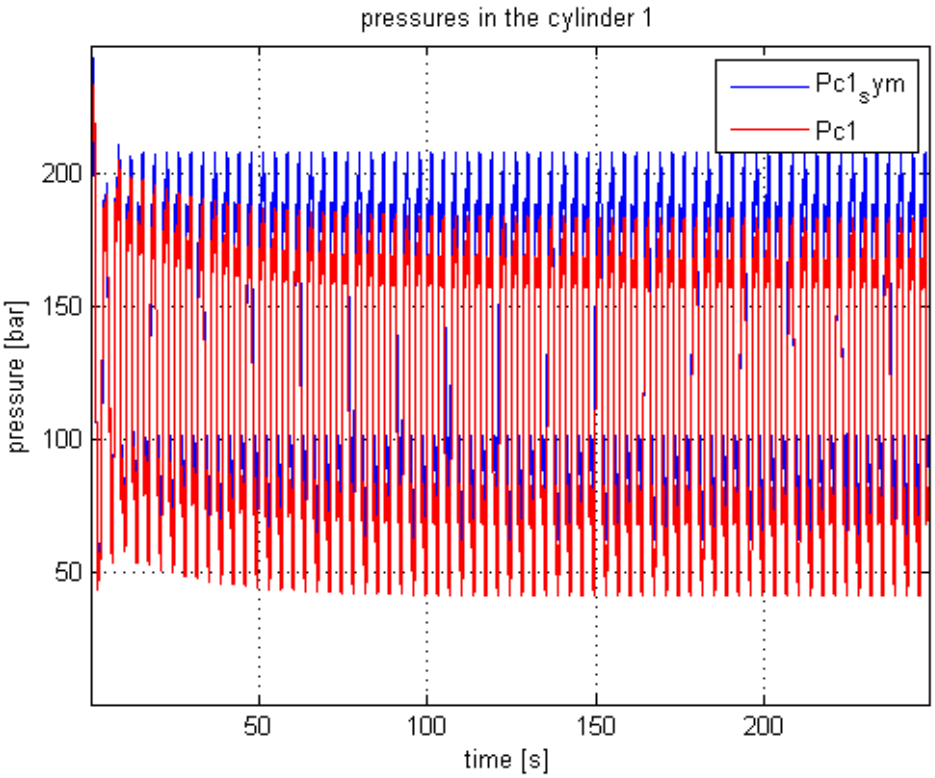

The pressure in the cylinder is influenced by the loss of pressure in the accumulators.

Pressure in high/low pressure accumulator

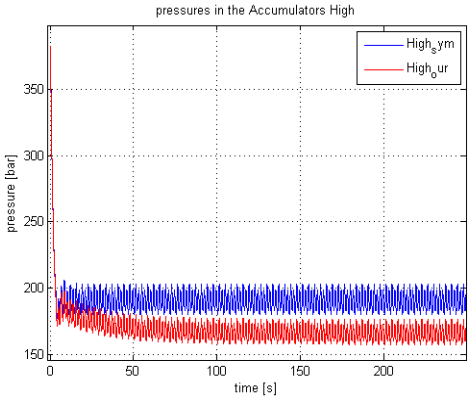

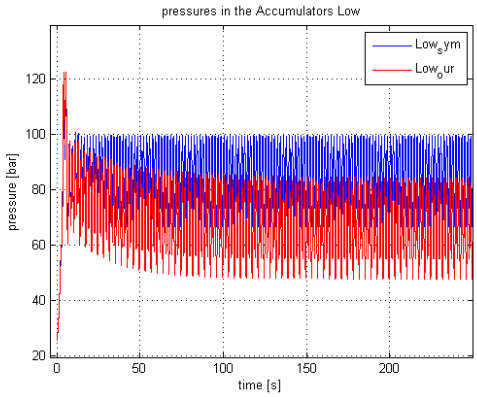

Volume of water in high/low pressure accumulator

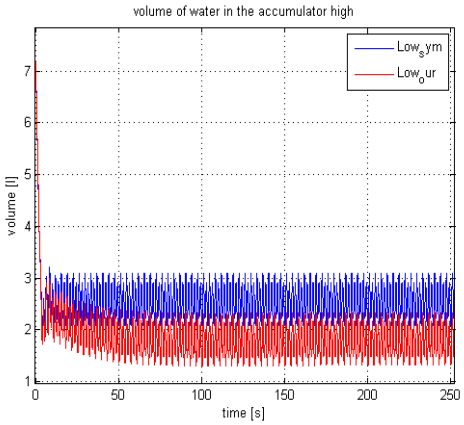

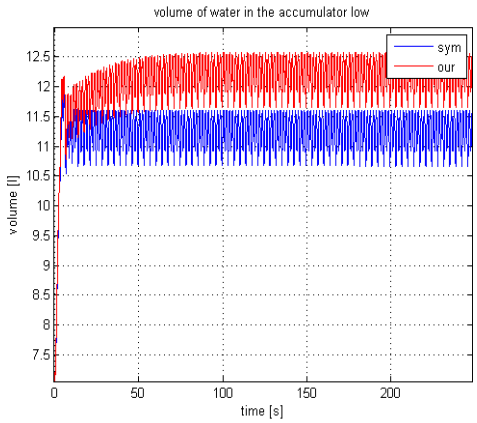

The accumulator finds an equilibrium when the equilibrium between the average energy stored and the heat exchange is reached. In fact, at the beginning, when the gap of temperature between the gas and the external surface is

maximum (the internal temperature is set equal to the wall one when the accumulator is empty of oil) the heat exchange prevails on the work.

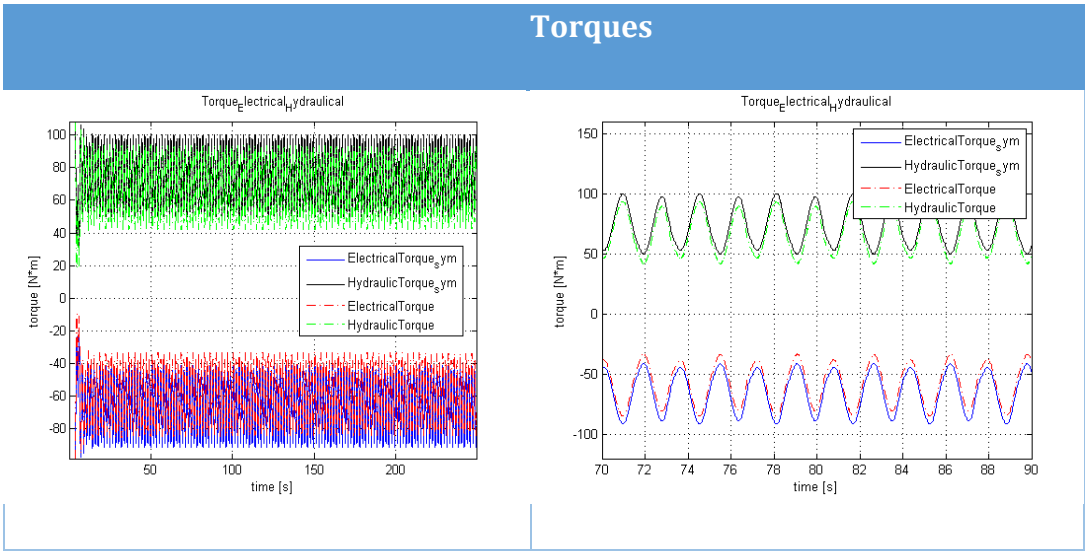

2.7 SIMULATION WITH A RANDOM WAVE INPUT

After the validation of our model, we finally give the random input and we may re-dimension some part of the system due to the different energy input with respect the sinusoidal one. In addition to that, our aim will be managing the conversion with different wave states, so that a unique and robust dimensioning of the component is require. Despite a regular regime condition won't be found by the system, anyway we will have to deal with a transient that turns out to find an equilibrium, where the mean of the variables will be almost constant (stationary condition).

When the equilibrium is globally found, it means that each component works in its stationary condition (if the input keeps stationary too). The pressure of the accumulators will adjust to a value that depends on the energy input from the wave, on the conversion strategy adopted (which varies the efficiency) and on the velocity of the motor. At these condition, the system occurs in a situation where the fluid pumped by the cylinder equals, on average, the sucked fluid by the motor. The accumulator themselves are needed to absorb the variance of the flow rate, but they will oscillate more irregularly around a mean value.

We tested the system with different wave conditions and we collect a table with the variables we are interested in, so that we will compare them with the optimized system. The variables collected are, hence, indicators of energy production and conversion. We will show the entire results in the finale chapter, when we will carry out the comparison. Before showing the results, in order to explain the meaning to these variable, we introduce the concept of efficiency for our system in the next chapter [2.8].

For the time being, we can look at the same variables we considered before, in chapter [2.6], in order to make the model validation.

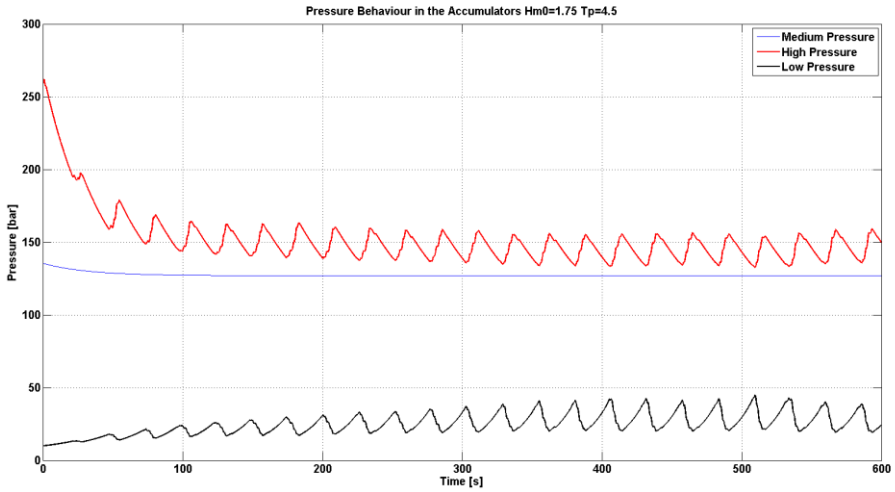

Figure 2-46 Pressures in the Accumulators

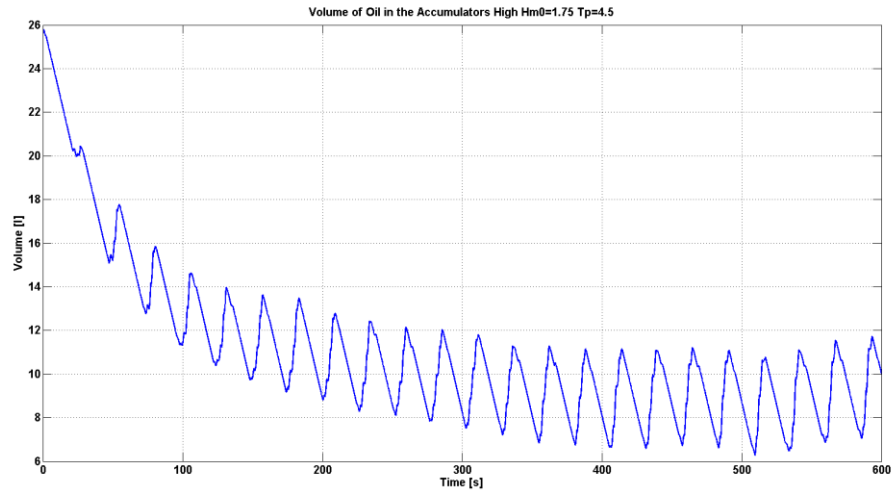

Figure 2-47 Volume of Oil in the High Pressure Accumulator

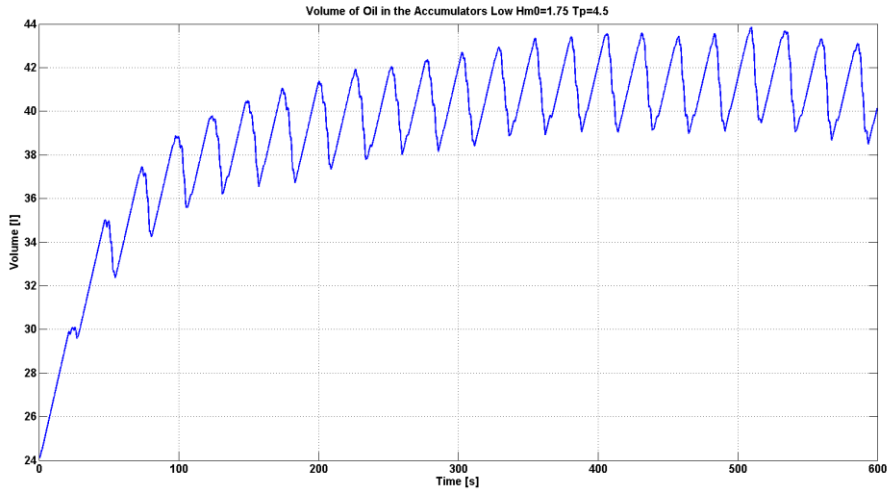

Figure 2-48 Volume of Oil in the Low Pressure Accumulator

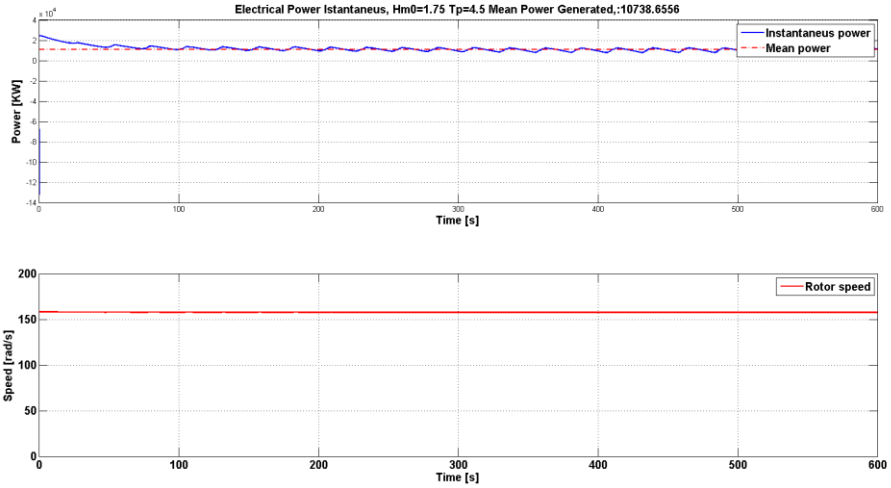

Figure 2-49 Instantaneous and Average Power

2.8 EFFICIENCY OF THE SYSTEM

The whole system as expected has an efficiency. In order to have a better representation of the whole efficiency, we split the energy conversion in 5 steps. This means that we consider five efficiencies of the system, everyone representing one step in the energy conversion process. The total efficiency is the product of the five. These efficiencies are the following:

1. Efficiency of the process of conversion from the energy contained in the wave to the one that moves the buoy
2. Efficiency of the process of conversion from the energy that moves the buoy and the energy extracted by the cylinder
3. Efficiency of the process of conversion from the energy extracted by cylinder and the energy available between the high pressure and low pressure accumulators
4. Efficiency of the process of conversion from the energy available between the accumulators and the mechanical energy that the hydraulic motor use to move the generator.
5. Efficiency of the process of conversion from mechanical energy that aliments the generator to the electrical energy direct output of the generator, before any action from the inverters.

We will see how these efficiencies, calculated as ratio of energies, will reach a regime condition, as the system does. In particular, since the system contains the accumulators, at the beginning the efficiency will result greater than one, due to the exploitation of the storage volumes in the accumulator while

the system is still pumping upstream. In particular, the efficiencies that will show these phenomenon are the number 3 and of course the total one.

The calculation of the efficiency is done as the ratio between the energy produced between time zero and the actual time. This mean that this calculation is absorbing the transitory, implying an over estimation of the efficiency, even at regime condition, unless we reset the integrals after the transient is over.

We can have a look to the following representation to better understand what conversion processes we are talking about:

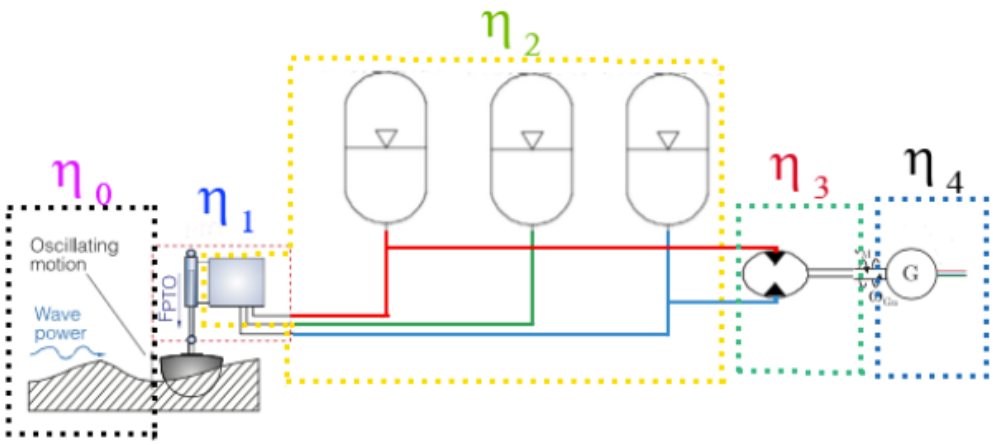

Figure 2-50 Scheme of the system with Efficiencies Definition

We can have a look at the value of these efficiencies for our system undergoing the latter random input (Hm0=1.75 Tp=4.5).

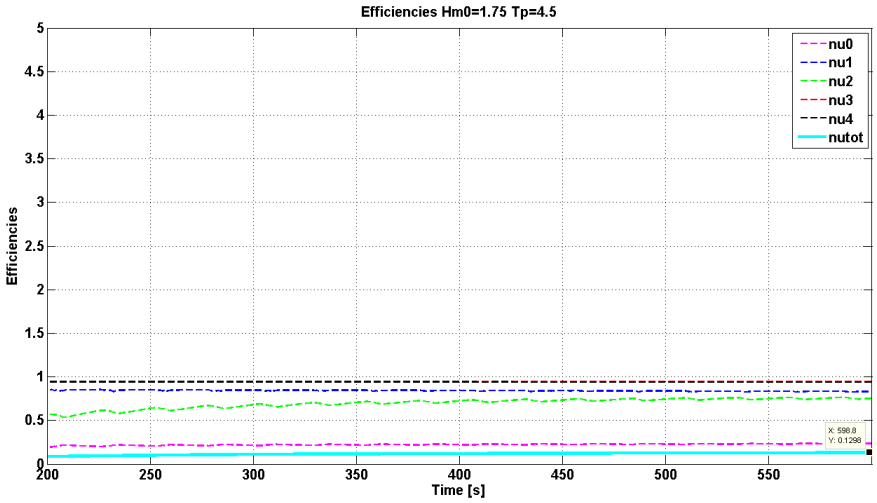

Figure 2-51 Efficiencies of the System

The total efficiency is around 13%. Our aim is to optimize the energy extraction, which means the total efficiency, since we will consider the same input wave to compare. By a more optimized control technique, which will imply a different strategy of the valves opening, we can achieve a better performance of the energy extraction process, both improving the energy input for the system and the ratio between the same energy input and the extraction. We will then optimize also parameters that belong to the downstream part of the system, in order to improve also the last efficiencies. In the next chapter we will explain how we carried out all the improving procedure for the PTO efficiency.

3 THIRD CHAPTER: CONTROL OF THE PLANT

In order to test our numerical model we had to apply a simple control strategy to the system. The idea, as already explained, was to exploit the piston merely like a simple volumetric pump. This implied that there are plenty of moments where the valve are closed and the fluid is not pumped. In addition to that, we were using just two pressure lines, without exploiting the medium accumulator that, as we will see, gives us great advantages.

This control made the system work, but it did not optimize its performance. Our aim in this and in the following chapters is to find a strategy in order to optimize the energy extraction. We know that we deal with an irregular and non-causal phenomenon like the wave one.

Due to the latter reason, it has been shown that the optimal control for a PTO is reactive and non casual. Reactivity implies that the PTO is 4-quadrant, meaning that sometimes it applies a force that introduces energy to the wave absorber. This could seem energy dispersive, but it's not, since it implies an investment of energy from the PTO to the absorber in order to get even more energy back. Non casual means, like explained in the previous chapters, that we should foresee the future waves in order to make an optimal control. This property makes an optimal control unfeasible and not implementable in its raw way. We classify this like a first problem to face while dealing with the optimization problem.

A second problem is the difference between the wave spectrum and the FRF of the point absorber. While the latter is really narrow banded, due to the little damping, the former is a broad-banded spectrum. In addition to that the peaks of the two spectrum are almost never aligned. This implies that the bases for energy absorption are not good at all, and that we have to act in order to change the spectrum of the absorber, which means changing the resonance frequency of the body. While doing it in a mechanical way, for example modifying the mechanical mass of the system is dispersive and expansive (we saw however in the introduction that some water is already added inside the buoy), we can do it with forces through the PTO. We know, in fact, that feedback forces modify the dynamic of the system.

That's why the basic idea of a generic control of the PTO is to follow a reference force. In our case, since we are dealing with a hydraulic cylinder, we will ask it to follow a reference. This force has the task to extract energy from the mechanical system, while supplying it to the hydraulic one. For an optimal control, we can generally write the reference force as:

$$\tau_{PTO,ref} = f(\ddot{\vartheta}, \dot{\vartheta}, \vartheta, n_w(t + t_{fut}))$$

Where we put in evidence the dependence of the force from the same dynamic of the system, and from a function which depends on the future. The future time t_{fut} stands for the non-causality of the feedback law. The law represents the so called WPEA (wave power extraction algorithm). The function to optimize is the extracted energy, or the extracted average power:

$$\overline{P_{extr}} = \frac{1}{T}\int_0^T P_{extr}(t)\,dt$$

For an optimal strategy, it's proved that excitation force must be always in phase with the velocity of the absorber, and that the added damping given by the PTO must match the hydrodynamic damping. For a regular wave case the optimization of the PTO parameter in order to achieve this condition is easy. For an irregular wave, meaning for the real case, the formulation becomes more difficult, and the implementation impossible due to the required knowledge of the future.

Before going on with the regular and irregular case algorithms, we introduce the linear control methods. A linear control method is a feedback law that contains just linear terms, which in time domain implies multiplication and convolutions. We can write, in the Laplace domain, a generic feedback law for the PTO torque:

$$\tau_{PTO} = h_c(t) * w_{arm}(t) = \mathrm{Z}_c(s)\,\mathrm{w(s)}$$

Thinking about a linear system with one translational degree of freedom, the reference force can be written as:

$$F_{pto} = M_{PTO}\ddot{x} + R_{PTO}\dot{x} + K_{PTO}x$$

Where the convention is the force to be positive towards the negative x direction. The linear part is the one proportional to the velocity, while the reactive part is given by the proportionality with the displacement or the inertia.

This two terms, in fact, displace the phase between force and velocity far from 90 degrees. If we think to a system composed by a mass, a damper and a spring and excited by an external force, we can have the following graphical representation:

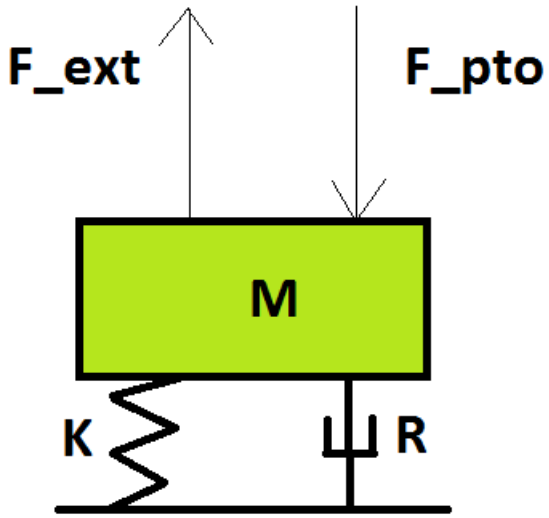

Figure 3-1 Most Schematic Representation of our Mechanical System

The aim of the PTO force is to extract the energy from the mechanical system and give it downstream. The reactive term moves the resonance peak of the system. Generally speaking, it can be spring based or inertia based, if not both. It can be proved that a spring based term is better for the performances, since it gives a broader resonance peak, meaning a better off-resonance behavior (we will show it in the next chapter).

3.1 REGULAR WAVES: PARAMETERS OPTIMIZATION

Our aim is to extract the most of the energy available from the body, given F(t). It's easy to show how there are optimal values of R and K that allow us to achieve this goal. This is straightforward with a regular force, described by a sinusoidal function and consequence of a sinusoidal wave. The results are independent from the magnitude of the force. We can develop the result considering a speed condition:

$$\left(J_{add}(\Omega)+J_{\inf}\right)\ddot{\vartheta}+B_{hyd}(\Omega)\dot{\vartheta}+k_{res}\vartheta=C(t)-C_{PTO}\left(\ddot{\vartheta},\dot{\vartheta},\vartheta\right)=C(t)-R_{PTO}\dot{\vartheta}-K_{PTO}\vartheta$$

$$\left(J_{add}(\Omega)+J_{\inf}\right)\ddot{\vartheta}+\left(B_{hyd}(\Omega)+R_{PTO}\right)\dot{\vartheta}+\left(k_{res}+K_{PTO}\right)\vartheta=C(t)$$

$$C(t)=C_0\sin(\Omega t+\delta)\quad \vartheta(t)=\vartheta_0\sin(\Omega t+\delta+\delta_{F,\vartheta})\quad \dot{\vartheta}(t)=\Omega\vartheta_0\sin(\Omega t+\delta+\delta_{F,\vartheta}+\frac{\pi}{2})$$

$$\vartheta_0=\frac{C_0}{\sqrt{\left(-\left(J_{add}(\Omega)+J_{\inf}\right)\Omega^2+\left(k_{res}+K_{PTO}\right)\right)^2+\left(B_{hyd}(\Omega)+R_{PTO}\right)^2\Omega^2}}$$

$$\delta_{F,\vartheta}=-\arctan\left(\frac{\left(B_{hyd}(\Omega)+R_{PTO}\right)\Omega}{-\left(J_{add}(\Omega)+J_{\inf}\right)\Omega^2+\left(k_{res}+K_{PTO}\right)}\right)$$

The expression of the average power can be achieved by using mathematical theorems and physical concepts. We can write the followings:

$$\overline{P_{in}} = \frac{1}{T}\int_0^T C(t)\dot{\theta}(t)\,dt \qquad \overline{P_{extr}} = \frac{1}{T}\int_0^T C_{PTO}\dot{\theta}(t)\,dt \qquad \eta_{extr} = \frac{\overline{P_{extr}}}{\overline{P_{in}}} = \frac{\frac{1}{T}\int_0^T C_{PTO}\dot{\theta}(t)\,dt}{\frac{1}{T}\int_0^T C(t)\dot{\theta}(t)\,dt}$$

Where we put in evidence the extracted energy, the inner energy and their ratio, which is the extraction efficiency. We will see how the optimal points of these functions are different. Our aim, though, is to maximize the extracted energy. These integral, thanks to the sinusoidal theorems, are easy to express:

$$\overline{P_{in}} = \frac{1}{T}\int_0^T C(t)\dot{\theta}(t)\,dt = C_0\Omega\vartheta_0\cos(\gamma_{C,\vartheta})$$

$$\overline{P_{extr}} = \frac{1}{T}\int_0^T C_{PTO}\dot{\theta}(t)\,dt = \underbrace{\frac{1}{T}\int_0^T K_{PTO}\vartheta(t)\dot{\theta}(t)\,dt}_{\text{is null due to the phae shift of } \pi/2} + \frac{1}{T}\int_0^T R_{PTO}\dot{\theta}^{\,2}(t)\,dt = \frac{1}{T}\int_0^T R_{PTO}\dot{\theta}^{\,2}(t)\,dt = R_{PTO}\Omega^2\vartheta_0^{\,2}\cos(0) =$$

$$= R_{PTO}\Omega^2\vartheta_0^{\,2}$$

$$\eta_{extr} = \frac{R_{PTO}\Omega^2\vartheta_0^{\,2}}{C_0\Omega\vartheta_0\cos(\gamma_{C,\vartheta})}$$

Where in the expression of the extracted energy we put in evidence how the reactive part produces a null average power, while the linear part is at 0 phase with the angular velocity (we consider the PTO torque positive when the angular velocity is positive, despite we know that this is an extracted energy such that the sign should be negative). All these functions are depending on K and R of the PTO torque.

3.1.1 Maximizing input energy

In order to maximize the average input energy we need to compute the gradient of the first function above and set it to zero:

$$\nabla\left(\overline{P_{in}}\right) = C_0 \Omega \nabla\left(\vartheta_0 \cos(\gamma_{C,\vartheta})\right) = 0$$

After the development of the partial derivatives:

$$\frac{\delta \overline{P_{in}}}{\delta K_{PTO}} = 0 \text{ -> } \mathrm{K}_{PTO,opt} = \Omega^2 \left(J_{add}(\Omega) + J_{\inf}\right) - k_{res}$$

$$\frac{\delta \overline{P_{in}}}{\delta R_{PTO}} = 0 \text{ -> } \mathrm{R}_{PTO,opt} = -B_{hyd}(\Omega) + \left(-\Omega\left(J_{add}(\Omega) + J_{\inf}\right) + \left(\frac{k_{res} + K_{PTO}}{\Omega}\right)\right)$$

$$\frac{\delta \overline{P_{extr}}}{\delta R_{PTO}}_{K_{PTO}=K_{PTO,\mathrm{OPT}}} = 0 \text{ -> } R_{PTO,opt} = -B_{hyd}(\Omega)$$

Where the idea is to annihilate the damping of the system if the system is in resonance. If the system is not in resonance, the optimum point is not cancelling the damping.

3.1.2 Maximizing output energy

$$\nabla\left(\overline{P_{extr}}\right) = \Omega^2 \nabla\left(R_{PTO}\vartheta_0^{\,2}\right) = 0$$

After the development we obtain the partial derivatives set to zero:

$$\frac{\delta \overline{P_{extr}}}{\delta K_{PTO}} = 0 \text{ -> } \mathrm{K}_{PTO,opt} = \Omega^2 \left(J_{add}(\Omega) + J_{\inf}\right) - k_{res}$$

$$\frac{\delta \overline{P_{extr}}}{\delta R_{PTO}} = 0 \text{ -> } R_{PTO,opt} = \sqrt{B_{hyd}(\Omega)^2 + \left(-\Omega\left(J_{add}(\Omega) + J_{\inf}\right) + \left(\frac{k_{res} + K_{PTO}}{\Omega}\right)\right)}$$

$$\frac{\delta \overline{P_{extr}}}{\delta R_{PTO}}_{K_{PTO}=K_{PTO,\mathrm{OPT}}} = 0 \; -> \; R_{PTO,opt} = B_{hyd}\left(\Omega\right)$$

Where we can observe how the optimal reactive term is independent from the linear term, while is not vice versa.

3.1.3 Maximizing extraction efficiency

$$\nabla\left(\eta\right) = \frac{\Omega^2}{C_0\Omega}\nabla\left(\frac{R_{PTO}\vartheta_0^{\,2}}{\vartheta_0\cos(\gamma_{C,\vartheta})}\right) = \frac{\Omega}{C_0}\nabla\left(\frac{R_{PTO}\vartheta_0}{\cos(\gamma_{C,\vartheta})}\right) = 0$$

If we develop the calculations we obtain:

$$\frac{\Omega}{C_0}\nabla\left(\frac{R_{PTO}\vartheta_0}{\cos(\gamma_{C,\vartheta})}\right) = \frac{\Omega}{C_0}\nabla\left(\frac{R_{PTO}\vartheta_0}{\frac{\sqrt{\left(-\Omega^2\left(J_{add}\left(\Omega\right)+J_{\inf}\right)+k_{res}+K_{PTO}\right)^2+\left(\Omega\left(R_{PTO}+B_{hyd}\left(\Omega\right)\right)\right)}}{R_{PTO}+B_{hyd}\left(\Omega\right)}}\right) =$$

$$= \frac{\Omega}{C_0}\nabla\left(\frac{R_{PTO}}{R_{PTO}+B_{hyd}\left(\Omega\right)}\right)$$

Without even studying the derivative, we can see how the function inside the gradient is monotone and has its maximum value when the linear term tends to infinite. The efficiency of extraction turns to be independent from the reactive term. Finally we can conclude the efficiency, if meant like this ratio, increases when the total damping increase. If this happens, though, both output and input energies decrease, despite in a different way (the input energy decreases more with R_{PTO} than the output).

We can hence see how the optimal points are not the same for the three functions. We want of course to maximize the extraction of energy. The development was made in order to specify how this won't maximize the extraction efficiency if we express it starting from the buoy energy input. In order to have the same optimum point between extraction and efficiency we should consider the energy coming from the sea, wholly contained in the waves.

We can conclude that there must be both linear and reactive term, and that there is an optimum point. We can give a qualitative description thinking about the action of these two terms. Rising the linear coefficient, we provoke a damping improvement, which would mean an increase of damping force and energy extraction if we consider the velocity constant. The behavior of the system, though, is not independent from the change of the linear term, since we are applying a feedback control, which change the dynamic answer of the whole system. Increasing the linear term, in fact, takes the displacement to diminish, so also its rate of change. Since R increases and the velocity decreases, we can expect that the energy, which comes from a product of them, has a maximum value.

To understand the effect of the reactive term, we have to be aware that this term is responsible of extracting zero energy, but it modifies the poles of the system. The result achieved brings the system in resonance with the external force, optimizing the process of energy conversion.

Let's consider our system with its parametric values at a certain frequency, and let's see how the transfer function of the system changes after the control has been applied.

If we consider a reactive spring based control, we can write:

$$\mathrm{K}_{PTO,opt} = \Omega^2 \left(J_{add}\left(\Omega\right) + J_{\inf} \right) - k_{res}$$

$$R_{PTO,opt} = B_{hyd}\left(\Omega\right)$$

Considering, instead, an inertial based control, we achieve the following (it can be easily shown, since the reactive term should always bring the resonance to the excitation frequency):

$$J_{PTO,opt} = -\left(J_{add}\left(\Omega\right) + J_{\inf} \right) + \frac{k_{res}}{\Omega^2}$$

$$R_{PTO,opt} = B_{hyd}\left(\Omega\right)$$

What we can conclude is that, in the case of optimization applied, the answer to the force will be:

$$\frac{\overline{\dot{\theta}}}{\overline{\overline{C_{ext}}}} = \frac{1}{2B_{hyd}\left(\Omega\right)}$$

Meaning the velocity is always in phase with the force and has a certain magnitude. This result is independent from the excitation frequency, which influence just the values of the optimal parameters in order to obtain this condition. This answer is real, and the physic is characterized by a perfect equilibrium between the elastic force and the inertial one.

Let's consider a regular torque with a certain frequency and all the parameters at the same frequency.

$$\Omega = 0.28Hz \quad B_{hyd}\left(\Omega = 0.28Hz\right) = 1.5311\text{MN/s} \quad J_{add}\left(\Omega = 0.28Hz\right) = 1.2237\text{MN/s}^2$$
$$J_{mech} = 2.45MN/s^2 \quad \mathrm{k}_{res} = 14MN$$

We can hence calculate the natural frequency of the system and the non-dimensional damping:

$$w_0 = \sqrt{\frac{k_{res}}{J_{mech} + J_{add}\left(\Omega{=}0.28\text{Hz}\right)}} = 1.952\,\text{rad/sec} = 0.317Hz \quad \xi = \frac{\mathrm{B}_{hyd}\left(\Omega{=}0.28\text{Hz}\right)}{2\left(J_{mech} + J_{add}\left(\Omega{=}0.28\text{Hz}\right)\right)w_0} = 0.107$$

We can calculate easily the value of the optimal parameters:

$$if \quad C_{PTO} = R_{PTO}\dot{\vartheta} + K_{PTO}\vartheta$$
$$K_{PTO,opt} = -2.63MN; \quad R_{PTO,opt} = 1.53\text{MN/s};$$

$$if \quad C_{PTO} = R_{PTO}\dot{\vartheta} + J_{PTO}\ddot{\vartheta}$$
$$J_{PTO,opt} = 0.85MN/s^2; \quad R_{PTO,opt} = 1.53\text{MN/s};$$

We can recalculate the dynamic parameters of the system once the two controls have been installed. We can see how, despite the resonance frequency is the same, the damping ratio differs, meaning that the broadness of the two curves are different too. We remind that in order to see that the resonance frequency has been moved down to the excitation one, we have to look at the frequency response function of the angular velocity to a torque input. This function in fact has its peak almost at the resonance frequency of the system, while the peak of the frequency response function between the angular

displacement and the torque input depends more strongly on the damping of the system.

We watch at the results and write down the new dynamic parameters:

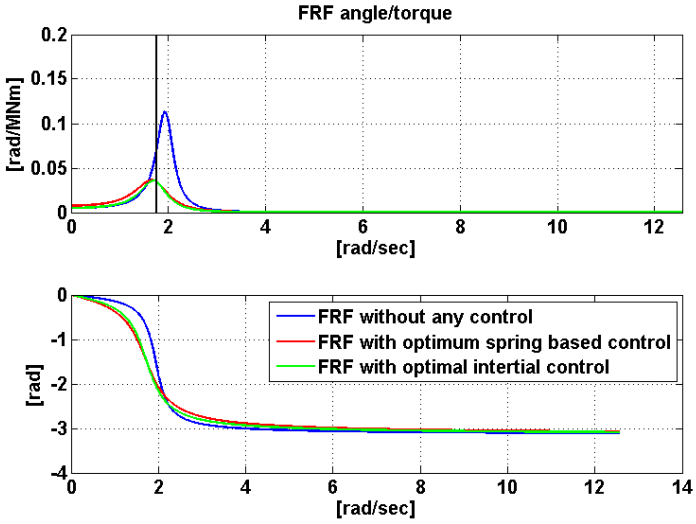

Figure 3-2 FRF of the Angle

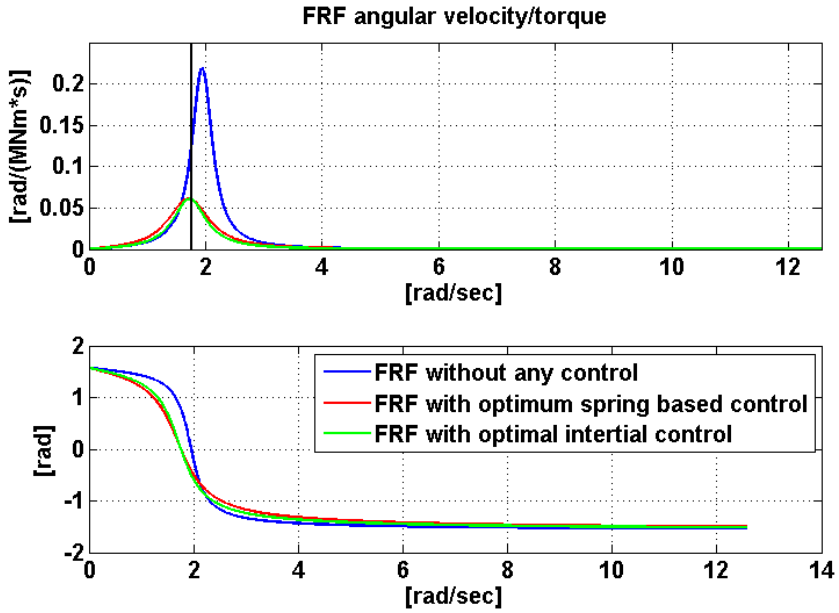

Figure 3-3 FRF of the Angular Speed

Zooming the angular velocity frequency response function:

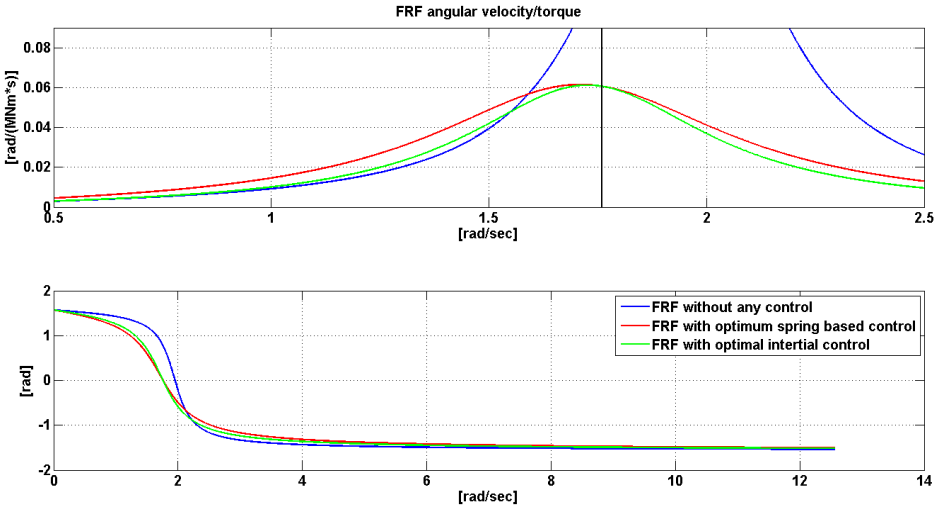

Figure 3-4 FRF of the Angular Speed

Calculating the parameters for the two cases we obtain:

- Spring based control:

$$w_0 = 1.7593 rad/\sec = 0.28\,\text{Hz} \quad \xi = 0.237$$

- Inertia based control:

$$w_0 = 1.7593 rad/\sec = 0.28\,\text{Hz} \quad \xi = 0.192$$

And we can then conclude that a spring based control, since it's giving a wider spectrum, it's better for the control of the system.

Finally the optimal strategy for a regular wave control is given by:

$$C_{PTO} = \tau_{PTO} = R_{PTO}\dot{\vartheta} + K_{PTO}\vartheta$$

3.1.4 Considering a Real PTO:

We can consider three features that might influence the optimization procedures and its results, depending on their weight.

1. Saturation of the PTO: we ask the PTO to follow a reference force, but we don't know if our system is able, in the reality, to follow it. We should consider the saturation throughout optimization process.

$$C_{PTO,sat_{\min}} \le R_{PTO}\dot{\vartheta} + K_{PTO}\vartheta \le C_{PTO,sat_{\max}}$$

2. Dynamic of the PTO: the PTO has a dynamic, meaning a mass, damping and elasticity, which might influence the whole dynamic of the system. The hypothetic influence depends also from the external excitement. If our PTO has a FRF characterized by a high frequency resonance peak (light and rigid), it behaves like a low pass filter, implying no effective

influence on a low frequency excitation. This is our case, since the wave has all frequency quite lower than 1Hz. This means that in our case we will consider the force discharged on the absorber exactly equal to the force resulting from the pressures inside the chambers. If it weren't like this, we should consider the dynamic equation of the PTO and insert it inside the model and the block scheme.

3. Efficiency of the PTO: in case of reactive control, this characteristic of the PTO influences a lot the results. We have to consider, in fact, that a reactive PTO is a 4-quadrant PTO, meaning that gives energy to the absorber sometimes during the cycle. Due to the efficiency, the energy given to the absorber weights more on the produced power than the absorbed one. We can immediately figure it out looking at the new function to optimize:

$$P_{out}(t)=\begin{cases} P_{extr}(t)\eta_{PTO} & \text{if } P_{extr}(t)\geq 0 \\ \dfrac{P_{extr}(t)}{\eta_{PTO}} & \text{if } P_{extr}(t)<0 \end{cases} \rightarrow \bar{P}_{out}=\lim_{T\to\infty}\frac{1}{T}\int_0^T P_{out}(t)\,dt$$

Which strongly depends (as shown in the next figure) on the efficiency of the PTO. Basically the reactive energy does not have any more zero mean value but assumes a negative value, as more negative as less the efficiency is.

Considering just the PTO efficiency and not the saturation an analytical formulation for the average power output is achievable as shown in [9]:

$$\overline{P}_{out} = \frac{C_0^{\,2}\left(\eta - \frac{1}{\pi}\left(\eta - \frac{1}{\eta}\right) a\tan\left(\frac{-K_{PTO}/\Omega}{R_{PTO}}\right) R_{PTO} - \frac{1}{\pi}\left(\eta - \frac{1}{\eta}\right)\frac{K_{PTO}}{\Omega}\right)}{2\left(\left(B_{HYD}(\Omega) + R_{PTO}\right)^2 + \left(\Omega\left(J_{mech} + J_{add}(\Omega)\right) - \left(\frac{K_{res} - K_{PTO}}{\Omega}\right)\right)^2\right)}$$

Where we can see how it is function of three variables, R_{PTO}, K_{PTO}, η_{PTO} with the system parameters defined by the regular wave frequency.

We can understand how the optimal point of strongly depends on η_{PTO}. We then search for the optimum point of these function, varying the efficiency. Since an analytical solution is not straightforward, we decided to implement a series of simulations on Simulink that given an efficiency of the PTO give out the optimal parameters.

For a Wave period of 5.5 [sec] we achieve the following results:

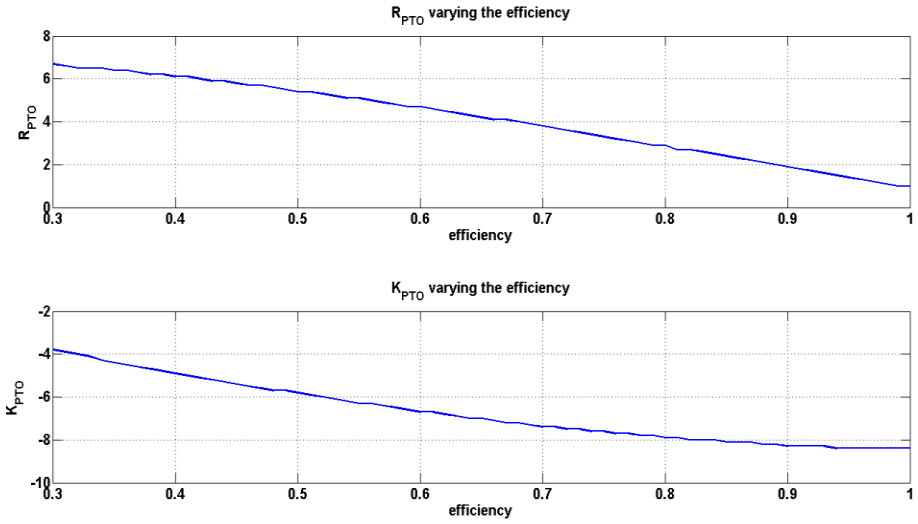

Figure 3-5 R and K with PTO Efficiencies

We can see how the reactive term loses its weight as the efficiency decrease. This occurs because the average negative reactive energy starts weighting for the whole system. The solution hence tends to the linear-no reactive solution. If we set n=1, the solution coincides with the ideal PTO one. We can show how these results match with the results of [9].

3.2 IRREGULAR WAVE OPTIMAL CONTROL:

We have to consider that we are not in the case of a simple sinusoidal force, but a discrete spectrum that approximate a continuous one. The optimal solution will be so different:

3.2.1 The complex conjugated control:

We know that in the optimal condition the exciting wave torque must always be in phase with the velocity and that the added damping must equal the hydrodynamic one. This should be occurring for all the frequencies of the spectrum. In order to convert it in numbers, we saw that when this happens, the frequency response function to the angular speed-force becomes:

$$\frac{w_{arm}(\Omega)}{\tau_{ext}(\Omega)} = \frac{1}{2 * B_{hyd}(\Omega)} \quad \forall \Omega$$

Meaning a real number. This, differently from before, should occur for all the frequencies, implying a whole cancellation of the dynamic of the system, which would behave like a pure damper, giving always a real response nonetheless the frequency of excitation.

Moving in time domain, we can express the external force in this optimal condition:

$$\tau_{ext} = 2h_b(t) * w_{arm}(t)$$

If we want this as external force, we can try to see which PTO force we might give in order to achieve it. Since the time domain equation is:

$$\left(J_{arm}+J_{add}\right)\ddot{\theta}_{arm}=\tau_{ext}-k_{res}\theta_{arm}-k_r\left(t\right)*w_{arm}-\tau_{PTO}$$

$$\text{if I want } \tau_{ext}=2h_b(t)*w_{arm}(t)$$

$$\tau_{PTO}=-\left(J_{arm}+J_{add}\right)\ddot{\theta}_{arm}-k_{res}\theta_{arm}-k_r\left(t\right)*w_{arm}+2h_b(t)*w_{arm}(t)$$

All terms are known except the last, which being the impulse response related to a real and symmetric transform, is symmetric as well, meaning it's not equal to zero before t=0 and so it's not casual.

This control is called conjugated control, since, if we consider the system through its transfer function, the result we obtain in terms of parameters are obtainable in terms of mechanical impedance, creating an obvious parallelism with the electrical world. In particular, given an intrinsic impedance of the absorber Z_i, the optimal result wants the impedance of the PTO Z_c to be the complex conjugated:

$$Z_i\left(s\right)=\frac{\tau_{ext,tot}\left(s\right)}{w_{arm}\left(s\right)}=\frac{\tau_{ext}\left(s\right)-\tau_{PTO}\left(s\right)}{w_{arm}\left(s\right)}\quad Z_c(s)=\frac{\tau_{PTO}\left(s\right)}{w_{arm}\left(s\right)}$$

$$Z_{c,OPT}(s)=\overline{Z_i\left(s\right)}$$

So:

$$\tau_{PTO}=Z_{c,OPT}(s)w_{arm}(s)=\overline{Z_i}(s)w_{arm}(s)$$

$$\tau_{PTO}(t) = h_i(-t) * w_{arm}(t)$$

Which required a future knowledge of the phenomenon.

This is the actual demonstration that a complex conjugated control is non implementable. This might be notice since from the equation we asked to obtain, because it's real (zero phase), but it has a variable gain, which is not feasible.

3.3 IRREGULAR WAVE SUB-OPTIMAL CONTROL:

We have then to implement a different kind of control that will be surely a sub-optimal one. We decided to maintain the same structure of the control introduced for the case of regular waves. We are going to develop the sub-optimal control both analytically and numerically. We are able in fact to develop an analytical procedure in case of an ideal PTO, which is a PTO that is allowed to achieve infinite forces. We won't be able to apply the same procedure, instead, when we consider a saturated PTO.

Let's consider a linear reactive control like the following generic formulation:

$$\tau_{PTO} = R_{PTO}\dot{\vartheta} + K_{PTO}\vartheta$$

3.3.1 Control optimization in case of an ideal PTO (Analytical Procedure):

In our case, this system is not even a mass-spring-damper system, since we saw that the state variables are five and we implemented an approximation in order to take into account the memory effect of the radiative forces.

Anyway, we are in front of a mechanical system that is excited by an external force whose spectrum is defined in amplitude (approximated after the calculation with a FEM technique) and whose phase is random (see chapter [2.3.1], where we explained how to generate a wave). After the transient is over, we have a movement of the buoy that can be analytically described as the sum of different components, having the same frequency of the external force (from the linearity of the system after linearization). The results is that we have different forces working on different velocity components. Thanks to the properties of these functions, which are sinusoidal, we can achieve a final function to optimize. Despite the existence of this function, due to its difficult shape, the optimization will be carried out through a numerical method.

We can hence write down the expression of the force (we saw how to achieve it from the wave), the displacement and the velocity of the buoy, given their transfer function in the Fourier domain. We saw then how the transfer function is modified by the PTO parameters, since they change the mechanical characteristic of the system through the feedback:

$$F(t) = \sum_{i=1}^{nf} F(\Omega_i) \cos\left(\Omega_i t + \delta_{rand,i}\right)$$

$$\vartheta(t) = \sum_{i=1}^{nf} F(\Omega_i) \left[{}^{\vartheta}\!/_{F}\left(\left(\Omega_i, R_{PTO}, K_{PTO}\right)\right)\right] \cos\left(\Omega_i t + \delta_{{}^{\vartheta}/_{F}(\Omega_i)} + \delta_{rand,i}\right)$$

$$\dot{\vartheta}(t) = \sum_{i=1}^{nf} \Omega_i F(\Omega_i) \left[{}^{\vartheta}\!/_{F}\left(\left(\Omega_i, R_{PTO}, K_{PTO}\right)\right)\right] \cos\left(\Omega_i t + \delta_{{}^{\vartheta}/_{F}(\Omega_i)} + \delta_{rand,i} + \frac{\pi}{2}\right)$$

$$C_{PTO} = R_{PTO}\dot{\vartheta}(t) + K_{PTO}\vartheta(t)$$

$$\overline{P_{extr}} = \frac{1}{T}\int_0^T C_{PTO}\dot{\theta}(t)\,dt$$

We can see how the latter expression involves products between sinusoidal function characterized by different frequencies. Despite the instantaneous power of one component of the force over one component of the velocity might be different from zero at a certain time t, just the component in quadrature produces average powers different from zero. This is easily understandable if we consider a product between two sinusoidal functions of different frequencies, we integrate it and we bring the time to infinite.

$$\mathrm{A}\cos(\Omega_i t+\varsigma_i)\,\mathrm{B}\cos(\Omega_j t+\varsigma_j) = \frac{AB\cos\left(\left(\Omega_i+\Omega_j\right)t+\varsigma_i+\varsigma_j\right)+AB\cos\left(\left(\Omega_i-\Omega_j\right)t+\varsigma_i-\varsigma_j\right)}{2}$$

hence

$$\lim_{T\to\infty}\frac{1}{T}\int_0^T \mathrm{AB}\cos(\Omega_i t+\varsigma_i)\cos(\Omega_j t+\varsigma_j) = \lim_{T\to\infty}\frac{1}{2T}\int_0^T \mathrm{AB}\cos\left(\left(\Omega_i+\Omega_j\right)t+\varsigma_i+\varsigma_j\right)+AB\cos\left(\left(\Omega_i-\Omega_j\right)t+\varsigma_i-\varsigma_j\right)dt$$

$$\lim_{T\to\infty}\frac{1}{2T}\int_0^T \mathrm{AB}\cos\left(\left(\Omega_i+\Omega_j\right)t+\varsigma_i+\varsigma_j\right)+AB\cos\left(\left(\Omega_i-\Omega_j\right)t+\varsigma_i-\varsigma_j\right)dt = \begin{cases} 0 & \text{if } \Omega_i \neq \Omega_i \\ \pi AB\cos\left(\varsigma_i-\varsigma_j\right) = \pi AB\cos\left(\varsigma_{rel_{i,j}}\right) & \text{if } \Omega_i = \Omega_i \end{cases}$$

Where from the latter we can confirm also what we gave for granted in the previous chapter, where we said that the average power given by the reactive component tends to 0. Considering that the displacement between the speed and the displacement at every component is equal to 90 degrees, we can easily write the function to optimize:

$$\overline{P_{extr}} = \lim_{T\to\infty}\frac{1}{T}\int_0^T C_{PTO}\dot{\theta}(t)\,dt = \lim_{T\to\infty}\frac{1}{T}\int_0^T \left(R_{PTO}\dot{\vartheta}(t)+K_{PTO}\vartheta(t)\right)\dot{\theta}(t)\,dt =$$

$$\lim_{T\to\infty}\frac{1}{T}\int_0^T\left(\begin{array}{l}R_{PTO}\left(\sum_{i=1}^{nf}\Omega_i F(\Omega_i)\left[\vartheta/_F\left((\Omega_i,R_{PTO},K_{PTO})\right)\right]\cos\left(\Omega_i t+\delta_{\vartheta/_{F(\Omega_i)}}+\delta_{rand,i}+\frac{\pi}{2}\right)\right)+\\ +K_{PTO}\left(\sum_{i=1}^{nf}F(\Omega_i)\left[\vartheta/_F\left((\Omega_i,R_{PTO},K_{PTO})\right)\right]\cos\left(\Omega_i t+\delta_{\vartheta/_{F(\Omega_i)}}+\delta_{rand,i}\right)\right)\end{array}\right)*$$
$$*\left(\sum_{i=1}^{nf}\Omega_i F(\Omega_i)\left[\vartheta/_F\left((\Omega_i,R_{PTO},K_{PTO})\right)\right]\cos\left(\Omega_i t+\delta_{\vartheta/_{F(\Omega_i)}}+\delta_{rand,i}+\frac{\pi}{2}\right)\right)dt$$

What results to influence this function is the product between the terms in quadrature:

$$\overline{P_{extr}}=2\pi R_{PTO}\sum_{i=1}^{nf}\left(F(\Omega_i)\left[\vartheta/_F\left(\Omega_i,R_{PTO},K_{PTO}\right)\right]\right)^2\Omega^2{}_i$$

In order to achieve the optimal values, we can fix Tp and Hm0, cycling the values of R and K, and save the ones which turns out to maximize the latter function. We can test that these values are not dependent on Hm0, but just on Tp. Tp modifies the center of spectrum of the force, so this function changes because the values of the forces at a determinate frequency change. Fixed Tp, when we vary Hm0 this just scale the value of the Force, that anyway is elided by the multiplication with the FRF.

We can hence build a map that gives the values of R and K optimal varying Tp. We built this map for our system, having both the transfer function and the spectrum of the force given Tp. The results are shown in the figures:

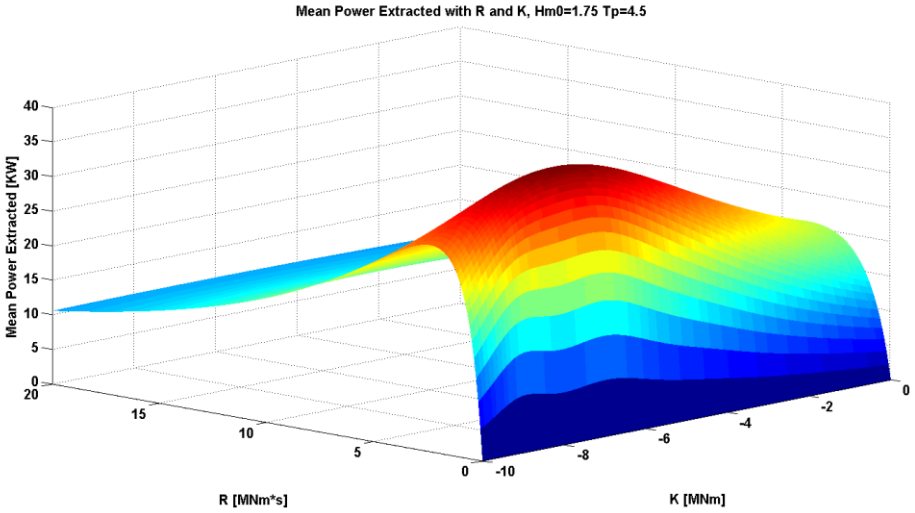

Figure 3-6 Energy varying R and K

Given a sea state, we know now the optimal values of the parameters. We confirmed the value obtained with this semi-analytical development through simulations of our system, in a way that corresponds to the purely numerical procedure that will be explained in the next chapter [3.3.2], regarding real PTOs.

If the PTO is real, in fact, we already saw how things change. Despite the presence of an efficiency could be easily face to achieve the function shown in [3.1.4], the saturation rends the problem highly nonlinear and dependent on the random behavior of the phase. In fact, depending on how the phase are, the saturation could be reached different times during one cycle. This brings to different results for a same wave state, which obliged us to use a numerical-statistical procedure.

3.3.2 Control optimization in case of a real PTO (Numerical Procedure):

We have seen how an analytical solution cannot be found if we want to consider a real PTO, we so have to build a simulation that can identify the optimal controller parameters. Schematically we have to design a system that receiving as an input the wave force gives us the resulting optimal parameters for the controller:

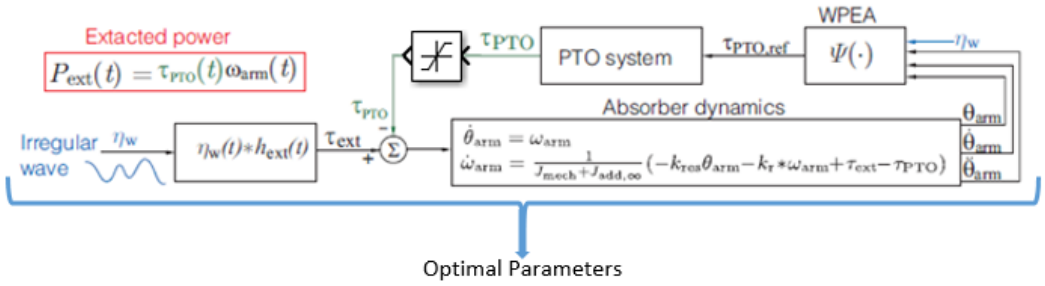

Figure 3-7 Scheme of our Optimization Technique

This black box needs as an input not just the wave force but also the values of the controller parameters, and this means that a priori we need to cycle on a grid of controller parameters to obtain as output the extracted energy. Finding so the controller parameters couple that maximizes the energy, mathematically:

$$\text{Given: } K_{PTO},\ R_{PTO},\ \eta_w(t),\ \eta_{PTO}\ \left(\eta_w(t) \text{ is the wave height story}\right)$$

$$\bar{P}_{PTO} = \begin{cases} \frac{1}{T}\int_0^T P_{ext}(t)\eta_{PTO}dt & \text{if } P_{ext}(t) > 0 \\ \frac{1}{T}\int_0^T \frac{P_{ext}(t)}{\eta_{PTO}}dt & \text{if } P_{ext}(t) < 0 \end{cases}, \qquad P_{ext}(t) = \underbrace{\left(K_{PTO}\vartheta(\eta_w(t)) + R_{PTO}\dot{\vartheta}(\eta_w(t))\right)}_{\text{limited by the saturation}} \cdot \dot{\vartheta}(\eta_w(t))$$

We understand how this maximization process is highly dependent on three parameters:

- The PTO efficiency
- The saturation (that is function of the available pressures in the accumulators)
- The wave force (the random phases will highly influence the saturation of the PTO)

By cycling for some wave states for some given efficiency and saturation, on a given grid we observed how there is only a maximum point of extraction, as it was for the analytical solution, and this point is both a local and global maximum even if we added a strong discontinuity as the saturation. By plotting, in fact, the exponential of the produced power, we can easily identify the maximum point:

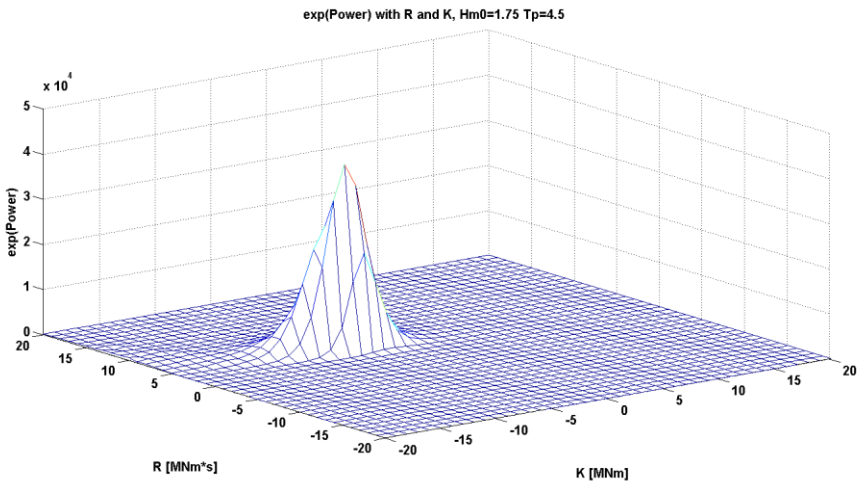

Figure 3-8 Exponential of the Energy with R and K

We can so proceed more cleverly than using a grid and computing the extracted energy. We know that there are numerical methods such as the gradient method that is able to identify local maximum or minimum of a function. Because our unknown function (the power produced) has a unique maximum we can use the latter method to obtain the optimizing parameters for each wave state.

To solve the fact that method as the gradient one needs to know the derivative of the function, something that obviously was for us unknown, we implemented a grid based gradient:

3.3.2.1 Grid Based Gradient

The idea is to move to create two grids:

1. The first one will identify all the possible control parameters couple: this grid can be very wide, in fact it will not be our "computational" grid.
2. The second one is the computation grid: this grid has nine points of the first grids, in which the PTO power will be computed. This second grid will move maintaining its center on the maximum ratio between the PTO power and the distance (an approximation of the derivative). In this way this grid will move in the direction identified by the highest slope until the central point is the maximum. The algorithm is implemented such that it does not run over points in the grid that have been already computed during the previous cycles.

The starting point to compute the computational grid is always chosen as the optimal point given by the ideal analytical solution, so the point that was the optimum without considering the efficiency and the saturation of the PTO.

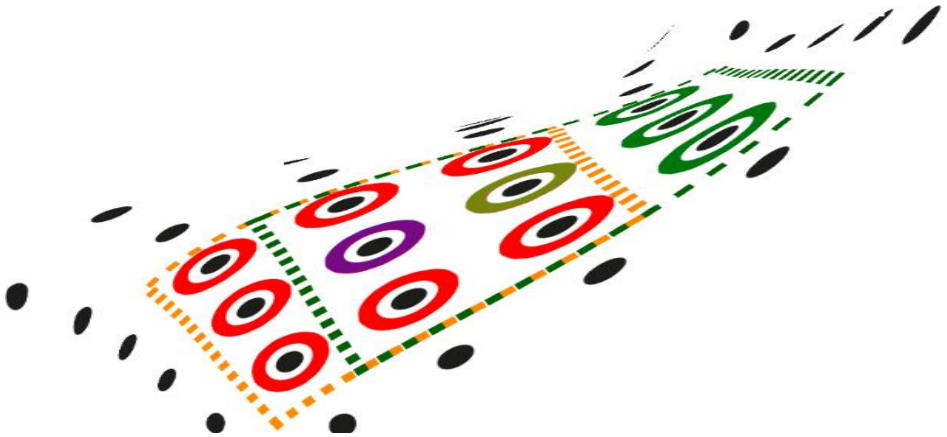

Figure 3-9 Grid Based Gradient: The black points represents the possible computational points, the red circles represents the first bunch of point where the computation is done where the purple one is the analytical optimal point, the yellow one is the one where the grid center is moved after the computation on the red points. Afterwards only the green circles will be considered for the next computation.

We can observe how just the necessary points are computed, and how the system reaches the maximum of PTO power.

In future chapters, we will obtain the optimum PTO efficiency and the saturation values by optimizing the behavior of different parts of the whole system. The effect of the wave random behavior will be studied in a statistical way. In fact considering for a moment known both the PTO efficiency and the torque saturations we can cycle over 40 different waves that have the same characteristic.

Our aim right now is to follow a reference force in order to create it with a cylinder. We know that we have three different pressure available and three chambers with three different areas. This implies that we can have, given three pressure, 27 different forces. We will develop a strategy in order to follow the reference force in a sort of "digital way", using the pressure in the accumulator. In addition to this, we will see how the real force will oscillate around the one

we ask, due to the dynamic of the system that influences the pressure inside the chambers.

3.4 CONTROL OF THE HYDRAULIC MOTOR

By analyzing the flux of power of the system is straightforward to understand how the motor absorbed a variable power absorption over time. In fact, having variable energetic waves we cannot extract a fixed amount of power from them. The power extraction (up to the hydraulic motor) can be defined as:

$$P_{hydraulic\ motor} = P_{wave}\eta_{PTO}\eta_{motor} \rightarrow P_{wave}\eta_{PTO}\eta_{motor} = \Delta P_{mot} D_w \omega$$

For a low energetic wave, we can act in two different way:

- Keeping the rotor speed constant and having a consistent oscillation of delta pressure between the accumulators (and consequently the motor head).
- Varying the rotor speed in order to maintain the ΔP_{mot} as much constant as possible.

The first strategy has a big drawback, in fact, as can be easily understood the ΔP_{mot} is strictly connected with the maximum and minimum PTO forces. With a small ΔP_{mot} the maximum forces available will be smaller. Considering our three-chamber cylinder the maximum and minimum forces can be defined as a function of two different parameters, the ΔP_{mot} and the pressure of the high-pressure accumulator (neglecting the pressure losses in the hoses):

$$\begin{cases} F_{PTO_{\min}} \approx -A_1 P_h + A_2 P_l - A_3 P_h \approx -A_1 P_h + A_2 \left(P_h - \Delta P_{mot} \right) - A_3 P_h \\ F_{PTO_{\max}} \approx -A_1 P_l + A_2 P_h - A_3 P_l \approx -A_1 \left(P_h - \Delta P_{mot} \right) + A_2 P_h - A_3 \left(P_h - \Delta P_{mot} \right) \end{cases}$$

The ΔP_{mot} and pressure of the high-pressure accumulator are not independent however. The decrease of ΔP_{mot} takes place by a flow of hydraulic liquid (done by the motor) from the high to the low-pressure accumulator. This means that $\Delta P_{mot} \downarrow$ means $P_h \downarrow$ so $F_{PTO_{\min}}$ and $F_{PTO_{\max}} \downarrow$ creating difficulties on the force following.

The hydraulic motor must so be controlled in speed, in order to maintain necessary gap of pressure and avoid a depletion of the high-pressure accumulator that would lead to a poor following of the reference force.

Since the hydraulic motor is connected mechanically to the asynchronous generator, the only way to reduce or increase the speed is to control the feed frequency of the generator by means of an inverter. This inverter will be connected to another inverter that will be connected to the three-phase grid.

The inverter connected to the asynchronous motor will define the characteristic of the alimentation electrical field (Voltage and frequency).

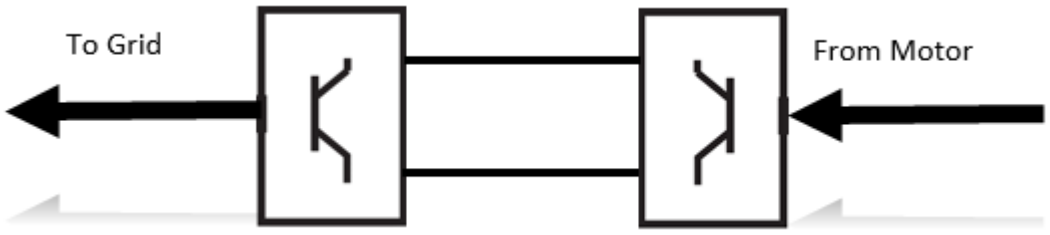

Figure 3-10 Schematic Representation of the Connection with the Grid

3.4.1 Controlling the alimentation frequency

We know that the asynchronous motor works at a speed that is very near to the feeding frequency. A change of even a radiant per second in the shaft speed, in fact, means a change of various kW of power produced (the slope of the curve near the operational point is steep). This means that by controlling the feeding frequency we are controlling quite precisely the rotor speed.

Considering defined the objective rotor speed, ω_{ref} , we will vary the feeding frequency of the double (having a two pair of pole asynchronous generator) and the feeding voltage.

Varying the alimenting frequency can have, obviously, two different effects on the system. If we are going to accelerate the frequency and so the rotor speed, being the rotor of the generator rigidly connected with the hydraulic motor, means that the generator will act for some milliseconds as a motor. This to win both the mechanical inertias and the hydraulic inertia of the fluid. The opposite will happen in case of decrease of rotor velocity; the inertias will work as a flywheel and give an extra power to the generator. This behavior can be limited by changing the frequency slowly enough to let the mechanical system adapt slowly to the new equilibrium. We have found experimentally that the maximum rate of change for the frequency was 5 rad/s. With this value we have in fact a good compromise between power quality and speed of adaptation. The slowly varying frequency permits us to avoid to consider the inverter dynamic,

and so it allows us not to vary our system model. However we consider some limit on the inverter capacity; we consider as limits value for the achievable alimentation frequencies 80 and 314 [rad/sec], limits that are compatibles with a various types of inverters in commerce.

Changing the alimenting frequency means also changing the alimentation voltage, in fact if we want to keep constant at the nominal level the magnetic flux the voltage must be changed proportionally with respect to the frequency:

$$V_{new} = \frac{\omega_{ref}}{2\pi} \frac{V_{nom}}{\omega_{nom}}$$

3.4.2 Choosing the reference speed:

Understood how we can vary the rotor speed (even with some upper and lower bound) we must now choose a reference speed. We want to define a reference speed such that the power extracted by the waves is fully (or at least as much as the losses permits) transformed in electrical one. Since the losses in the hydraulic and electrical motors are of the order of few percent of the total energy, we are going to neglect them for the choice of the reference speed. There are two main drivers to the choice of the reference speed:

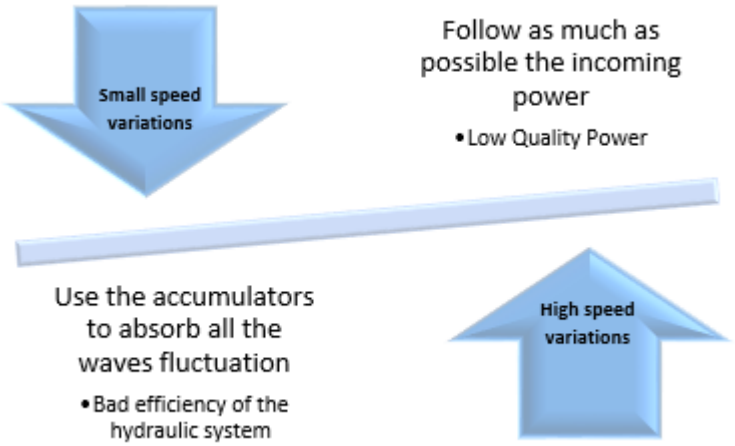

Figure 3-11 Effect of the Motor Speed Variation

We choose to give more weight to the power quality, this means that as much as it is possible we want to work with a constant generator speed. The efficiency of the hydraulic system can be improved and optimized in other ways described in chapter [3.6].

By the statistical optimization of the controller parameters, we have a statistical PTO power associated to all the wave states. This power is the average incoming power to the hydraulic motor: we are able to transform this power to electric one as much as the η_2 efficiency is higher. In fact, lower is the power stored variation, lower are the losses in the accumulators since it is more stable around the optimal ΔP_{acc} :

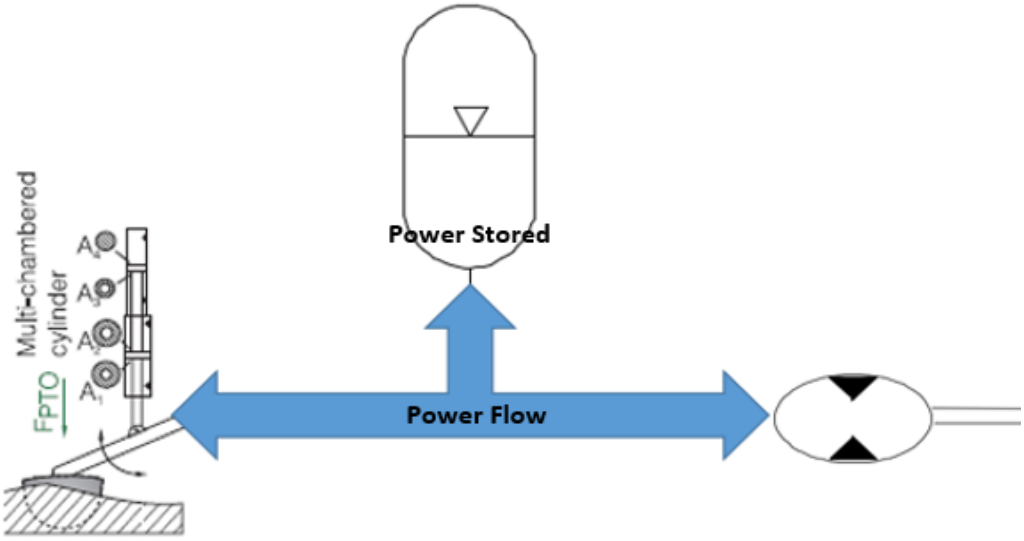

Figure 3-12 Scheme of the Power Flow

This means that we are going to make an average speed reference design:

$$P_{hyd} = \Delta P_{acc} D_w \omega_{rot} \approx \bar{P}_{PTO} \rightarrow \omega_{ref} = \frac{\bar{P}_{PTO}}{\Delta P_{acc} D_w}$$

Where $\bar{P}_{PTO}$ is the mean PTO power given a wave state and ΔP_{acc} is the optimized delta pressure, see chapter [3.6.2].

This ω_{ref} defined as now is firstly not considering the fluctuation of the power, secondly the possibilities of occurrence of long periods in which the wave is not producing enough power, that implies a condition in which the power flow is maintained only by the accumulators. Being the power of the wave defined in a statistical way, problems related to its variance could rise. Waves

that produces the same power may have, in fact, different power distribution even with the same mean value.

The idea is so to add a variable gain to this reference speed to consider an eventual depletion of the high-pressure accumulator and to maintain the optimal ΔP_{acc} in the system. We do not want to make a control defined just on the actual ΔP_{acc} because as described before, not just the ΔP_{acc}, but also the pressure in the high-pressure accumulator defines the range of forces available to the system.

To create a criterion based on the high-pressure accumulator depletion, we need to define a limit high-pressure value. This value is obtained considering the average pressure of the medium accumulator in the last 30 seconds and adding half of the ΔP_{acc} optimal. We decided to base this control on the average pressure of the medium accumulator in the last 30s once we observed that. In fact, while the pressures of low and high accumulators during a transient (that occurs during a change of wave condition) can change a lot, the medium pressure is usually always bounded in a ± 20 [bar] bound. Considering all of this the gain is defined mathematically as:

$$\phi_{depl} = \begin{cases} 1 & \text{if } P_{medium,acc} + \Delta P_{acc} - P_{high,acc} \leq 0 \\ \dfrac{1}{e^{\frac{\left|\bar{P}_{medium,acc} + \Delta P_{acc} - P_{high,acc}\right|}{5}}} & \text{else} \end{cases}$$

So that the reference speed will be given by:

$$\omega_{ref} = \frac{\bar{P}_{PTO}}{\Delta P_{acc} D_w} \phi_{depl}$$

Meaning that the reference alimentation frequency, since we have two pair of poles, will have to reach the double of ω_{ref} .

3.5 CONTROL OF THE CYLINDER VALVES:

In the previous paragraphs we have defined a reference force/torque that the cylinder must follow. In this paragraph we will design a control that, by means of opening and closing the nine valves, will allow to follow as much as possible the optimal force.

As said in the introduction chapter the choice of a three chamber and three level of pressures hydraulic system was done to have a possible choice of 27 available forces for the cylinder. From the figure below we can understand why we needed a so wide force distribution:

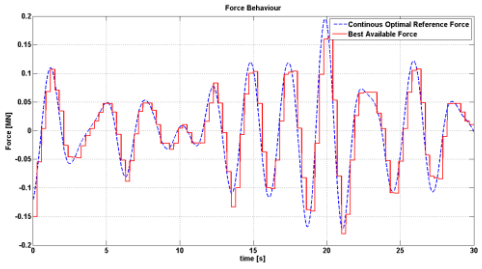

Figure 3-13 Torque with Time

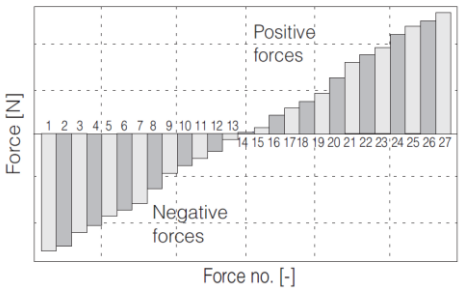

Figure 3-14 All the Possible Forces

The valves controller has however some other important objectives, in fact it must:

- Follow as best as possible the reference force
- Avoid the emptying or filling of the medium-pressure accumulator, and at the same time a useful positioning for it.
- Assure that the pressure in the low-pressure accumulator does not pass the one in the high-pressure one in case of very low energetic waves.

We will treat each problem differently in order to have an overview of the whole control picture, and we will then proceed with the assembly of all the parts to obtain the final control.

3.5.1 Follow the reference:

The best way to follow the reference force is to create a table in which we define all the available forces given the pressures in the accumulators. Every force is associated with a unique set of valve disposition (open/close). We then compare each possibility with the required force and we choose the closest one.

This choice is done with a discrete time: in fact, following constantly the force is impossible due to the opening and closing time of the valves and to the transient that occurs in the chamber pressure. We can define approximately a minimum of 0.05 second to switch from a chosen force to another; this time will be optimized in future paragraph.

The force choice is so based on:

$$F_{possible} = \begin{bmatrix} F_{1,1} & \cdots & F_{1,9} \\ F_{2,1} & \cdots & F_{2,9} \\ F_{3,1} & \cdots & F_{3,9} \end{bmatrix} \rightarrow F_{i,j} : \min\left(\left|F_{i,j} - F_{ref}\right|\right)$$

Where:

- $F_{i,j} = -A_1 P_x + A_2 P_y - A_1 P_z$ with P_x, P_y, P_z pressures either of the high, medium or low accumulator.
- $F_{ref} = \dfrac{K_{PTO}\vartheta(t) + R_{PTO}\dot{\vartheta}(t)}{d_{arm}(t)}$
- i, j will define the set of valves to open

The approximation we make is to neglect the losses between the cylinder and the accumulators when we calculate the available forces. However, we will see how this approximation is not strong at all.

3.5.2 Medium-Pressure accumulator control:

If we are not controlling the medium-pressure accumulator in order to keep its pressure in the middle of the low and the high, we will lose the well distributed availability of forces. This will lead to a lower power absorption and consequently to a reduction of available forces, leading to a non-optimal behavior of the system.

We have so to consider a medium-pressure accumulator reference pressure and we need to try to follow it as much as possible. To follow the reference forces we have to act in two different ways considering that when $P_{med,acc}$ is lower than $P_{med,ref}$ we need somehow to fill the medium accumulator, otherwise we need to foster the emptying. We need so to identify which force

uses the medium pressure accumulator and to define if the latter has an action of emptying or filling it.

Let's consider for a moment the cylinder:

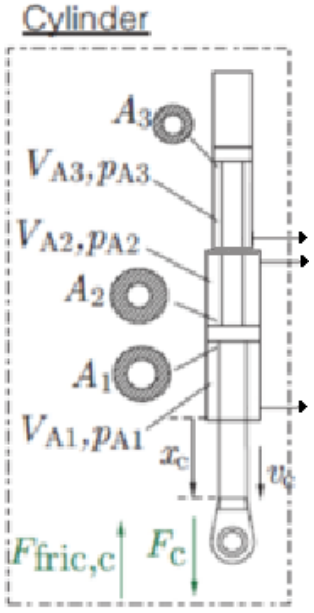

From the figure we can understand how knowing the actual sign of the piston velocity we can define which chamber is filling and which one is emptying the accumulators.

For example, let's consider a positive velocity, so a downward motion of the piston, we can see how chamber 2 is expanding, that corresponds to an incoming flow in the chamber, while chamber 1 and 3 are compressing, that implies an out coming flow. In this case if $P_{med,acc} < P_{med,ref}$,the medium accumulator needs a refill and we have to foster the connection of the medium pressure accumulator with chamber 1 and 3, while we have to penalize its connection with chamber 2.

Obviously, the penalization must be done in function of how far is the $P_{med,acc}$ from $P_{med,ref}$,so to not penalize too much the tracking of the force. As for the previous strategy adopted for the motor, we decided to apply an exponential gain. The gain will be defined to penalize or to endorse a choice of the valve combination. The penalization/abetment of a selected force will be defined in an additive way, so, for example, if the force selected has two chambers to be penalized and the other one is not connected with the medium accumulator the

penalization will be doubled. On the other hand, a force that has a chamber to be penalized and one to be endorsed will be counted as one with no connection with the medium accumulator. It's so a gain that is proportional to the difference between the chambers that endorse and the ones that penalize the requirement (n in the formula, where the definition just given is for the combinations of valves that endorse. For the ones that penalize, n is defined with the opposite sign).

$$\chi_{medium} = \begin{cases} n * e^{\frac{\left|P_{med,acc} - P_{med,ref}\right|}{10}} & \text{to endorse} \\ \dfrac{1}{n * e^{\frac{\left|P_{med,acc} - P_{med,ref}\right|}{10}}} & \text{to penalize} \\ 1 & \text{if there is no connection with the medium accumulator} \end{cases}$$

$$\text{With } P_{med,ref} = \frac{P_{acc,\text{high}} + P_{acc,\text{low}}}{2}$$

3.5.3 Emergency Strategy:

If our system is subjected to low power waves a situation in which the high pressure and low pressure accumulators tend to reach the same value of pressure or even to exchange their "role". In fact we observed how, due to the limited amount of accumulators (to avoid an excessive cost of the system), the ΔP across high and low pressure accumulators could reach oscillation of even 15 bar. While in case of energetic wave, so when the ΔP is great enough to avoid the exchange of the two pressure, we don't face this problem, in case of low

energetic wave we need to design a control strategy to avoid the occurrence of this condition.

In case of a $\Delta P < 40$ [bar] this emergency strategy will be used. The strategy is based on three main points:

- Penalize all the forces combination that fill the low-pressure accumulator or empty the high-pressure one with a strategy similar to the one used to keep the medium-pressure accumulator around its reference pressure.
- Avoiding the usage of the medium pressure accumulator
- As will be seen afterwards, an increase of the plausible forces

As for the medium-pressure accumulator, the strategy for this control is based on a gain. This gain is again an exponential one, with the same additive behavior, defined as:

$$\varepsilon_{emergency} = \begin{cases} n * e^{\frac{|\Delta P_{\lim} - \Delta P_{actual}|}{5}} & \text{to endorse} \\ \dfrac{1}{n * e^{\frac{|\Delta P_{\lim} - \Delta P_{actual}|}{10}}} & \text{to penalize} \\ \inf & \text{if there is a connection with the medium accumulator} \end{cases}$$

This will have a slight effect on the possibility to follow the reference force since the two pressures are so near that is not necessary to have a third, medium, pressure value.

3.5.4 The Final Control:

We have seen how to treat all these three different problems. We need now to design the final control strategy. In order to be able to apply different

gains we need to release the requirement of the force following. In fact it is obvious that by asking $F_{i,j} : \min\left(\left|F_{i,j} - F_{ref}\right|\right)$ we are not able to make a choice based on a compromise between chasing the force reference and the "necessity" of the system.

We decided to release this requirement by introducing a range defined with a percentage; in fact we will consider the group of force that have an absolute error with the reference one smaller than the 25% of it. This is done in a normal working condition, while we are going to increase this percentage linearly in case of emergency condition [3.5.3]. This means that:

$$\begin{cases} F_{sel} = F_{i,j} : \left|F_{i,j} - F_{ref}\right| < 0.25 F_{ref} & \text{not in emergency} \\ F_{sel} = F_{i,j} : \left|F_{i,j} - F_{ref}\right| < \underbrace{\left(0.25 + 2^{\left|\Delta P_{\lim} - \Delta P_{actual}\right| / \Delta P_{\lim}}\right)}_{\text{saturated to a maximum of 0.5}} F_{ref} & \text{emergency} \end{cases}$$

If we have this bunch of plausible forces we are going to weight their error with the exponential gain given by the mid-pressure accumulator control or the emergency gain so:

$$\begin{cases} F_{weight_{i,j}} = \chi_{medium_{i,j}} F_{sel_{i,j}} & \text{not in emergency} \\ F_{weight_{i,j}} = \varepsilon_{emergency_{i,j}} F_{sel_{i,j}} & \text{emergency} \end{cases}$$

We are then going to select the minimum weighted force. In case that there are no forces nearer enough to be selected, the choice will be done in the classical way, so by choosing the force that gives the minimum error.

We can now describe the process in a graphical way:

IF WE ARE NOT IN AN EMERGENCY SITUATION:

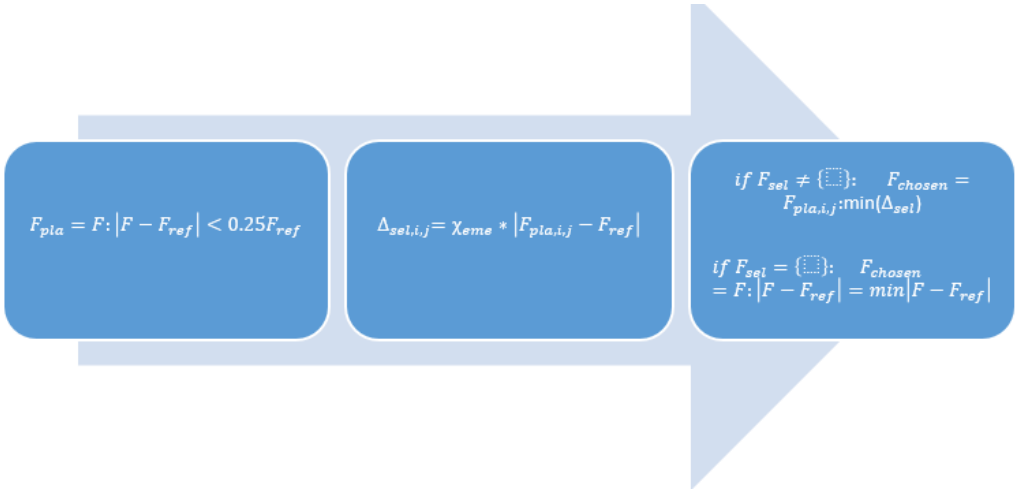

IF WE ARE IN AN EMERGENCY SITUATION:

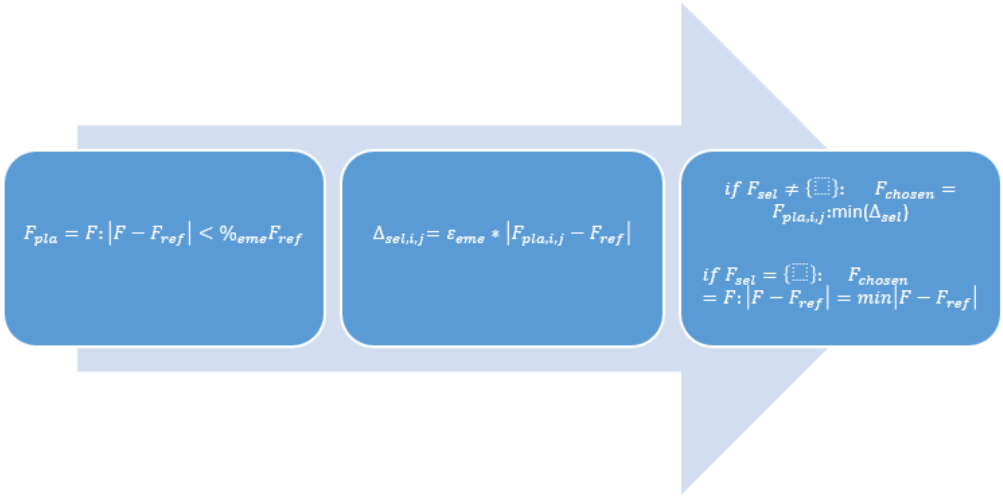

3.6 INCREASING THE EFFICIENCY

Up until now, we have been concentrated more on the mechanical system. Despite the importance of the WPEA, we have also to care about the hydraulic system, since we will see how the hydraulic losses strongly influence on the whole system. Performing an optimization considering solely the upstream part, we were obtaining a big increase in the energy extraction, but looking at the single efficiencies of the components (every step in the energy conversion), we understood that we could do better. Above all, we achieved a bad conversion from the cylinder to the hydraulic motor, meaning a bad hydraulic conversion of energy.

In addition to that, we anticipate that we will see how optimizing the downstream part of the system could influence the optimization point of the upstream part (for example the saturations we considered before, to perform the previous optimization, change). We will explain in the last chapter how an approximation of the whole system optimization point could be achieved, for each wave state.

We now consider a reference force to follow, and we introduce the problem due to compressibility losses.

The whole idea is to find the best compromise between the tracking of the force and these losses. The question, hence, is: is there a force that follows less the reference one, but allows us to save more energy?

3.6.1 A new tracking algorithm: considering losses inside the chambers

We saw in the last chapter how the reference force might not be chosen in certain cases, due to prohibited conditions of the medium accumulator. In order to avoid an excessive or too low volume in the medium accumulator, we so explained that we impose some weight to the choices of the valve combination, in order to privilege some solutions with respect others. This solution sometimes could have been different from the one that more nearly approached the force.

The idea now is to follow a similar procedure, setting another gain that is related to compressibility losses. Given a shift of pressure inside a cylinder chamber, we can write the energy loss in the following way:

$$E_{\beta}[J] = \frac{1}{2}\left(P_{old} - P_{new}\right)^2 \frac{V}{\beta}$$

Where we put in evidence the bulk coefficient, which we consider constant for approximation, and the volume of the chamber. From the expression, we can see how this loss, which is in Joule if the international system is used for the other variables, depends on the square of the pressure drop.

For a three-chamber cylinder we can write this loss as:

$$E_{\beta}[J] = \sum_{i=1}^{3} \frac{1}{2}\left(\Delta P_i\right)^2 \frac{V_i}{\beta}$$

Every valve connection switches, since it does not occur in a pressure equilibrium like in our original non-optimized control, causes some loss. In order to create a compromise between the force tracking and the losses

minimization, our first criteria is about creating a gain for all the 27 possible choices, defined like the following:

$$\gamma_{en} = \sum_{i=1}^{3} \frac{V_{chamberchosen,i}}{\beta} \left(P_{accchosen,i} - P_{cylchosen,i} \right)^2$$

Where we put in evidence how every choice implies three couple of accumulator-chamber. Of course a single accumulator might be connected to more than one chamber, while the opposite is not allowed (we can't connect one chamber to more the one accumulator).

We can create, hence, a table of 27 values, each of it connected to one new state of the manifold. Of course, the choice that implies no change of connection will provoke zero loss.

After having create this table, we select (in the same way we did to control the pressure of the medium accumulator), the forces whose difference with the reference one is no more than 25%. If there is just one force, in case we are not in emergency condition (see previous paragraph), this will be the choice, regardless any energy loss. If, instead, there is more than one choice, the penalty weight introduced before is multiplied by the energy gain, giving origin to one single gain. The procedure, then, follows at the same way. The choice is the one associated with the smallest gain.

The scheme so is:

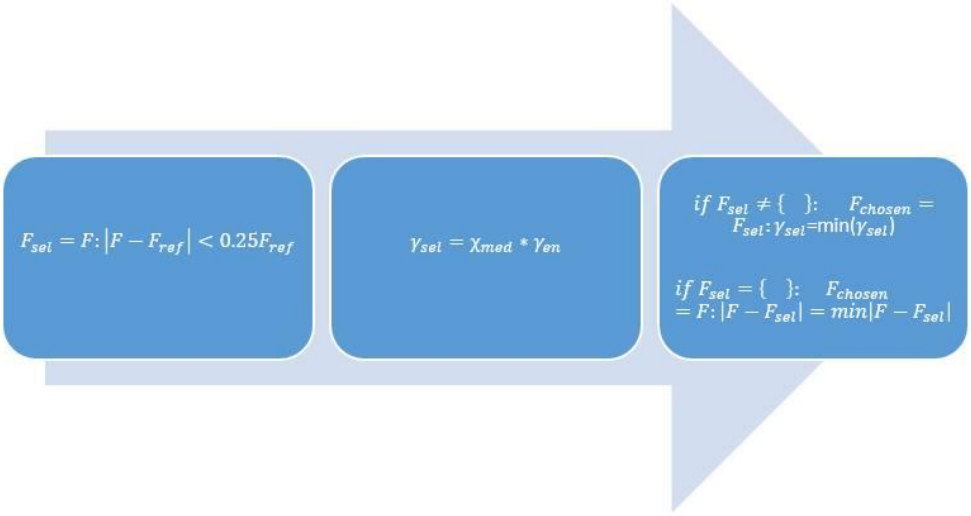

Doing this multiplication and the previous selection, we are doing a compromise between the tracking, the losses due to compressibility, and the medium accumulator urgencies.

3.6.2 Optimization of the gap of pressure inside the system

This procedure we just explained is not the only one which aims to achieve a better whole performance of the system. We can in fact understand how the value of the pressures inside the accumulators, and as a consequence inside the chambers, strongly influence the absolute values of the hydraulic losses. The idea is to optimize the pressure drop across the hydraulic motor.

Going more in depth, we put in evidence three effects of the drop of pressure:

1. Capability of tracking a force: given a force reference, if by diminishing the difference between the higher and the lower pressure, considering the medium always in the between, we will start to be less able to follow the reference, above all at its peaks. This because the maximum force available does not reach the maximum required anymore.
2. Compressibility losses: we saw how increasing the drop of pressures inside a chamber implies a hydraulic loss more consistent.
3. Hydraulic motor efficiency: in the second chapter, where we model all our components, we saw how the whole efficiency of the hydraulic motor improves with the pressure gap.

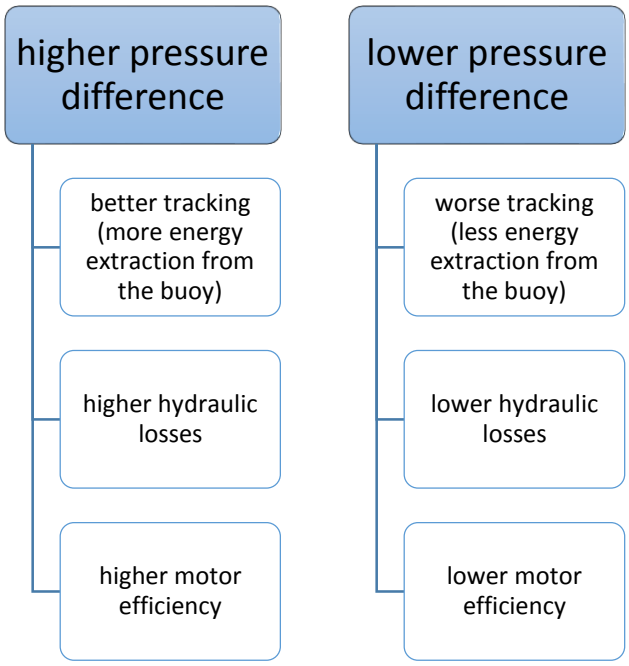

Since the process of energy conversion pass by all of these steps, meaning the extraction, the conversion into hydraulic power and finally the conversion

into mechanical power to aliment the asynchronous generator, we can imagine how there is an optimal point for the pressures.

We implemented an optimization process in the following way

- We gave a security limit for the gap of pressure, given by a maximum torque from the cylinder equal to 1MN, which correspond to 240 bars.
- We are aware about the dependence of the torque also from the medium pressure, but this dependence is weaker than from the difference between the high and the low pressure. Throughout the simulation, hence, we will keep constant the medium pressure to 130 bars.
- The system we run to achieve the results is simpler than the detailed model: similarly to the case of the R, K optimization of the PTO, we implement a Simulink model describing dynamically the mechanical buoy, subjected to the wave input. At this time, we consider the model of the cylinder connected, since we want to model the hydraulic losses. An approximation is given by neglecting the transient in the cylinders, implying the pressure in the chambers to be always equal to the pressures inside the accumulator connected. To do that, we avoid the dynamic of the valve and we consider every switch instantaneous. This approximation, though, is not influencing that much the energy loss calculation, but it could slightly modify the energy extraction.
- We cycle for different value of DP, from 40 to 240, and we save the maximum value of energy output, meaning the energy that arrives upstream the motor. Finally, we need to consider the efficiency of the hydraulic motor, which depends on both the pressure drop and the

angular velocity. Given the energy and the pressure drop, we can calculate the ideal angular speed, being aware that this value might not be available from the system due to the saturation of the asynchronous generator alimentation frequency. Anyway, this happens just in extreme condition of high energy or extremely low one, which are cases that do not regards us very much.

We can sum up the procedure:

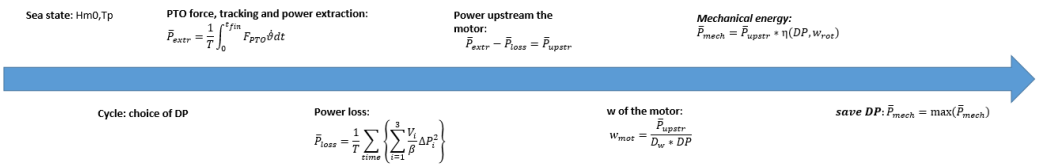

Figure 3-15 Procedure to Optimize the DP

We save the optimal value of DP for every sea state. We can show an example, for some sea state, looking at the shape of the mechanical energy. The result are the following:

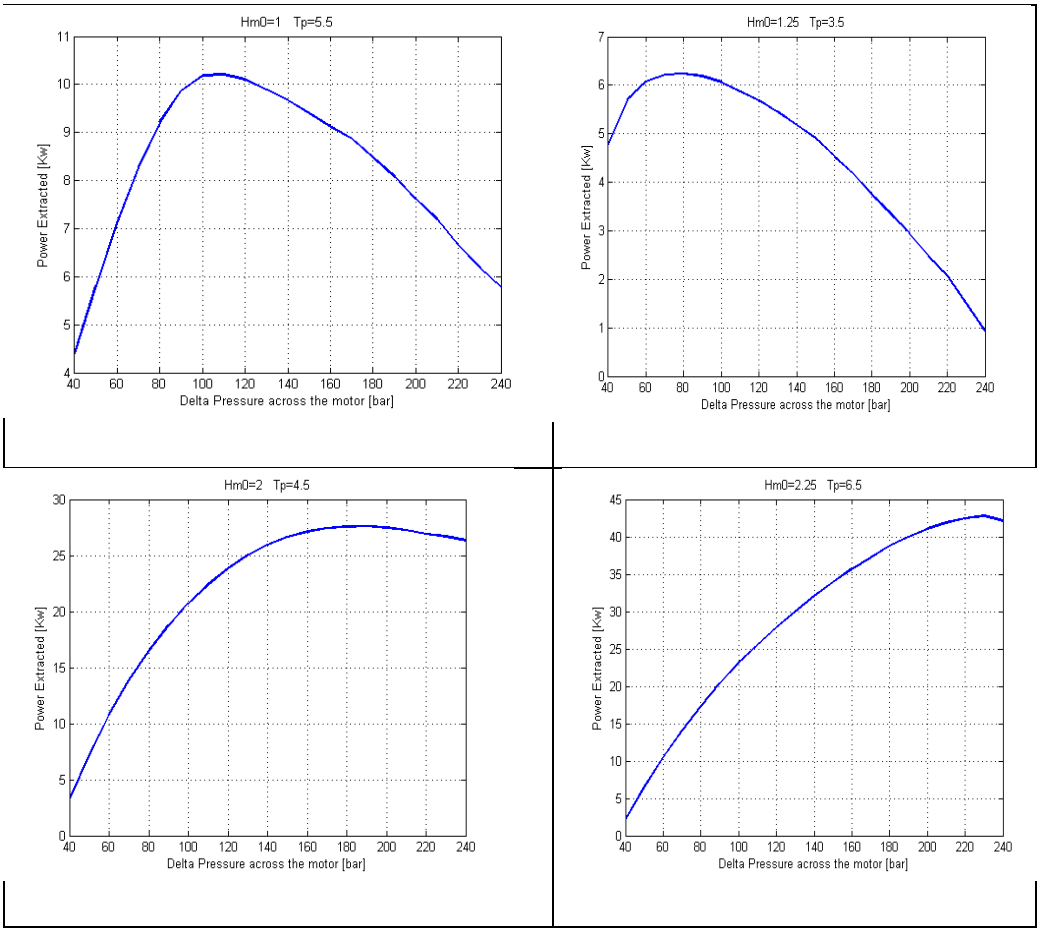

Figure 3-16 Some Results for different Wave States

We can see how the optimal DP varies a lot with the wave sea state. In particular, it grows with the energy input, but not proportionally. We are going to build a table for each wave state and, how we will see, we are going to use these tables for a reiteration process (re-optimization of R and K).

3.6.3 Optimization of the control time

We already introduce our control system. The aim is to manage the manifold in the appropriate way and the control is discrete, meaning that the control action is taken at determined time, equally spaced one from the other. The control choice, hence, is done depending on an evaluation made at that same time t. We witness how the reference force cannot be reached perfectly, since our system provides a discrete force that approximates it. Our investigation is how the control time influences the energy production.

As we did for the pressure, we can put in evidence some effects of the control time:

1. Tracking the force: since the system is digital, switching the valves more slowly implies a longer step of the actual PTO force. This means that being the actual force constant for a longer time, it will get further from the reference one, which is constantly changing during the control time.
2. Energy losses: every switch of the manifold arrangement implies an energy loss. If this switch is done more often, the total losses grow in global terms, meaning that the power loss increases.

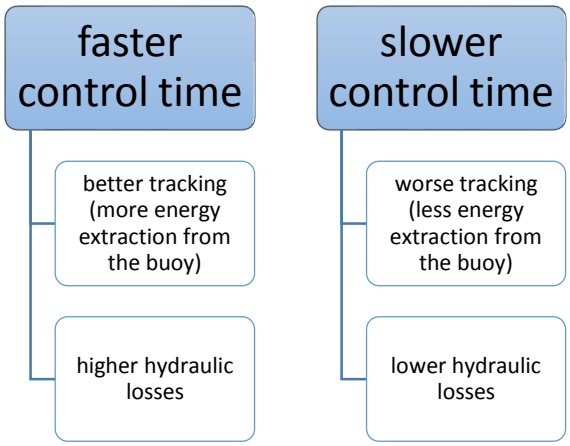

Figure 3-17 Effect of the Control Time

We noticed how the optimal point for this value is around 0.35s for each wave state, so we decide to keep this value equal to it for each wave state. It is the best compromise, on average, between tracking requirement and energy losses.

To implement the simulation we use the same Simulink scheme we used before to optimize the pressure gap, varying the control time.

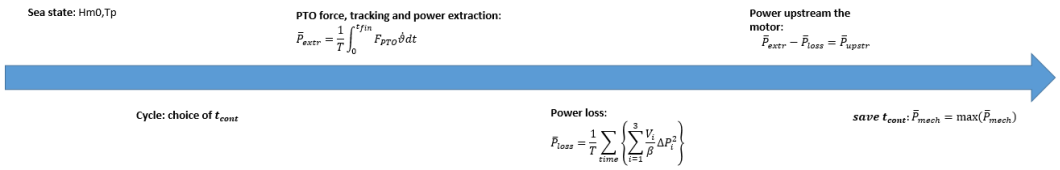

Figure 3-18 Procedure to Optimize the Control Time

We can watch the result for a main wave height of 2m and a main wave period of 4.5s

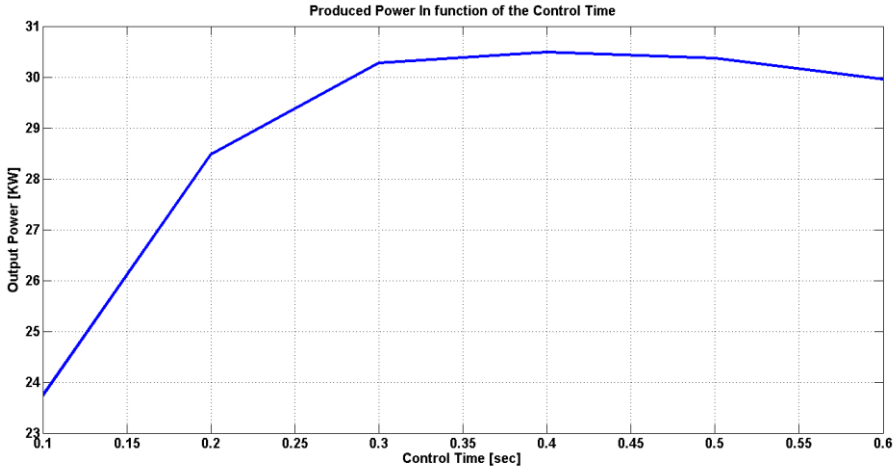

Figure 3-19 Energy with Control Time

We can see how shortening the time far from the optimal point strongly influences on the energy conversion. We were running the first simulations with a control time of 0.1s and the whole efficiency was negatively influenced by this choice.

3.6.4 Valve superimposition time

The opening of a valve is not immediate, but there is a maximum speed of opening. The value of the area is assumed to grow and decrease linearly. If we open one and close the valves when the digital command arrives, we have a maximum superimposition time, meaning that a chamber is connected contemporary to two accumulators, which is not an efficient way to act. From literature [9], we use to have a 10% of superimposition time, over the total opening time (or closing). This is another compromise between a force tracking

and energy saving. We avoid an immediate opening to save an unwanted leakage between accumulators. Moreover, this procedure adopted allows us to reduce the simulation time consistently. We cannot wait too long, though, to avoid a very bad tracking.

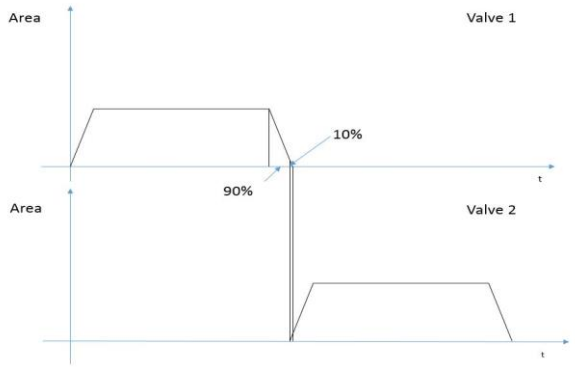

Figure 3-20 Valve Strategy Adopted

3.7 PRACTICAL IMPLEMENTATION: OPTIMIZATION OF THE WHOLE SYSTEM

We have seen in the previous paragraphs how there are many variables that influence the energy extraction. Hence the optimization procedure should consider somehow all of them. Summing up the variables, we can write:

$$\frac{P_{output}}{P_{wave}} = f\left(WPEA, \Delta P, t_{contr}, t_{\sup valve}, P_{accmedium}\right) \text{ where } WPEA = f\left(R_{PTO,}, K_{PTO}\right)$$

If we wanted to carry out a global optimization we should run a huge number of simulations running over a grid of 6 dimension. Moreover the number of simulations would increase if we consider the statistical nature of the wave phenomenon (R and K are chosen in a statistical way).

We have to find a compromise between precision and whole optimization time.

We chose to follow a particular procedure that exploits just one iteration, since we arrive to a satisfactory convergence.

Some of the variables are optimized independently exploiting the fact that we observed their optimum value is not strongly influenced by the variations of the other parameters. These variables are the control time and the superposition time. In addition to that, as already explained, we will keep the medium accumulator pressure around the average of two pressure lines to have a better distribution of available forces.

This optimization, since it is function of the wave state, must be done for each wave state.

Schematically we can summarize the procedure in the following way:

1. ***We need a starting point for our optimization process:*** we supposed the PTO efficiency to be equal to 0.7 and we set maximum saturation to 1MN, we then run the simplified system (just the PTO part) and we obtain the values of R,K and an rough estimation of the energy extraction, which we will use in the next step

2. ***Including a plausible saturation:*** Thanks to the energetic estimation we achieved in point 1 we can reiterate the simulation updating the value of saturation. Knowing the working range of our motor, we consider a more plausible level of saturation above all for low energetic waves where pressures would never give a 1MN torque.
3. ***Optimization of the gap of pressure:*** For a given reference force (R and K defined) we optimize through a simpler system the gap of pressure (see paragraph [3.6.2]).
4. ***Whole system simulation:*** We perform a simulation with the parameters obtained checking the efficiency values, above all the efficiency of the PTO. We will use this new value of efficiency in the next step.
5. ***New Optimization of R and K:*** Through the new efficiency and the new saturations given by the pressure gap achieved in point 3 we run again the optimization for the controller parameters. We check that these values of gap of pressure could be reached by our system. However, we keep as a safety maximum value 1MN.
6. ***Check of the convergence:*** We run again the simulation to optimize the drop of pressure with the new values of R and K. Checked that the ΔP has not changed of more than 10 bars we run the whole system simulation to check the convergence of the efficiency. The efficiency will change considering different wave states, we decided however to check if the average of this efficiency corresponds to the one supposed in point 5.

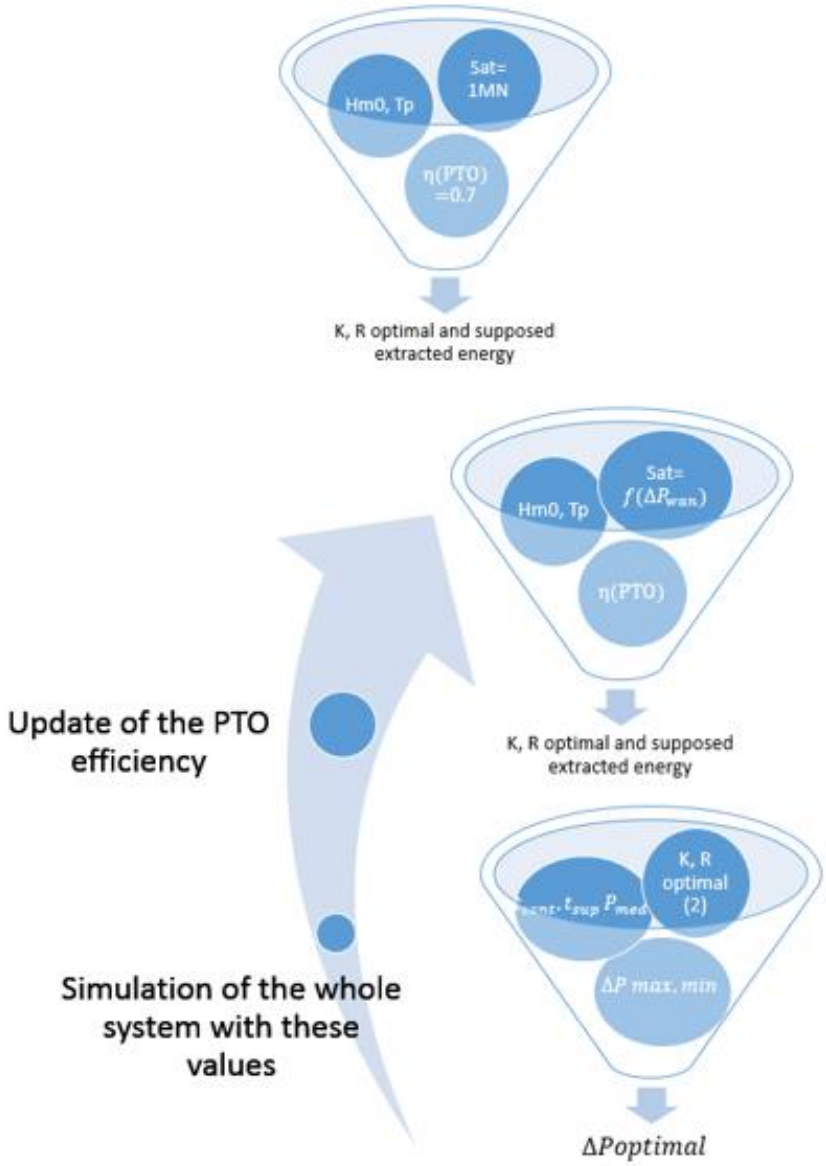

Figure 3-21 Procedure to Optimize the System Control Parameters

Through this method, we have obtained an optimal value for all the parameters, this values might be different from the one that we would have

achieved through the global optimization but as anticipated this choice is a reasonable compromise between time and precision.

We can have a look to our final parameters that will be used in the WPEA. We can observe that where the saturation does not occurs the optimal parameters do not depend on the wave height. This occurs however just for low energetic wave states.

K optimal								
Tp\Hm0	**1**	**1.25**	**1.5**	**1.75**	**2**	**2.25**	**2.5**	**2.75**
2.5	3.40	3.45	3.35	3.45	3.25	3.45	3.40	3.45
3.5	-3.25	-3.20	-3.10	-3.05	-3.00	-3.05	-3.35	-3.20
4.5	-6.85	-6.15	-6.15	-5.70	-5.40	-5.40	-6.20	-6.55
5.5	-9.51	-8.46	-9.46	-9.11	-8.71	-5.51	-6.66	-6.76
6.5	-8.65	-7.40	-8.45	-7.00	-9.25	-8.50	-7.90	-8.10

Table 3-1 Optimal values of K coefficient

R optimal								
Tp\Hm0	**1**	**1.25**	**1.5**	**1.75**	**2**	**2.25**	**2.5**	**2.75**
2.5	2.31	2.31	2.31	2.31	2.31	2.31	2.31	2.31
3.5	2.33	2.28	2.28	2.28	2.53	2.33	2.38	2.28
4.5	4.26	3.46	3.51	3.91	3.56	3.06	4.66	4.66
5.5	6.36	6.01	6.36	6.46	6.66	5.06	6.31	5.86
6.5	6.85	5.75	7.00	5.55	9.55	10.40	9.50	12.25

Table 3-2Optimal values of R coefficient

After having collected the results for each wave states we run the final simulations collecting and comparing the results with the old control.

4 FOURTH CHAPTER: RESULTS AND CONCLUSIONS

We decided to arrange the chapter of the results in the following way:

1. Showing a whole simulation of 2000s with a particular wave state where we can appreciate some important results and trends given by the control. We choose a significant wave state (Hm0=1.75m, Tp=4.5s).
2. Compare different control for this wave state: the oldest one, a couple of partially optimized control and the final control adopted.
3. The results obtained for the entire possible northern sea wave states.

4.1 SIMULATION OF THE SYSTEM FOR A WAVE STATE

We run a long simulation for a wave characterized by a significant wave height of 1.75m and a main wave period of 4.5s. We then have a look at the main variables trends, at the energy production and at the efficiencies, whose structure and meaning has been explained in [2.8]

The results are the following:

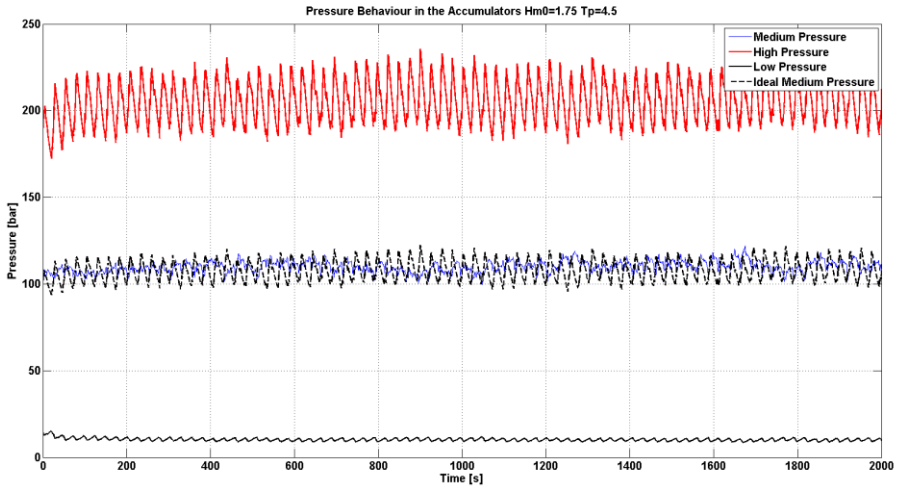

Figure 4-1 Pressure Trends inside the Accumulators

Where we see how the pressure of the medium accumulator is controlled and stays always around the reference one, which is the average between the high and the low pressure. To avoid to have a long transient we set initial conditions near the regime ones.

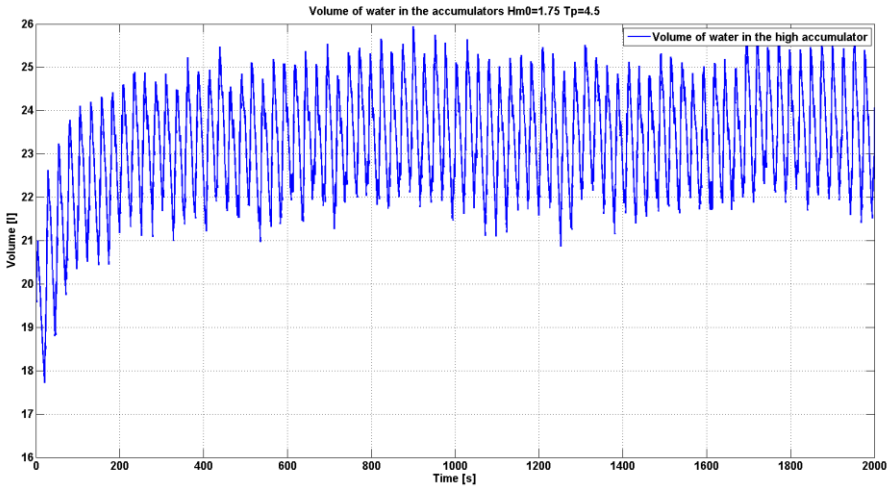

Figure 4-2 Volume of Oil in the High Pressure Accumulator

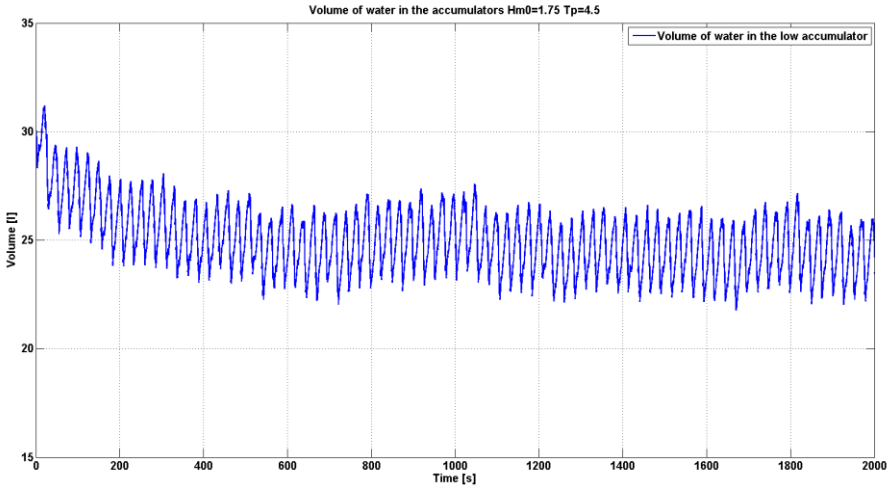

Figure 4-3 Volume of oil inside the Low Pressure Accumulator

The volume of oil in the accumulators are linked to their respective pressures. We could check how they don't occur into any depletion.

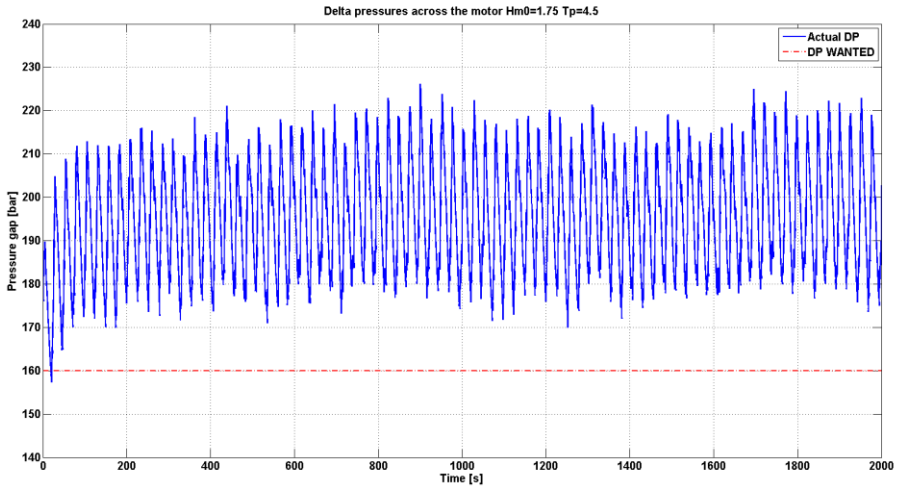

Figure 4-4 Drop of Pressure across the Motor

If we go across the motor we can check the gap of pressure. We can see how this gap can't reach the desired one do to an excessive energy input and a limited angular speed. We will see in the next graph how the motor runs at its maximum allowed speed. If we had a faster motor, we could reach the desired pressure gap. Despite this impossibility, we are anyway working nearest to the optimum point given our capability. Any gap of pressure higher than this, in fact, will go further from the real optimum point, unreachable for us.

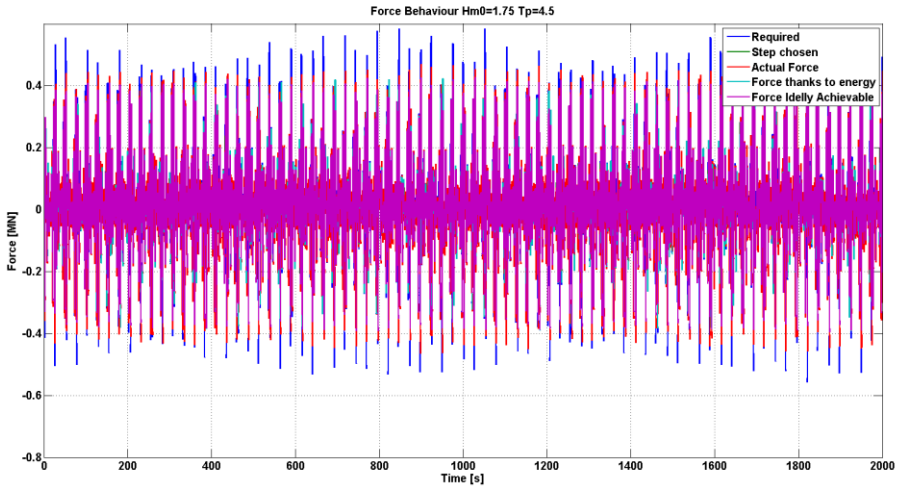

Figure 4-5 PTO Force

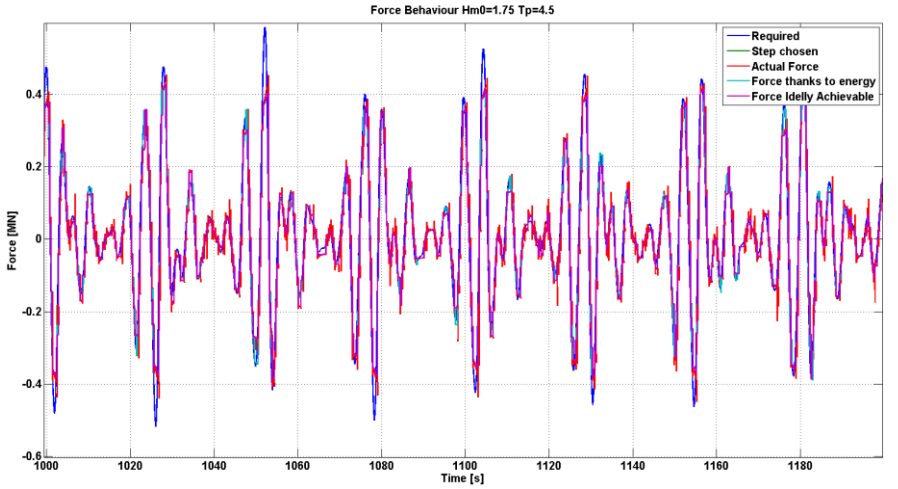

Figure 4-6 PTO Force Zoom 1

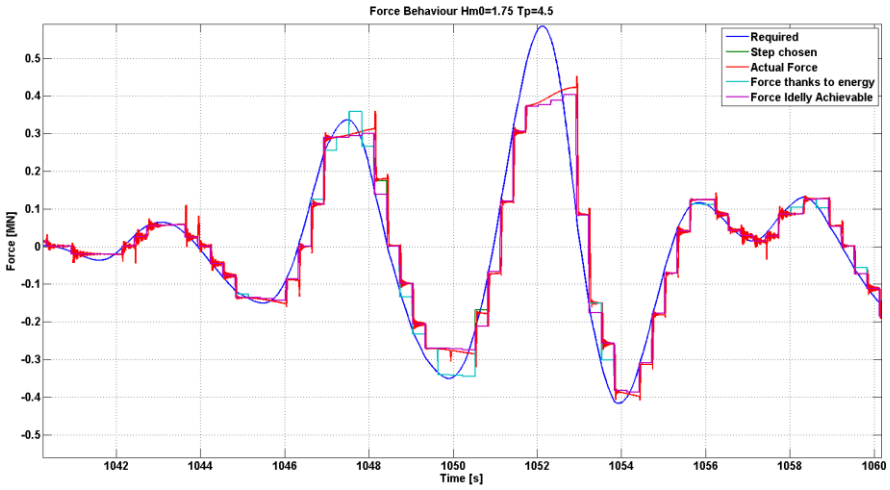

Figure 4-7 PTO Force Zoom 2

The latter graphs shows, one in a more detailed way, how the reference force is followed. Sometimes, above all when there are peaks of torque, our system does not follow the force, or because it's not able with its optimize gap of pressure, or because it decided not to follow it by strategy, see [3.5.2,3.6.1].

We put in evidence the reference torque, the torque ideally achievable, the torque chosen by the algorithm, the torque that would be chosen just by considering the energetic issue [3.6.1], without considering the medium accumulator issues, and finally the torque nearest to the reference one.

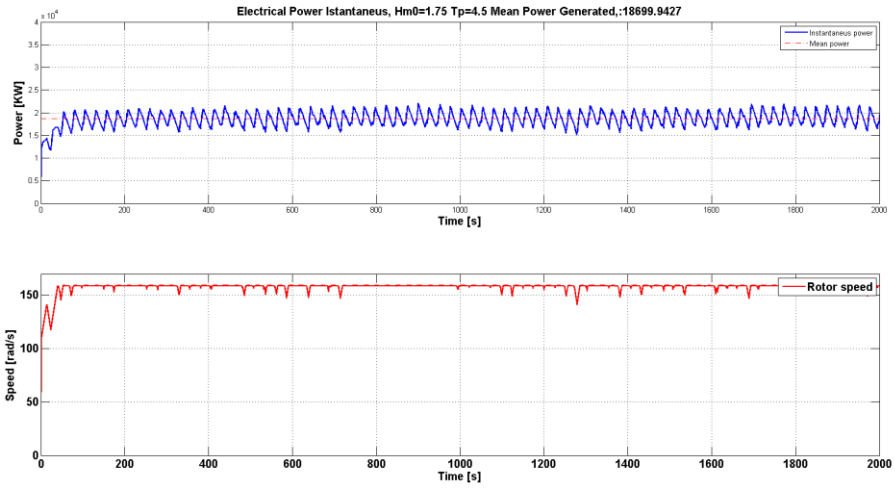

Figure 4-8 Power and Angular Speed

We can have a look at the instantaneous power and at the mean one, calculated starting from 100s, in order to neglect the transient, conditioned by the presence of the accumulator action. We see how the power production is about 18.6kW. This is a great improvement with respect our previous control and the others not completely optimized.

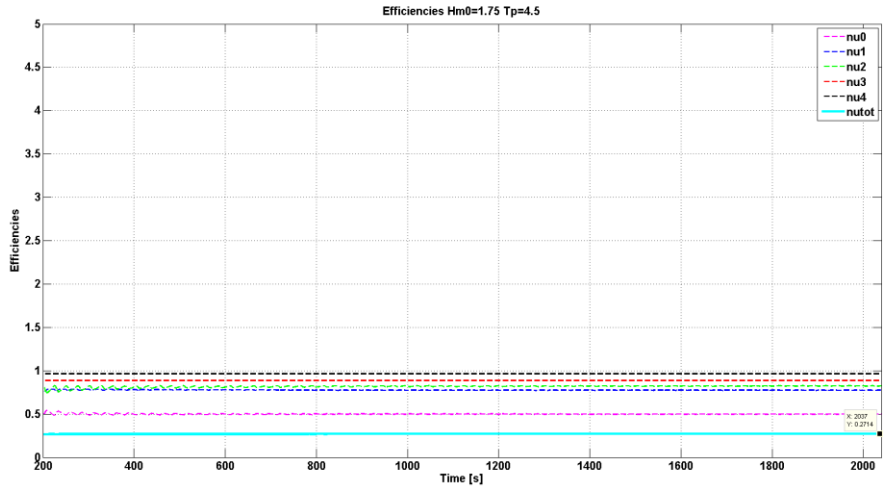

Figure 4-9 Efficiencies

We can finally watch at the efficiencies, whose meaning has been explained in [2.8]. The total efficiency is 0.27, starting from the energy contained inside the wave. This efficiency can vary depending on the wave state, since the system doesn't work exactly in the same way for every condition. We will list all the energy production and efficiencies, for all wave states, in [4.3]. We can summarize the results in the following table:

RESULTS	
Power Production	18.7 kW
ηu0	0.5
ηu1	0.77
ηu2	0.82

ηu3	0.89
ηu4	0.96
ηutot	0.27

Table 4-1 Results Obtained

4.2 COMPARISON BETWEEN CONTROLS

We can now compare some control strategy between each other. We decided to compare the following four controls:

- Our optimized control
- A control partially optimize, just in R and K, and not in the pressure gap. In particular, we set a gap of pressure of 230 bar, while the optimal one is 160 bar.
- A control partially optimize, just in the gap of pressure, and not in the R K. In particular, we set the WPEA parameters calculated without considering the saturation and the efficiency (see [3.3.1]).
- Our oldest control, which treats the cylinder like a simple volumetric pump.

We build a table where we compare the results obtained for each control

	POWER OUTPUT	TOTAL EFFIFICINCY	ηu0	ηu1	ηu2
Our control	18.6 kW	0.27	0.50	0.77	0.82
Not opt DP	17.3 kW	0.25	0.49	0.73	0.78
Not opt R,K	16.8 kW	0.24	0.48	0.71	0.8
Oldest control	10.7 kW	0.13	0.24	0.83	0.75

Table 4-2 Comparison between Results

We can see how, despite we don't optimize every single efficiency, the result is the optimization of the total one. This confirms how our system is composed by different parts, each of which has its own optimization, but it can't be optimize singularly, without considering the other parts of the system.

4.3 Final Results for Different Wave States

We are now proposing the resulting power for different wave states:

Average Power Produced [kW]								
Tp\Hm0	**1**	**1.25**	**1.5**	**1.75**	**2**	**2.25**	**2.5**	**2.75**
2.5	1.10	1.77	2.62	3.61	4.84	6.14	7.23	9.24
3.5	3.62	5.77	8.28	11.40	14.23	18.34	22.16	26.36
4.5	6.38	10.37	14.81	18.54	24.15	30.31	32.27	37.93
5.5	8.54	12.89	18.29	23.27	29.41	33.74	40.07	47.31
6.5	10.09	15.17	21.05	28.17	32.54	35.42	42.12	44.90

Table 4-3 Average Power Produced

We can observe how the system is able to produce energy even with low energetic waves. The efficiencies are not constant with the wave states, but as already explained this is normal since different operational condition point of the plant arise in different components performance.

Total Efficiency [%]								
Tp\Hm0	**1**	**1.25**	**1.5**	**1.75**	**2**	**2.25**	**2.5**	**2.75**
2.5	8.82	9.08	9.31	9.43	9.69	9.70	9.89	9.77
3.5	20.67	21.11	21.02	21.26	20.33	20.70	20.26	19.92
4.5	28.36	29.49	29.26	26.90	26.84	26.61	22.95	22.29
5.5	31.06	30.00	29.55	27.63	26.74	24.24	23.31	22.75
6.5	31.04	29.87	28.78	28.30	25.03	21.53	20.73	18.27

Table 4-4 System Total Efficiency

Since we supposed a PTO efficiency equal to 0.85 in order to obtain the controller values, we must check that the mean value of the accumulator efficiency (ηu2) is near to the guessed value. Here we present the efficiency table and its mean value:

ηu2 [%]								
Tp\Hm0	**1**	**1.25**	**1.5**	**1.75**	**2**	**2.25**	**2.5**	**2.75**
2.5	83.68	88.52	87.94	87.49	90.25	88.19	89.67	89.58
3.5	90.77	88.47	89.52	87.31	83.91	80.13	77.09	76.03
4.5	86.84	91.04	86.94	81.00	79.18	74.48	71.90	67.95
5.5	92.93	85.12	87.34	83.90	77.78	74.09	71.37	68.31

6.5	88.54	88.89	85.28	80.63	80.50	76.29	74.29	71.15

Table 4-5 PTO Efficiency

We can observe how this supposed efficiency value was approximately correct, this means that we were allowed to stop to the first iteration during the optimization procedure for the controller parameters.

Another important parameter was the optimal DP that was used to position the pressure lines in an optimal point. However, it could happen that the plant can't reach this value due to a limited speed of the motor (purple and red colored) as we have seen in [4.1].

Pressure Gap Desired								
Tp\Hm0	**1**	**1.25**	**1.5**	**1.75**	**2**	**2.25**	**2.5**	**2.75**
2.5	50	50	60	70	80	90	100	100
3.5	60	80	90	110	120	140	150	170
4.5	90	110	120	160	190	200	220	230
5.5	110	160	160	180	210	230	230	230
6.5	140	170	190	210	230	230	230	230

Table 4-6 Pressure Gap Wanted by the Control

In some cases, as anticipated, the reached delta pressure is too high to be feasible for our plant, since it goes over the maximum rated pressure of the accumulator of 330bars (red colored). The solution could be either switch on a parallel motor/generator that will help the original one assuring the necessary

flow sucking the excessive flowrate, or through a control that dump the power adsorption. The solution in which we pass to a single pole generation is might be problematic for low waves state. How was possible to imagine, due to the variance of the phenomena, is almost impossible to generate in a feasible and efficient way energy for all waves states.

Like indicated in [9] every wave states has its distribution all over the year, meaning that all the wave states we analyzed do not occur with the same probability.

Tp\Hm0	Hm0<=1	1<Hm0<=1.5	1.5<Hm0<=2	2<Hm0<=2.5	Hm0>2.5
2<Tp<=3	3.87	0	0	0	0
3<Tp<=4	27.38	6.84	0.33	0.02	0.01
4<Tp<=5	13.24	13	9.58	3.34	0.22
5<Tp<=6	2.59	2.96	3.05	4.60	3.89
6<Tp<=7	0.32	0.3	0.29	0.2	0.21

Table 4-7 Wave Yearly Distribution

Having the table for the power generation and for the wave distribution over the year we can calculate the average yearly power production by multiplying the mean power associated to each wave state with the relative probability. The final result is:

$$\bar{P}_{year} = \sum_{j=1}^{n_{H_{m0}}} \sum_{i=1}^{n_{T_p}} \bar{P}_{ij} * p_{ij} = 12.6\,\mathrm{KW}$$

4.4 CONCLUSION:

We optimized the plant choosing one kind of control, which involves a so called WPEA. Comparing this control with the old one [4.2], the procedure took to a visible improvement, since the energy extraction enhance of more than double. The mechanical system we took in consideration is a buoy that exploits the vertical force available from the wave in order to create a torque that is the start of the conversion process. This of course is not the only movement that an incoming wave could generate, and since we are exploiting just the vertical one, we are losing some energy at the entrance. To improve the total efficiency, in particular ηu0, we should be able to exploit other movements (like the Pelamis plant, see [1.3])

We used as a PTO a cylinder with three chambers and to optimize the control we chose a reference force to follow. This force is described by two parameters, R and K [3.5.1]. In our system, then, there are energy storage devices, which are the accumulators [2.5.4]. Two of them are connected to the hydraulic motor, while the third is needed to follow better the reference force and to limit the pressure drops inside the chambers (efficiency improvement). These accumulators allow from one side to smooth the energy output, from another side to supply the reactive energy required by the PTO.

By the end, a fixed stroke hydraulic motor drives an asynchronous generator [2.5.5] that, being connected to the grid through a couple of inverters, has the possibility to change its alimentation frequency. This is done in order to prevent the high-pressure accumulator from depletion but with the prudency of

maintaining a good energy quality at the same time (no sudden changes in the alimentation frequency).

Regarding our control, there are different parts of this plant to manage. Like we thoroughly described in the respective chapters, we optimized the parameters of the reference force to follow [3.3.2], the gap of pressure between the two pressure line [3.6.2] and the control time [3.6.3]. In addition to that, which regards mainly the force control, controls over the accumulators have been applied. In particular, we want to avoid the high pressure accumulator to lower its pressure too much, and this is guaranteed by the motor that slows down its speed when this condition occurs [3.4.1]. Secondly, we don't want the medium accumulator to stop behaving like a medium accumulator. That's why we develop a strategy that, in parallel with tracking the force, checks the medium accumulator situation and acts to position it in a right range [3.5.2]. We saw how this strategy was even more modified taking into account the energy losses inside the cylinder chambers [3.6.1]. Finally, we wanted to avoid the high pressure accumulator and the low pressure to approach too much, and that's the reason why we develop an emergency strategy that, in these cases, switches off the valves connected to the medium accumulator and starts pumping fluid in the high with more urgency [3.5.3].

Finally we obtain a system that manages to work with different wave conditions in an efficient way, even if this efficiency is not constant. For medium high wave energies, the performance of the plant reaches its maximum up to 30%.

5 NOMENCLATURE:

ϑ_{arm}	Arm angle from equilibrium condition
a_c	Distance between the hinge of the arm and the cylinder one
b_c	Distance between the hinge of the arm and the piston one
c_c	Minimum distance between the cylinder and piston hinges
x_c	Cylinder stroke (from minimum distance of the hinges)
$x_{c,0}$	Cylinder stroke (from minimum distance of the hinges) at equilibrium condition
d_c, d_{arm}	Action arm of the cylinder
H_{m0}	Significant wave height
T_p	Peak wave period
S_{PM}	PM-Spectrum
S_{JS}	JonSwap-Spectrum
J_{mech}	Arm moment of inertia considering the buoy in production configuration
λ	Wave length
η_{wave}	Wave height
d_{mech}	Distance from the hinge of the arm equivalent concentrated mass
A_w	Crossectional area of the float at the draft line
J_{add}	Added moment of inertia
B_{hyd}	Radiation damping

ω	Angular frequency
$\hat{K}_{r,n}(s)$	Approximated transfer function of the radiated wave torque of order n
$k_r(t)$	Radiated wave torque time function
$k_{elastic}$	Linearized spring term related to the buoyancy force
V_{sub}	Submerged volume at equilibrium
H	Hydraulic head
ε	Fitting loss coefficient
$Q, \dot{V}$	Flow rate
Q_m, M	Mass flow rate
β	Bulk modulus
$V_{0,An}$	Cylinder dead volume of chamber n
α	Percentage of trapped air
μ	Static friction coefficient
k_v	Oil viscosity
δ_v	Nonlinear coefficient that relates the viscous friction to the velocity
v_σ	Stribeck Velocity
δ_σ	Gradient of friction decay
C_d	Discharge coefficient
γ	Adiabatic index
α_v	Percentage of the valve opening
D_w	Flow rate parameter linked to angular velocity of the hydraulic motor
C	Torque

6 REFERENCES:

[1] BP, “BP Statistical Review of World Energy June 2014,” 2014.

[2] N. Stern, G. Britain, and H. Treasury, *Stern Review: The economics of climate change*. 2006.

[3] J. Cunha and R. Onofrei, “Energia Oceânica.”

[4] A. T. Jones and W. Finley, “Recent Developments in Salinity Gradient Power,” pp. 2284–2287.

[5] B. Drew, a R. Plummer, and M. N. Sahinkaya, “A review of wave energy converter technology,” *Proc. Inst. Mech. Eng. Part A J. Power Energy*, vol. 223, no. 8, pp. 887–902, Dec. 2009.

[6] A. Falcão, “Modelling of Wave Energy Conversion,” *fenix.tecnico.ulisboa.pt*, 2013.

[7] “Marine and Hydrokinetic Technology Database | Open Energy Information.” [Online]. Available: http://en.openei.org/wiki/Marine_and_Hydrokinetic_Technology_Database. [Accessed: 01-Oct-2014].

[8] R. Hansen, M. Kramer, and E. Vidal, “Discrete Displacement Hydraulic Power Take-Off System for the Wavestar Wave Energy Converter,” *Energies*, vol. 6, no. 8, pp. 4001–4044, Aug. 2013.

[9] R. H. Hansen, M. M. Kramer, and P. All, “Modelling and Control of the Wavestar Prototype.”

[10] G. Diana and F. Cheli, *Dinamica dei sistemi meccanici*. 2010.

[11] J.-B. Saulnier, P. Ricci, and A. H. Clément, “Mean power output estimation of wecs in simulated sea,” in *Proceedings of the 8th EWTEC*, 2009.

[12] A. Falcão, “Modelling of Wave Energy Conversion,” *fenix.tecnico.ulisboa.pt*, pp. 1–119, 2013.

[13] P. Tristan and F. Thor, “Parametric Time-domain models based on frequency-domain data.” [Online]. Available: http://www.marinecontrol.org/pdf/Tutorial/CAMS_M7_time_domain_models_short_II.pdf. [Accessed: 25-Nov-2014].

[14] T. Perez and T. Fossen, “Identification of Dynamic Models of Marine Structures from Frequency-domain Data Enforcing Model Structure and Parameter Constraints,” *ARC Cent. Excell. Complex …*, pp. 1–28, 2009.

[15] E. C. Levi, “Complex-Curve Fitting,” in *IRE Trans. on Automatic Control*, 1959, pp. 37–44.

[16] G. Diana and F. Resta, *Il Controllo Di Sistemi Meccanici*. 2006.

[17] N. D. Manring, *Hydraulic Control Systems*. 2005.

[18] A. Heinze, “Modelling, simulation and control of a hydraulic crane,” no. September 2007, 2008.

[19] B. Armstrong and C. C. de Wit, “Friction Modeling and Compensation,” in *The Control Handbook*, CRC Press, 1996, p. 1566.

[20] P. Luchini and M. Quadrio, *Aerodinamica*. 2003, pp. 217–230.

[21] A. Pourmovahed and D. Otis, “An experimental thermal time-constant correlation for hydraulic accumulators,” *J. Dyn. Syst. Meas. Control*, 1990.

[22] “Poclain Hydraulics.” [Online]. Available: http://www.poclain-hydraulics.com/en/products/motors/m-mv.

[23] T. Pradella, “Generatore asincrono a doppia alimentazione,” Università degli studi di Padova, 2010.

APPENDIX A

Here is attached the ANSYS AQWA report. The report was a direct output from AQWA program; we can observe how the inertias and mass are given randomly, in fact as discussed in the section regarding the *Exciting Wave Torque* and *Radiated Wave Torque* these coefficients are computed just by considering the geometry characteristic of the buoy [12].

Project

Name	Project
Data Folder Root	C:\Users\Gianmarco\Desktop\provaacaso_files\dp0\AQW\AQW
Date of Creation	11/18/2014 1:35:49 PM
Last Modified	11/19/2014 1:15:23 PM
Product Version	15.0.7 RELEASE

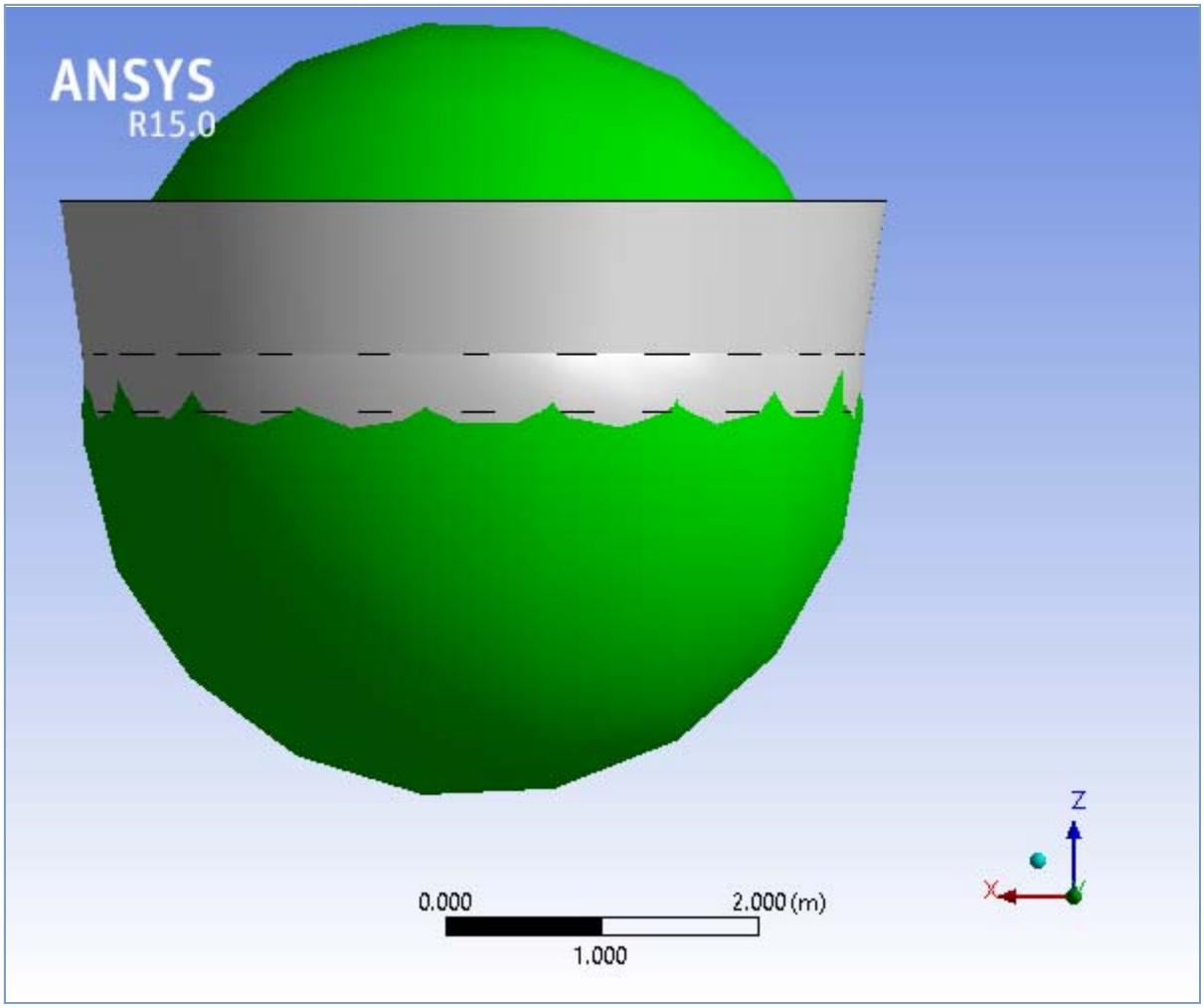

Contents

Units

TABLE 1

Length	Metre
Mass	Kilograms
Rotational Velocity	Degrees
Force	Newton
Frequency	Hertz
Time	Second

Model (A3)

Geometry

TABLE 2
Model (A3) > Geometry

Object Name	*Geometry*
State	Fully Defined
Details of Geometry	
Attached Assembly Name	C:\Users\Gianmarco\Desktop\provaacaso_files\dp0\AQW\DM\AQW.agdb
Sea Geometry	
Water Depth	40 m
Water Density	1025 kg/m³
Water Size X	1000 m

Water Size Y	1000 m
Import Preferences	
Import Solid Bodies	No
Import Surface Bodies	Yes
Import Line Bodies	Yes

Part

TABLE 3
Model (A3) > Geometry > Part

Object Name	*Part*
State	Fully Defined
Details of Part	
Part Visibility	Visible
Suppressed	Not Suppressed
Total Structural Mass	26144.6632385254 kg
X Position of COG	2.92173254479167E-08 m
Y Position of COG	0.0 m
Z Position of COG	0.0 m
Generate Internal Lid	No
Current Calculation Depth	0.0 m
Fixity Options	
Structure Fixity	Structure is Free to Move
Force Factors	
Drag Factor	1
Mass Factor	1
Slam Factor	0.0
Advanced Options	
Submerged Structure Detection	Program Controlled
Override Calculated GMX	No
Override Calculated GMY	No
Non-Linear Roll Damping	
Non-Linear Roll Damping	Excluded from Calculations

TABLE 4
Model (A3) > Geometry > Part > Axes

Object Name	*Part Axes*
State	Fully Defined
Details of Part Axes	
Visibility	Visible
Alignment Method	Global Axes
Rotation About Global Z	0.0 °
Rotation About Local Y	0.0 °
Rotation About Local X	0.0 °
Unit Vector X	[1, 0.0, 0.0]
Unit Vector Y	[0.0, 1, 0.0]
Unit Vector Z	[0.0, 0.0, 1]

TABLE 5
Model (A3) > Geometry > Part > Point Mass

Object Name	*Point Mass*
State	Fully Defined

Details of Point Mass	
Visibility	Visible
Suppressed	Not Suppressed
X	2.92173254479167E-08 m
Y	0.0 m
Z	0.0 m
Mass definition	Program Controlled
Mass	26144.6632385254 kg
Define inertia values by	Direct input of Inertia
Kxx	9.70009588924813 m
Kyy	9.70009588924813 m
Kzz	9.70009588924813 m
Ixx	2460000 kg.m²
Ixy	0.0 kg.m²
Ixz	0.0 kg.m²
Iyy	2460000 kg.m²
Iyz	0.0 kg.m²
Izz	2460000 kg.m²

TABLE 6
Model (A3) > Geometry > Part > Body

Object Name	*Surface Body*
State	Fully Defined
Details of Surface Body	
Body Visibility	Visible
Suppressed	Not Suppressed
Structure Type	Physical Geometry
Surface Type	Program Controlled

TABLE 7
Model (A3) > Geometry > Part > Body

Object Name	*Surface Body*
State	Fully Defined
Details of Surface Body	
Body Visibility	Visible
Suppressed	Not Suppressed
Structure Type	Physical Geometry
Surface Type	Program Controlled

Connections

TABLE 8
Model (A3) > Connections

Object Name	*Connections*
State	Fully Defined
Details of Connections	

TABLE 9
Model (A3) > Connections > Catenary Data

Object Name	*Catenary Data*
State	Fully Defined
Details of Catenary Data	

Mesh

TABLE 10
Model (A3) > Mesh

Object Name	*Mesh*
State	Meshed
Details of Mesh	
Defaults	
Global Control	Basic Controls
Mesh Parameters	
Defeaturing Tolerance	0.001 m
Max Element Size	0.1 m
Max Allowed Frequency	1.919 Hz
Meshing Type	Combined Meshing
Generated Mesh Information	
Number of Nodes	30156
Number of Elements	30176
Number of Diff Nodes	14211
Number of Diff Elements	14094

Hydrodynamic Diffraction (A4)

TABLE 11
Model (A3) > Analysis

Object Name	*Hydrodynamic Diffraction (A4)*
State	Solved
Details of Hydrodynamic Diffraction	
Analysis Type	Hydrodynamic Diffraction/Radiation

TABLE 12
Model (A3) > Hydrodynamic Diffraction (A4) > Analysis Settings

Object Name	*Analysis Settings*
State	Fully Defined
Details of Analysis Settings	
Sea Grid Size Factor	2
Output File Options	
Output Full QTF Matrix	No
Do Not Output .LIS Banner Page	No
No Wave Elevation at Field Points	No
Output Source Strengths	No
Output Potentials	No
Output Centroid Pressures	No
Output Element Properties	No
Output ASCII Hydrodynamic Database	No
Output Example of Hydrodynamic Database	No
QTF Options	
Calculate Full QTF Matrix	Yes
Common Analysis Options	
Ignore Modelling Rule Violations	Yes
No Drift Coefficients	No
No Pressure Post-Processing	No
Near Field Solution	No

Linearized Morison Drag	No

TABLE 13
Model (A3) > Hydrodynamic Diffraction (A4) > Gravity

Object Name	*Gravity*
State	Fully Defined
Details of Gravity	
Gravity, g	9.80665 m/s²

TABLE 14
Model (A3) > Hydrodynamic Diffraction (A4) > Structure Selection

Object Name	*Structure Selection*
State	Fully Defined
Details of Structure Selection	
Structures to Exclude	None
Group Of Structures	
Interacting Structure Groups	None
Structure Ordering	
Structure 1	Part

TABLE 15
Model (A3) > Hydrodynamic Diffraction (A4) > Wave Direction

Object Name	*Wave Directions*
State	Fully Defined
Details of Wave Directions	
Type	Range of Directions, No Forward Speed
Required Wave Input	
Wave Range	-180° to 180° (-PI to PI)
Interval	45 °
Number of Intermediate Directions	7
Optional Wave Directions A	
Additional Range	None
Optional Wave Directions B	
Additional Range	None
Optional Wave Directions C	
Additional Range	None
Optional Wave Directions D	
Additional Range	None

TABLE 16
Model (A3) > Hydrodynamic Diffraction (A4) > Wave Frequency

Object Name	*Wave Frequencies*
State	Fully Defined
Details of Wave Frequencies	
Frequency / Period definition	
Range	Program Controlled
Total Number of Frequencies	50
Equal Intervals Based Upon	Frequency

Solution (A5)

TABLE 17

Model (A3) > Hydrodynamic Diffraction (A4) > Solution (A5) > Hydrodynamic Graph Results

Object Name	*Added Mass, Global X (Force/Moment vs Frequency)*
State	Solved
Details of Added Mass, Global X (Force/Moment vs Frequency)	
Presentation Method	Line
Axes Selection	Force/Moment vs Frequency
Frequency or Period Scale	Frequency
Line A	
Structure	Part
Type	Added Mass
SubType	Global Z
Component	Global Z
Position of Min in X	0.482
Position of Max in X	0.016
Minimum Value	11884.704
Maximum Value	29575.205
Line B	
Structure	Not Defined...

FIGURE 1
Model (A3) > Hydrodynamic Diffraction (A4) > Solution (A5) > Added Mass, Global X (Force/Moment vs Frequency)

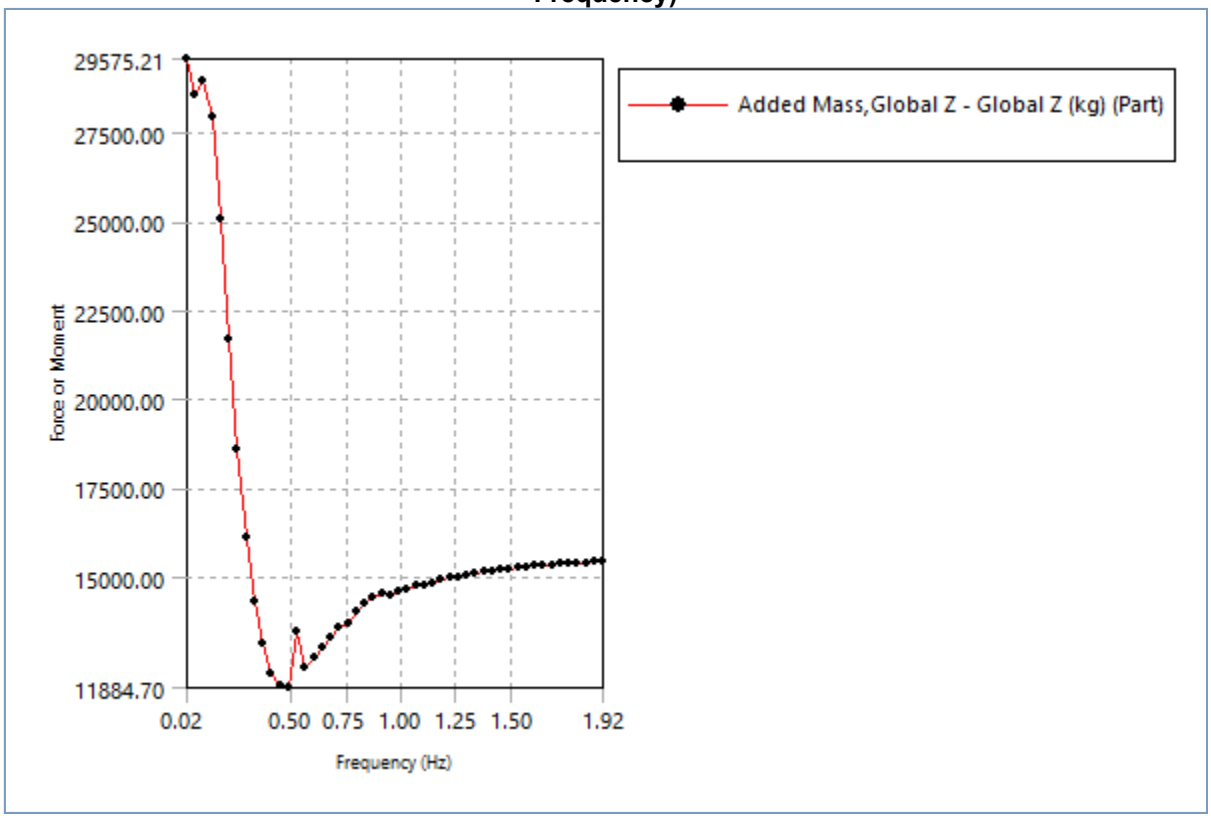

TABLE 18
Model (A3) > Hydrodynamic Diffraction (A4) > Solution (A5) > Added Mass, Global X (Force/Moment vs Frequency)

Frequency (Hz)	Line 1
0.016	29575.205
0.055	28587.637
0.094	28941.26

0.132	27967.457
0.171	25050.676
0.21	21688.924
0.249	18598.1
0.288	16109.516
0.327	14308.614
0.365	13098.331
0.404	12251.619
0.443	11929.165
0.482	11884.704
0.521	13454.784
0.56	12450.36
0.599	12708.702
0.637	12999.561
0.676	13288.354
0.715	13561.017
0.754	13696.423
0.793	14043.69
0.832	14251.98
0.87	14440.272
0.909	14509.823
0.948	14471.002
0.987	14582.129
1.026	14654.39
1.065	14732.568
1.103	14737.232
1.142	14840.52
1.181	14907.096
1.22	14979.554
1.259	15004.012
1.298	15053.108
1.337	15098.614
1.375	15127.663
1.414	15164.05
1.453	15199.896
1.492	15222.888
1.531	15250.8
1.57	15263.622
1.608	15297.418
1.647	15317.927
1.686	15337.62
1.725	15355.011
1.764	15372.5
1.803	15388.27
1.841	15400.058
1.88	15415.615
1.919	15426.87

TABLE 19
Model (A3) > Hydrodynamic Diffraction (A4) > Solution (A5) > Hydrodynamic Graph Results

Object Name	*Radiation Damping, Global X (Force/Moment vs Frequency)*
State	Solved

Details of Radiation Damping, Global X (Force/Moment vs Frequency)	
Presentation Method	Line
Axes Selection	Force/Moment vs Frequency
Frequency or Period Scale	Frequency
Line A	
Structure	Part
Type	Radiation Damping
SubType	Global Z
Component	Global Z
Position of Min in X	1.57
Position of Max in X	0.288
Minimum Value	157.803
Maximum Value	19888.545
Line B	
Structure	Not Defined...

FIGURE 2
Model (A3) > Hydrodynamic Diffraction (A4) > Solution (A5) > Radiation Damping, Global X (Force/Moment vs Frequency)

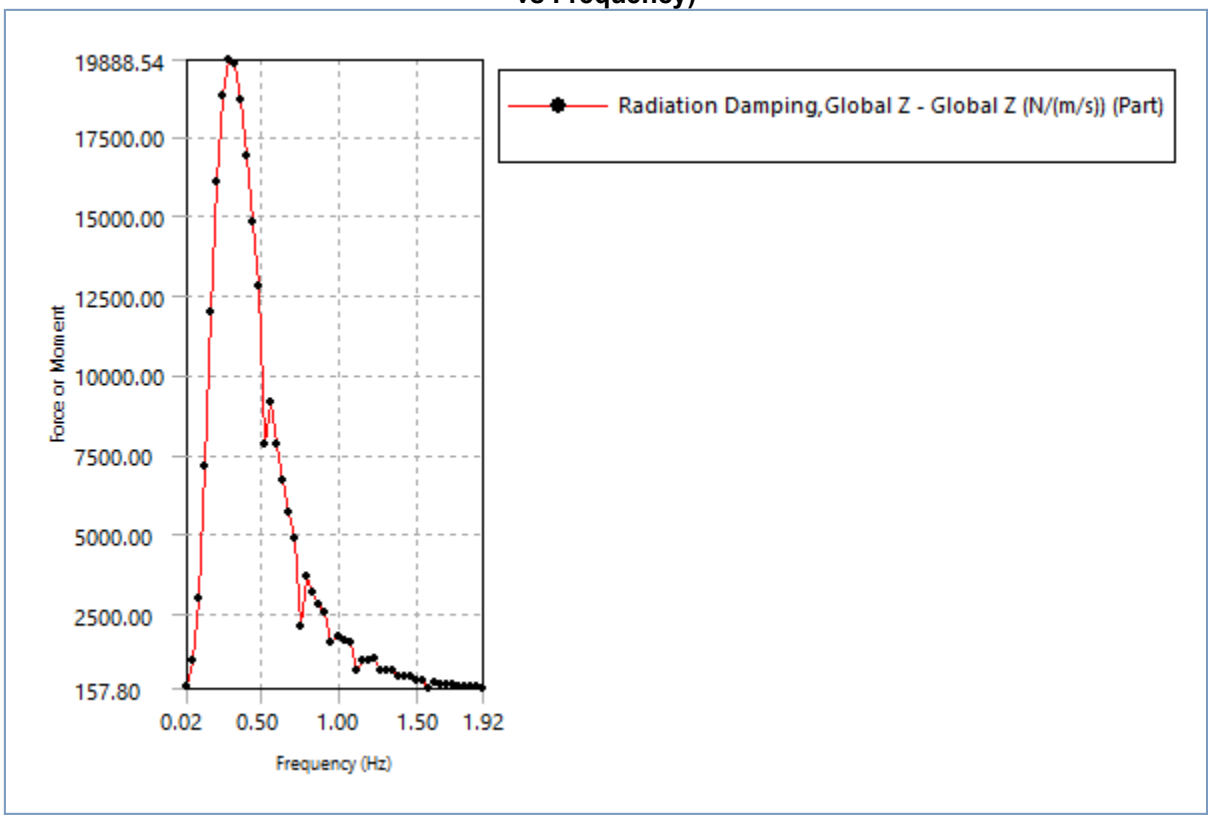

TABLE 20
Model (A3) > Hydrodynamic Diffraction (A4) > Solution (A5) > Radiation Damping, Global X (Force/Moment vs Frequency)

Frequency (Hz)	Line 1
0.016	242.53624
0.055	1062.1456
0.094	3001.3931
0.132	7140.0288
0.171	11986.945
0.21	16049.438

0.249	18729.006
0.288	19888.545
0.327	19736.461
0.365	18619.393
0.404	16855.592
0.443	14802.059
0.482	12789.635
0.521	7807.6582
0.56	9148.0215
0.599	7842.1147
0.637	6693.2515
0.676	5703.9258
0.715	4841.7676
0.754	2126.5193
0.793	3705.1052
0.832	3194.2153
0.87	2798.8906
0.909	2526.3958
0.948	1633.7478
0.987	1788.6102
1.026	1657.625
1.065	1612.5508
1.103	732.63
1.142	1068.5437
1.181	1022.7937
1.22	1130.7799
1.259	715.03351
1.298	693.29211
1.337	696.9599
1.375	519.57336
1.414	508.45859
1.453	526.91705
1.492	402.15756
1.531	389.15744
1.57	157.80278
1.608	319.48682
1.647	308.80792
1.686	267.6265
1.725	256.94681
1.764	226.2986
1.803	219.53296
1.841	201.63164
1.88	191.50879
1.919	170.28493

TABLE 21
Model (A3) > Hydrodynamic Diffraction (A4) > Solution (A5) > Hydrodynamic Graph Results

Object Name	*Diffraction + Froude-Krylov (Phase Angle vs Frequency)*
State	Solved
Details of Diffraction + Froude-Krylov (Phase Angle vs Frequency)	
Presentation Method	Line
Axes Selection	Phase Angle vs Frequency

Frequency or Period Scale	Frequency
Line A	
Structure	Part
Type	Diffraction + Froude-Krylov
Component	Global Z
Direction	-180 °
Position of Min in X	1.88
Position of Max in X	0.637
Minimum Value	-175.085
Maximum Value	161.729
Line B	
Structure	Not Defined...

FIGURE 3
Model (A3) > Hydrodynamic Diffraction (A4) > Solution (A5) > Diffraction + Froude-Krylov (Phase Angle vs Frequency)

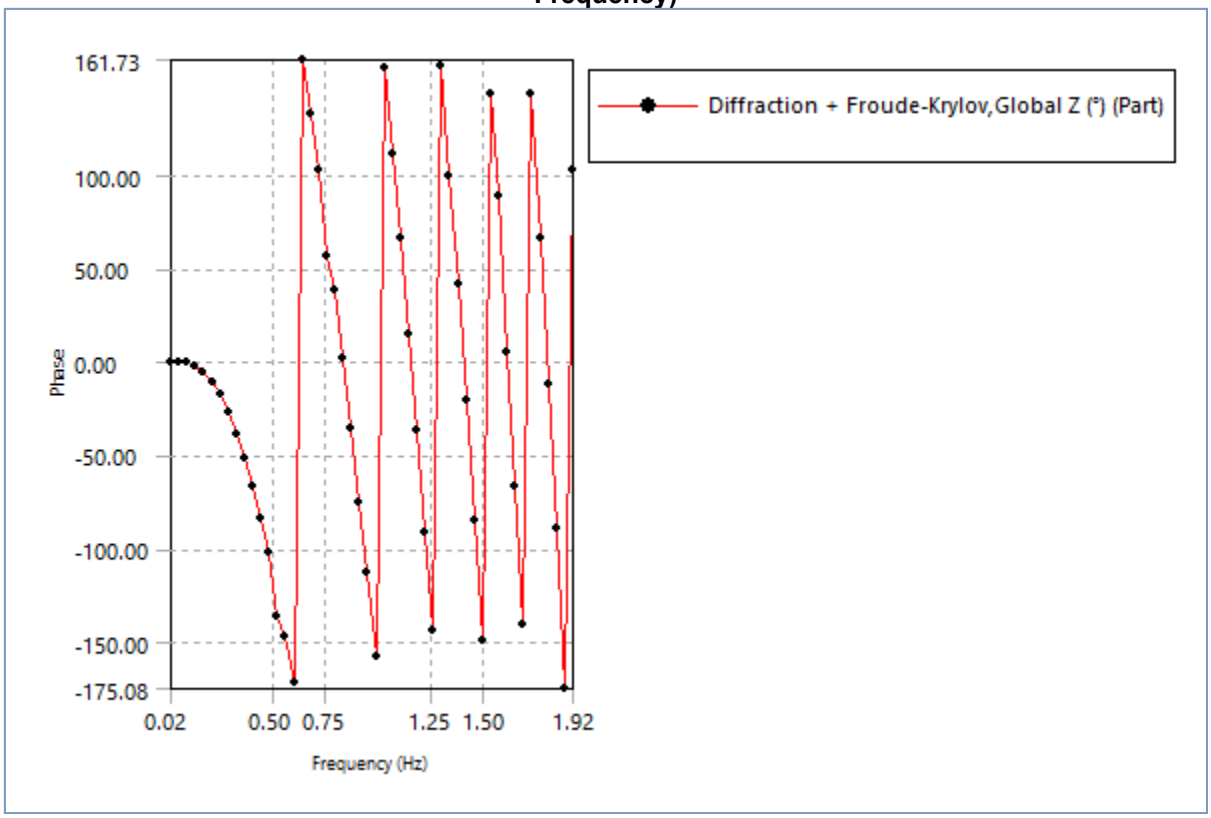

TABLE 22
Model (A3) > Hydrodynamic Diffraction (A4) > Solution (A5) > Diffraction + Froude-Krylov (Phase Angle vs Frequency)

Frequency (Hz)	Line 1
0.016	-7.2264e-3
0.055	-0.1122257
0.094	-0.5809338
0.132	-2.183588
0.171	-5.4736274
0.21	-10.66867
0.249	-17.9163
0.288	-27.220863
0.327	-38.547955

0.365	-51.832861
0.404	-66.860865
0.443	-83.761444
0.482	-102.34474
0.521	-136.9424
0.56	-147.3348
0.599	-171.76017
0.637	161.72913
0.676	133.2957
0.715	102.88509
0.754	56.745618
0.793	37.928556
0.832	2.0754855
0.87	-35.453535
0.909	-74.975697
0.948	-113.02641
0.987	-157.53292
1.026	157.81126
1.065	111.26998
1.103	66.049835
1.142	14.650375
1.181	-37.004302
1.22	-91.357332
1.259	-144.15163
1.298	158.88367
1.337	100.00409
1.375	41.225748
1.414	-20.883209
1.453	-84.838026
1.492	-149.12105
1.531	143.79884
1.57	88.94995
1.608	5.0631928
1.647	-66.840019
1.686	-140.73198
1.725	144.02258
1.764	65.87296
1.803	-12.056429
1.841	-89.774306
1.88	-175.08491
1.919	102.42942

TABLE 23
Model (A3) > Hydrodynamic Diffraction (A4) > Solution (A5) > Hydrodynamic Graph Results

Object Name	*Diffraction + Froude-Krylov (Force/Moment vs Frequency)*
State	Solved
Details of Diffraction + Froude-Krylov (Force/Moment vs Frequency)	
Presentation Method	Line
Axes Selection	Force/Moment vs Frequency
Frequency or Period Scale	Frequency
Line A	
Structure	Part

Type	Diffraction + Froude-Krylov
Component	Global Z
Direction	-180 °
Position of Min in X	1.57
Position of Max in X	0.016
Minimum Value	341.61
Maximum Value	192565.063
Line B	
Structure	Not Defined...

FIGURE 4
Model (A3) > Hydrodynamic Diffraction (A4) > Solution (A5) > Diffraction + Froude-Krylov (Force/Moment vs Frequency)

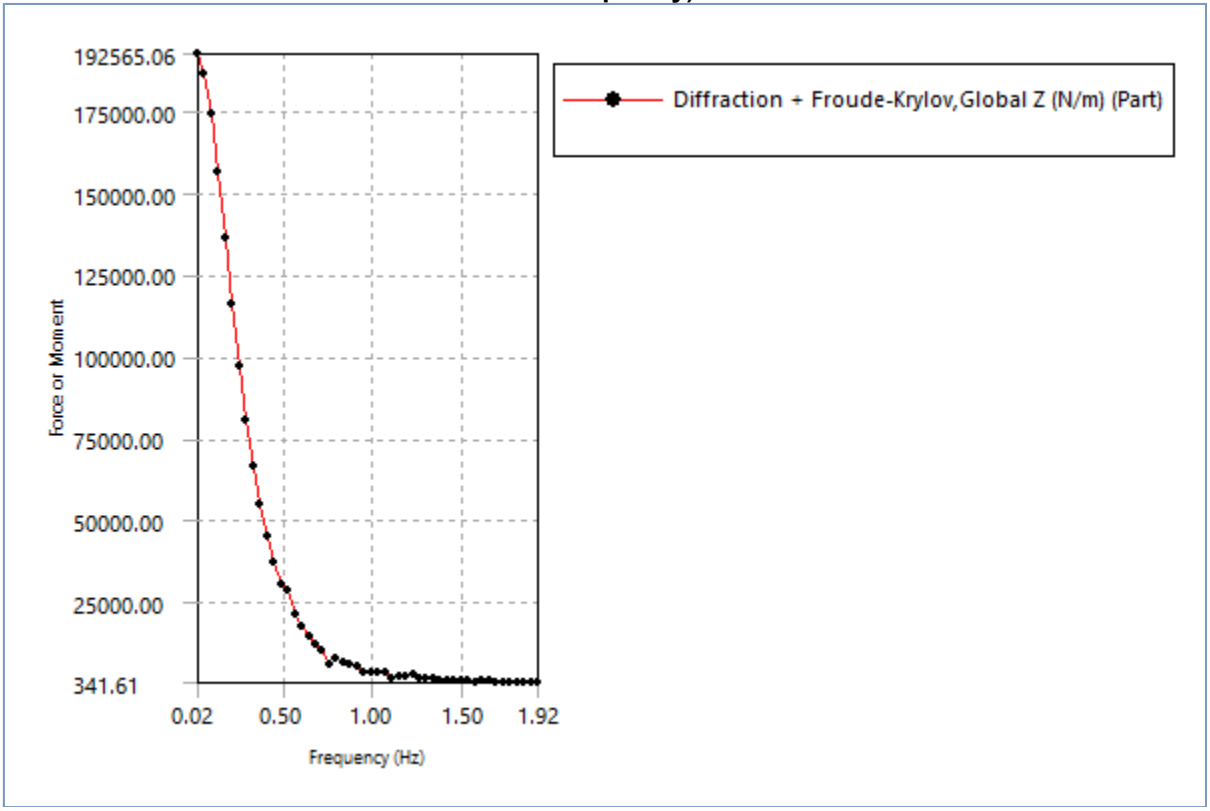

TABLE 24
Model (A3) > Hydrodynamic Diffraction (A4) > Solution (A5) > Diffraction + Froude-Krylov (Force/Moment vs Frequency)

Frequency (Hz)	Line 1
0.016	192565.06
0.055	186682.33
0.094	174251.81
0.132	156367.05
0.171	136176.17
0.21	115908.53
0.249	97090.758
0.288	80500.906
0.327	66328.688
0.365	54529.488
0.404	45123.699
0.443	37188.492

0.482	30482.504
0.521	28457.658
0.56	20990.648
0.599	17332.629
0.637	14419.563
0.676	12063.792
0.715	10126.445
0.754	5746.918
0.793	7507.4224
0.832	6453.4385
0.87	5642.042
0.909	5107.6206
0.948	3209.7002
0.987	3592.6934
1.026	3352.1594
1.065	3297.9404
1.103	1479.3022
1.142	2229.124
1.181	2179.7944
1.22	2485.9663
1.259	1566.2603
1.298	1543.7568
1.337	1575.1277
1.375	1173.9812
1.414	1160.4037
1.453	1215.2744
1.492	926.42267
1.531	902.92847
1.57	341.60971
1.608	746.53888
1.647	723.54022
1.686	628.37183
1.725	603.10614
1.764	534.95685
1.803	516.245
1.841	466.11578
1.88	449.83899
1.919	395.51779